RÉPUBLIQUE ALGERIENNE DÉMOCRATIQUE ET POPULAIRE

MINISTÈRE DE L'ENSEIGNEMENT SUPERIEUR ET DE LA RECHERCHE SCIENTIFIQUE

UNIVERSITÉ ABDELHAMID IBN BADIS - MOSTAGANEM

FACULTÉ DES SCIENCES ET DE LA TECHNOLOGIE

DÉPARTEMENT DE GÉNIE CIVIL

THÈSE

Présentée pour obtenir

LE DIPLÔME DE DOCTORAT 3ème Cycle

Spécialité : Génie civil

Option : Structures

Par

BRAHIMI Mahi Eddine

Analyse numérique des performances thermiques d'une paroi à base de matériaux à changement de phase

Numerical analysis of the thermal performances of a wall based on phase change materials

Soutenue publiquement le …../…./2025 devant le jury composé de :

Mr. MEBROUKI Abdelkader	Professeur	Président	UMAB - Mostaganem
Me. BELAS Nadia	Professeure	Examinateur	UMAB - Mostaganem
Mr. HOUAT Samir	Professeur	Examinateur	UMAB - Mostaganem
Mr. MENAD Kamel	M.C.A	Examinateur	Université de Relizane
Mr. MALIKI Mustapha	Professeur	Rapporteur	UMAB - Mostaganem
Mr. SARDOU Miloud	Professeur	Co-rapporteur	UMAB - Mostaganem
Mr. Kuznik Frédéric	Professeur	Invité	INSA de Lyon - France

Année Universitaire: 2024-2025

ACKNOWLEDGMENTS

Praise be to Allah, the Most Gracious, the Most Merciful. I thank Him with abundant and sincere praise, for it is by His grace and mercy that this work has come to completion.

I would like to express my deepest gratitude to my supervisor, Professor Mustapha Maliki, for his constant support, valuable guidance and scientific insight throughout the course of this research. His encouragement and expertise have been instrumental in shaping the direction and quality of this thesis.

My sincere thanks also go to Professor Miloud Sardou, my assistant supervisor, for his kind support.

I would also like to express my sincere appreciation to Professor Missoum Hanifi and Professor Laredj Nadia for their constructive feedback, scientific input and encouragement, which greatly enriched my work.

A special thanks goes to Professor Frédéric Kuznik from the Université de Lyon for his academic support and fruitful collaboration, which contributed meaningfully to the progress of this research.

I am also grateful to my doctoral colleagues: Sebahi Lakhal, Bennaceur Djihad and Belhamideche Kheira, for their friendship, cooperation and for sharing this journey with me. My sincere thanks also extend to my colleague, Ali Hadj Brahim. I would like to extend my heartfelt gratitude to Dr. Abdeljalil, Head of the Thermal Analysis Laboratory at the Innovation Center, University of Bab Ezzouar.

I am also deeply thankful to Mr. Ibrahim, Head of the Laboratories at the Faculty of Technology, for his kind facilitation and unwavering support.

I am especially grateful to Dr. Ahcen Keziz from the University of M'sila, whose expertise and generous contributions in the laboratory greatly enriched my work.

I also extend my sincere thanks to those in charge of the Mechanical Engineering Laboratory at the University of Mostaganem.

Most of all, I thank my beloved parents for their endless love, prayers and sacrifices throughout my life. I am deeply grateful to my dear wife for her patience, encouragement and unwavering support, and to my precious children who have been my greatest source of motivation and joy.

May Allah accept this humble work and make it useful for science and society.

الملخص

يمثل استهلاك الطاقة في المباني أكثر من 40٪ من إجمالي استهلاك الطاقة في الجزائر، وتُعتبر أغلفة المباني المصدر الرئيسي لفقدان الحرارة. خلال السنوات الأخيرة، تناولت العديد من الدراسات فوائد دمج المواد ذات التغير الطوري (PCM)بشكل ايجابي داخل جدران المباني. وتُعد هذه المقاربة حلاً واعدًا لتحسين الراحة الحرارية الداخلية من خلال تنظيم تقلبات درجات الحرارة وتحسين استخدام الطاقة.

تركز هذه الدراسة على المواد العضوية ذات التغير الطوري المستمدة من مصادر بيولوجية(BO-PCM) ، باعتبارها بدائل مستدامة للمواد ذات الأساس البترولي الشائعة الاستخدام في مجال البناء. الهدف هو تحديد المواد البيولوجية الأكثر ملاءمة والتي تقلل من التكاليف والتأثير البيئي، مع ضمان كفاءة عالية وأداء حراري مثالي. وقد تم تحديد خلطات يوتكتيكية من الأحماض الدهنية، مكونة من 70٪ حمض الميريستيك و30٪ حمض الستياريك، كخيارات واعدة من حيث الفعالية البيئية والاقتصادية. تتميز هذه المواد بدرجات حرارة تبلور وانصهار تتراوح بينC° 35 وC° 35.5 ، مما يجعلها مناسبة لتخزين الحرارة الكامنة كبديل عن PCM البترولية. وتُعد خصائصها الحرارية الجيدة، وتكلفتها المنخفضة، وأصلها المتجدد، وكثافتها الطاقوية المقاربة، من أبرز ميزاتها التي تجعلها مرشحة قوية لحلول بناء مستدامة.

تم اختيار مادة BO-PCM ذات مدى انصهار وتصلب بين 35.5 °C35و°C، وبسعة حرارية كامنة تبلغ 240.1 كيلوجول/كغ، وموصلية حرارية وسطية قدرها 0.17 واط/(م·ك) في الحالة الصلبة، و0.15 واط/(م·ك) في الحالة السائلة، وتم دمجها في مواد البناء بهدف تحسين الكفاءة الطاقوية عن طريق تقليل التبادلات الحرارية وتثبيت درجات الحرارة الداخلية. أُجري تحليل رقمي باستخدام برنامج COMSOL Multiphysics V6.0 لحل المعادلات التفاضلية الجزئية التي تحكم الظاهرة وتقييم فعالية دمج هذه المادة في مواد البناء.

كما تستكشف هذه الدراسة تطوير مركب عضوي مستدام قائم على ألياف نخيل التمر. حيث تم تشريب هذه الألياف تحت الفراغ بمزيج يوتكتيكي من حمض الميريستيك وحمض الستياريك بنسبة إدماج بلغت 52.39٪، لإنتاج مركب مستقر تم استخدامه في طوب الطين (الآدوبي) المعزز بمادة تغيير الطور. وقد تم توصيف الخصائص الحرارية للمواد باستخدام تقنيات مثل المسح الحراري التفاضلي(DSC) ، والتحليل الحراري الوزني(TGA) . أظهرت نتائج DSC أن المركب MA-SA/DPF يتمتع بدرجات حرارة انصهار وتصلب تبلغC° 34.5 ، مع إنثالبيات انصهار وتصلب تبلغ 240.1 جول/غ و124 جول/غ على التوالي. وأكد تحليل TGA الاستقرار الحراري للمركب حتى درجة حرارة C° 125 ، مما يجعله مناسبًا لتطبيقات البناء. تم تقييم الأداء الحراري لطوب الطين المدعم بمادة التغير الطوري في حالتين مختلفتين.

كما أُجريت دراسة عددية لتقييم تأثير دمج PCM في مواد البناء التقليدية. تم اقتراح وتحليل جدار من الطوب المجوف يتكون من 8 و12 تجويفًا، وهو شائع في البناء بالجزائر، وذلك باستخدام تكوينات مختلفة لمواقع PCM .وأظهرت النتائج تحسنًا كبيرًا في القصور الحراري للجدار، ظهر في انخفاض درجة حرارة السطح الداخلي مقارنة بالحالة المرجعية بدون PCM.

الكلمات المفتاحية: مواد تغير الطور، الجدار، التوصيل الحراري.

Résumé

La consommation d'énergie dans les bâtiments représente plus de 40 % de la consommation totale d'énergie en Algérie, l'enveloppe du bâtiment étant la principale source de pertes thermiques. Ces dernières années, de nombreuses recherches ont exploré les avantages de l'intégration passive des matériaux à changement de phase (PCM) dans les murs des bâtiments. Cette approche constitue une solution prometteuse pour améliorer le confort thermique intérieur en régulant les fluctuations de température et en optimisant l'utilisation de l'énergie.

Cette étude porte sur les matériaux à changement de phase organiques biosourcés (BO-PCM) comme alternatives durables aux PCM à base de pétrole couramment utilisés dans la construction. L'objectif est d'identifier les PCM biosourcés les plus adaptés, minimisant les coûts et l'impact environnemental tout en garantissant une efficacité élevée et des performances thermiques optimales. Des mélanges eutectiques d'acides gras, spécifiquement 70 % d'acide myristique et 30 % d'acide stéarique, ont été identifiés comme des alternatives économiques et écologiques prometteuses. Ces matériaux présentent des températures de cristallisation et de fusion comprises entre 35°C et 35,5°C, ce qui les rend viables pour le stockage de chaleur latente en remplacement des PCM pétroliers. Leurs propriétés thermophysiques favorables, leur faible coût, leur origine renouvelable et leur densité énergétique comparable en font de solides candidats pour des solutions de construction durables.

Un PCM biosourcé sélectionné, ayant une plage de fusion et de solidification de 35,5°C à 35°C, une capacité thermique latente de 240,1 kJ/kg et des conductivités thermiques moyennes de 0,17 W/(m·K) à l'état solide et 0,15 W/(m·K) à l'état liquide, a été intégré aux matériaux de construction pour améliorer l'efficacité énergétique en réduisant les échanges thermiques et en stabilisant les températures intérieures. L'analyse numérique a été réalisée à l'aide du logiciel COMSOL Multiphysics V6.0 afin de résoudre les équations différentielles partielles régissant le phénomène et d'évaluer l'efficacité de l'intégration du PCM dans les matériaux de construction.

Cette étude explore également le développement d'un composite biosourcé à base de fibers de palmier dattier. Ces fibers ont été imprégnées sous vide avec un mélange eutectique d'acide myristique et d'acide stéarique (MA-SA) à un taux d'incorporation de 52,39 %, produisant un composite stabilisé utilisé pour des briques en adobe enrichies en PCM. Les propriétés thermiques des matériaux ont été caractérisées par calorimétrie différentielle à

balayage (DSC), analyse thermogravimétrique (TGA) et Analyseur de conductivité thermique (TCi). Les résultats DSC ont révélé que le composite MA-SA/DPF présentait des températures de fusion et de solidification de 35,5°C, avec des enthalpies de fusion et de solidification respectives de 240,1 J/g et 124 J/g. L'analyse TGA a confirmé la stabilité thermique du composite jusqu'à 125°C, ce qui le rend adapté aux applications de construction. Les performances thermiques des briques en adobe enrichies en PCM ont été évaluées dans deux conditions différentes.

Une étude numérique a été menée pour évaluer l'impact de l'intégration des PCM dans les matériaux de construction conventionnels. Un mur en briques creuses avec 8 et 12 cavités, couramment utilisé dans la construction en Algérie, a été proposé et analysé avec différentes configurations de placement du PCM. Les résultats ont montré une amélioration significative de l'inertie thermique du mur, illustrée par une réduction de la température de surface intérieure par rapport au cas de référence sans PCM.

De plus, l'étude a examiné le positionnement optimal du PCM dans le mur de briques dans des conditions réelles extérieures. Les résultats ont indiqué que la meilleure performance thermique était obtenue lorsque le PCM était placé dans la rangée vide de la brique, proche de la surface extérieure.

L'analyse numérique de l'intégration des PCM biosourcés dans les murs des bâtiments en Algérie a mis en évidence une amélioration considérable de la capacité de stockage d'énergie durant l'été dans différentes villes. L'impact sur la performance de stockage énergétique variait selon les conditions climatiques, avec une réduction notable des températures de pointe à l'intérieur : jusqu'à 2,4°C à Adrar, 2,1°C à Tindouf et 1,6°C à Aïn Salah. Ces résultats démontrent le potentiel des PCM biosourcés comme matériaux efficaces pour améliorer la régulation thermique dans les constructions.

Mots-clés : matériaux à changement de phase, paroi, conductivité thermique.

Abstract

Energy consumption in buildings accounts for more than 40% of the total energy usage in Algeria, with the building envelope being the primary source of heat loss. In recent years, extensive research has explored the benefits of passive integration of phase change materials (PCM) into building walls. This approach offers a promising solution for enhancing indoor thermal comfort by regulating temperature fluctuations and optimizing energy use.

This study focuses on bio-based organic phase change materials (BO-PCM) as sustainable alternatives to petroleum-based PCMs commonly used in construction. The goal is to identify the most suitable bio-based PCMs that minimize costs and environmental impact while ensuring high efficiency and effective thermal performance. Eutectic mixtures of fatty acids, specifically 70% myristic acid and 30% stearic acid, have been identified as promising economic and eco-friendly alternatives. These materials exhibit crystallization and melting temperatures between 35°C and 35.5°C, making them viable substitutes for petroleum-based PCMs in latent heat storage applications. Their favorable thermophysical properties, low cost, renewable origin, and comparable energy density position them as strong candidates for sustainable building solutions.

A selected bio-based PCM with a melting and solidification range of 35.5°C to 35°C, a latent heat capacity of 240.1 kJ/kg, and average thermal conductivities of 0.17 W/(m·K) in solid form and 0.15 W/(m·K) in liquid form was integrated into building materials to enhance energy efficiency by reducing heat exchange and stabilizing indoor temperatures. The numerical analysis was conducted using COMSOL Multiphysics V6.0 to solve the governing partial differential equations and assess the effectiveness of incorporating the new PCM into construction materials.

This study also explores the development of a bio-based PCM composite using date palm fibers. The fibers were vacuum-impregnated with a eutectic mixture of myristic acid and stearic acid (MA-SA) at an incorporation rate of 52.39%, resulting in a stabilized composite used for PCM-enhanced adobe bricks. The thermal properties of the materials were characterized using Differential Scanning Calorimetry (DSC), Thermogravimetric Analysis (TGA), and Thermal Conductivity Analyzer. (TCi). DSC results revealed that the MA-SA/DPF composite exhibited melting and solidification temperatures of 35.5°C, with enthalpies of fusion and solidification of 240.1 J/g and 124 J/g, respectively. TGA analysis confirmed the composite's thermal stability up to 125°C, making it suitable for building applications. The

thermal performance of the PCM-enhanced adobe was evaluated under two different conditions.

A numerical study was conducted to assess the impact of integrating PCMs into conventional building materials. A hollow brick wall with 8 and 12 cavities, commonly used in Algerian construction, was proposed and analyzed with different PCM placements. The results demonstrated a significant improvement in the thermal inertia of the wall, as evidenced by a reduction in the indoor surface temperature compared to the reference case without PCM.

Additionally, the study investigated the optimal positioning of the PCM within the brick wall under real outdoor conditions. The findings indicated that the best thermal performance was achieved when the PCM was placed in the empty row of the brick, positioned close to the outer surface.

The numerical analysis of bio-based PCM integration into building walls in Algeria highlighted a considerable enhancement in energy storage capacity during summer across various cities. The impact of energy storage performance varied based on climatic conditions, with a noticeable reduction in peak indoor temperatures: up to 2.4°C in Adrar, 2.1°C in Tindouf, and 1.6°C Ain Salah. These results demonstrate the potential of bio-based PCMs as effective materials for improving thermal regulation in building construction.

Keywords: Phase change materials, wall, thermal conductivity.

Table of contents

List of figures

List of tables

Nomenclature

Latin Letters

Rating	Description	Unit
C_p	Specific heat capacity	[J/kg K]
h_i	Inside convective heat transfer coefficient	[W/m^2 K]
h_o	Outside convective heat transfer coefficient	[W/m^2 K]
L	Latent heat	[J/kg]
L_f	Latent heat of fusion	[J/g]
q_s	Solar radiation	[W/m^2]
T	Temperature	[°C]
T_a	Indoor ambient temperature	[°C]
T_{amb}	Outdoor ambient temperature	[°C]
T_i	Interior wall surface temperature	[°C]
T_o	Outdoor wall surface temperature	[°C]
T_m	Melting temperature	[°C]
t	Simulation time	(h)

Greek Letters

Rating	Description	Unit
ϕ	Heat flux density	[W/m^2]
λ	Thermal conductivity	[W/m K]
ρ	Density	[kg/m^3]
α_m	Solid PCMs mass fraction	
Δ	Variation	
σ	Stefan-Boltzmann constant	[W.m^{-2}.K^{-4}]

Clues

Rating	**Description**
$ended$	End of melting process
$onset$	Start the PCM melting process
$peak$	The peak phase transition between the solid and liquid states
s	Solid-state
l	Liquid state
f	Freezing
m	Melting
in	Interface
o	Outdoor
Loc	Location of PCM in hollow clay brick
CPCMW	Shape-stabilized composite PCM wallboard
CFD	Computational fluid dynamics
DPF	Date palm fibers
DSC	Differential scanning calorimetry
DTA	Differential Thermal Analysis
LHS	Latent heat storage
MA	Myristic acid
PCMIWB	PCM-integrated building walls
PCM	Phase change Materials
SA	Stearic acid
B	Brick
eq	Equivalent
i	Indoor

General introduction

Improving energy efficiency in buildings is a critical issue due to its significant environmental, economic and social impacts [1]. The building sector is a major contributor to global carbon dioxide emissions and plays a crucial role in climate change [2]. Economic growth and globalisation have led to a surge in energy demand, resulting in the over-exploitation of fossil fuel resources, with more than a third of this energy consumed by buildings [3]. Buildings experience constant temperature variations, whether between indoor and outdoor environments, during the day and night, or over different seasons. These variations affect the thermal performance of the building envelope and increase the need for additional energy to maintain comfortable indoor conditions, resulting in higher electricity consumption [4]. Heat transfer within buildings is a major cause of thermal discomfort. Rising outdoor temperatures exacerbate this problem, allowing heat waves to easily penetrate into indoor spaces. This reduces thermal comfort and puts additional strain on air-conditioning, ventilation and heating systems, further increasing energy demand [5]. Several studies have investigated potential solutions, including phase change materials (PCMs) and nano-PCMs, to improve the thermal efficiency of buildings. Many recommendations and results from experimental research have been considered in this field [6]. PCMs, in particular, are being incorporated into building envelopes as a passive strategy to improve heat storage, helping to regulate indoor temperatures more effectively while reducing reliance on mechanical heating and cooling systems [7]. In recent years, PCM have been increasingly used in building envelopes of arid climates [8].

Structure of the Thesis

Our research aims to numerically analyse the thermal performance of a wall based on PCM. To achieve this goal, the thesis is divided into six chapters as follows:

Chapter One provides a general overview of energy consumption in Algeria, with a particular focus on the buildings sector. It highlights the growing demand for energy in buildings and sets the context for the need for energy efficient solutions.

The second chapter explains the mechanisms of thermal insulation in buildings and emphasises the need for it. It discusses the role of insulation in reducing energy losses, maintaining indoor comfort and improving the overall energy performance of buildings.

Chapter three presents a comprehensive literature review of phase change materials (PCMs) used in buildings. It covers the different types of PCMs, selection methods, thermal properties and techniques for their integration into building components. It also highlights the benefits of using PCMs through a review of previous experimental and numerical studies.

Chapter Four details the fabrication process of the newly developed bio-based PCM and its thermal characterisation. It also describes the successful impregnation of the PCM into date palm fibers for the production of adobe bricks. The mechanical and thermal properties of these bricks are then analysed and discussed.

Numerical simulations were carried out to evaluate the effectiveness of the newly developed PCM. These simulations focused on temperature variations inside hollow bricks, which are widely used in Algeria. In addition, numerical simulations using COMSOL Multiphysics 6.0 were carried out to study walls with PCM layers in different Algerian cities. Therefore, chapter five presents the mathematical models governing the studied systems, along with detailed descriptions of the initial and boundary conditions applied to each case. The validation of the proposed numerical model is also included in this chapter.

Finally, chapter six presents an in-depth analysis and discussion of the results related to heat transfer in PCM-enhanced building walls. It examines the variations in indoor temperatures and heat flows in several Algerian cities. The chapter also identifies the optimal location of the PCM layer within the hollow brick and discusses the mechanical and thermal properties of the PCM-impregnated date palm fiber-reinforced clay bricks. The chapter concludes with a comprehensive general summary of the research findings.

Objectives of the Thesis

The aim of this thesis is to develop and evaluate a novel bio-based phase change material (PCM) derived from fatty acids that are readily available on the Algerian market. The aim is to provide a competitive and potentially superior alternative to conventional petroleum-based PCMs traditionally used in thermal energy storage systems.

The ultimate aim is to help improve the energy performance of existing buildings and other structures in Algerian neighbourhoods and cities. Building retrofitting is considered a key pillar in the decarbonisation process.

After characterising the thermal properties of the newly developed PCM, its thermal performance will be evaluated both experimentally and numerically by simulating indoor temperature variations in building walls.

The main objectives of this research can be summarised as follows:

- Providing a bio-based phase change material based on fatty acids as a sustainable alternative to petroleum-based PCMs.
- Improvement of thermal energy management in buildings by addressing the needs of the built environment with a focus on maintaining occupant comfort.
- Reduce energy consumption in buildings.
- Contribute to the decarbonisation of heating and cooling systems by promoting the valorisation of available thermal energy.
- Supporting the development of sustainable and innovative building envelope technologies for energy efficient construction.

Chapter 1

Global and National Energy Context – Challenges and Consumption Trends in the Building Sector

1.1 Introduction

The world has been facing a steady rise in energy consumption for several decades, challenging the sustainability of an economic model that relies heavily on vast amounts of energy for growth and development. The current global energy situation is alarming. Society's ever-growing energy demands and the continuous rise in greenhouse gas emissions have made energy one of the biggest challenges of the 21st century. This issue is worsened by the fact that the primary energy sources used to meet the high demand are either non-renewable (fossil fuels) or extremely polluting (nuclear energy). It is projected that global energy consumption could increase significantly in the coming decades, with energy demand expected to grow by 1% per year until 2040 [9].

The construction sector is the world’s largest energy consumer, using over a third of all final energy and half of the global electricity supply. This makes it one of the leading contributors to carbon dioxide emissions worldwide. Economic growth and globalization are driving the overuse of fossil fuel reserves globally, and the unchecked consumption of fossil fuels has raised serious concerns about climate change and global warming [10].

In Algeria, a study conducted in 2012 found that energy consumption in the building sector accounts for over 34% of the country’s total energy use, estimated at the equivalent of 30 million tons of oil (TOE) [11]. Buildings suffer from temperature differences, such as the temperature difference between inside and outside, day and night, summer and winter. These differences have a negative impact on the performance of building envelopes, resulting in higher electricity consumption [4]. As outdoor temperatures rise, heat waves easily penetrate into buildings, resulting in poor indoor thermal comfort. And an additional load on electrical equipment used in air conditioning, ventilation and heating systems [5]. Relying on mechanical systems to achieve moderate living conditions creates thermal disturbances in buildings, resulting in high energy requirements for space conditioning in these buildings. The physical barrier between the indoor and outdoor environments is the building envelope. It protects the building's internal environment from the extremes of the external environment, such as wind

and temperature. Conventional building envelopes are rendered helpless due to the increase in global warming. The main role of the building envelope is to provide effective thermal resistance so that external heat waves are not easily transmitted to the interior. Thus, it helps to maintain a good level of internal thermal comfort for people [12], [13], [14]. To fully understand energy issues, it's important to first look at the growth in energy demand over the decades at both the global and national levels, the diversity of energy resources based on geographic location, and the goals for reducing greenhouse gas.

1.2 Energy context world

1.2.1 World Energy Resources

Demand for energy continues to rise to meet the needs of a growing global population whose standard of living continues to improve. From the beginning to the end of the 20th century, global energy consumption increased nearly tenfold, with an average growth rate of 2.3% per year (IEA, 2014). However, the current energy system is far from sustainable, relying heavily on fossil fuels (coal, oil, and natural gas), which account for more than 88% of the primary energy mix. This increased reliance on fossil fuel resources raises concerns about energy security, while climate change underscores the need for a more sustainable energy system-factors that must be evaluated alongside economic issues, particularly those that affect competitiveness through energy choices [15]. The following figure 1.1 shows the evolution of global final energy consumption from 1990 to 2020. Global energy consumption increases from 258.65 EJ in 1990 to 395.68 EJ in 2020.

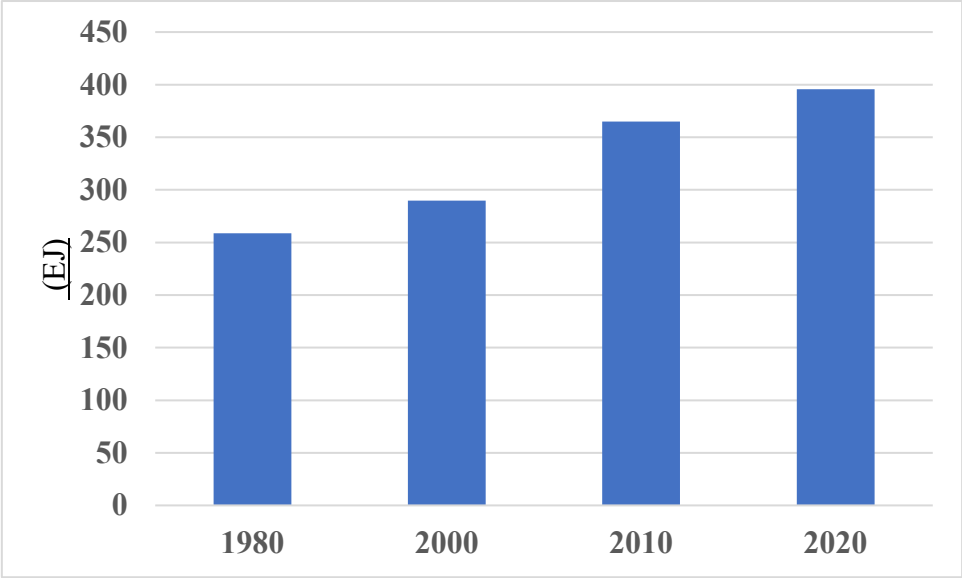

Figure 1.1. Final energy consumption worldwide[10].

1.2.2 Distribution of global energy consumption by resources

Figure 1.2 highlights the stark contrast between the types of fuels used for primary energy consumption and those used for primary energy storage. Currently, coal, oil, and gas account for 82% of the energy supply, while low-carbon energy sources account for a significant 18%- a share that is expected to grow significantly, especially in the wind and solar sectors [16].

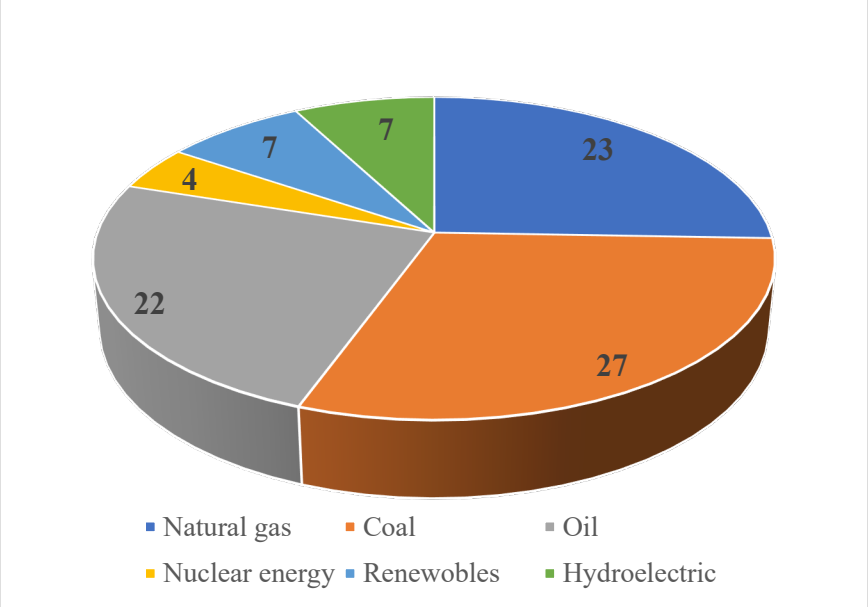

Figure 1.2. Primary Global Energy Consumption (2022 total= 167.9 PWh)

1.2.3 Environmental impact

Economic and population growth in emerging economies such as China, India, Russia, and Brazil are driving significant increases in energy demand. According to the IEA, global CO_2 emissions have reached 35 Gt, an increase of 140% since 1971. Global final energy consumption statistics show a steady increase in primary energy use from 64,321.87 TWh in 1971 to 167,787.67 TWh in 2022. The global temperature rise caused by greenhouse gases is amplifying the greenhouse effect, with climate impacts that far exceed those of other forms of pollution: reduced snow cover, increased drought and desertification in some regions, more frequent severe storms and heat waves, and the continued melting of glaciers.

1.2.4 Final energy consumption by sector in the word

Today, the entire world faces an escalating energy crisis, highlighted by the scarcity of natural resources and non-renewable fossil fuels. Since 1970, global energy demand has more than doubled [17]. In many countries, building energy use accounts for around 40% of global energy demand, with heating and cooling needs making up approximately 60% of the total energy consumed within buildings. This represents the highest percentage of energy usage overall [18]. Global final consumption in 2020 is shown in Figure 1.3. It is clear that the construction sector plays a major role in managing energy demand and improving energy efficiency. With the immediate availability of mature technologies and methods, the building sector can make a significant contribution to addressing the environmental challenges facing the world today.

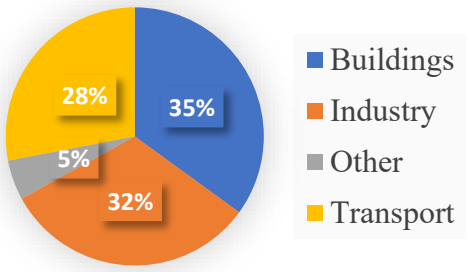

Figure 1.3. Percentage of global final energy consumption by sector in 2020 [19].

1.3 National energy context

1.3.1 Final energy consumption

Algeria is Africa's leading producer of natural gas, the second-largest supplier of natural gas to Europe, and one of the top three oil producers on the continent. Algeria joined the Organization

of Petroleum Exporting Countries (OPEC) in 1969, shortly after beginning oil production in 1958. As part of the global community, Algeria's energy consumption is reviewed in this study to highlight the importance of focusing on energy efficiency. This figure 1.4 compiles data published by the Algerian Ministry of Energy in its annual energy reports to observe the trend in Algeria's final energy consumption from 1980 to 2020, covering a span of 40 years. Notably, during this period, final consumption nearly increased sixfold, rising from 8.5 Mtoe in 1980 to 49.4 Mtoe in 2020. Final energy consumption is divided into three main sectors: industry and construction, transportation, and the residential sectors.

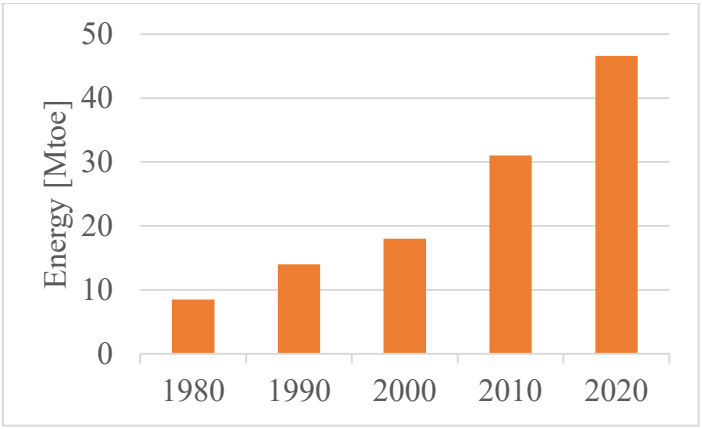

Figure 1.4. Summary of Algerian final energy consumption between 1980 and 2020 [19].

1.3.2 The way of energy consumption

The key concept in analyzing energy consumption is the stage at which energy is measured. Typically, energy is categorized according to how it is transformed from a natural resource to its final use by consumers[20]In Algeria's 2021 energy balance, these categories include primary energy, which consists of raw, unprocessed resources; final energy, which is delivered and billed to the consumer; and useful energy, which represents the portion used for specific household needs such as heating, cooling, refrigeration, cooking, and lighting.

1.3.3 Consumption by form of energy (Algeria):

Natural gas remains the dominant energy source at 37%, followed by petroleum products and electricity at 29%, as shown in the following figure 1.5.

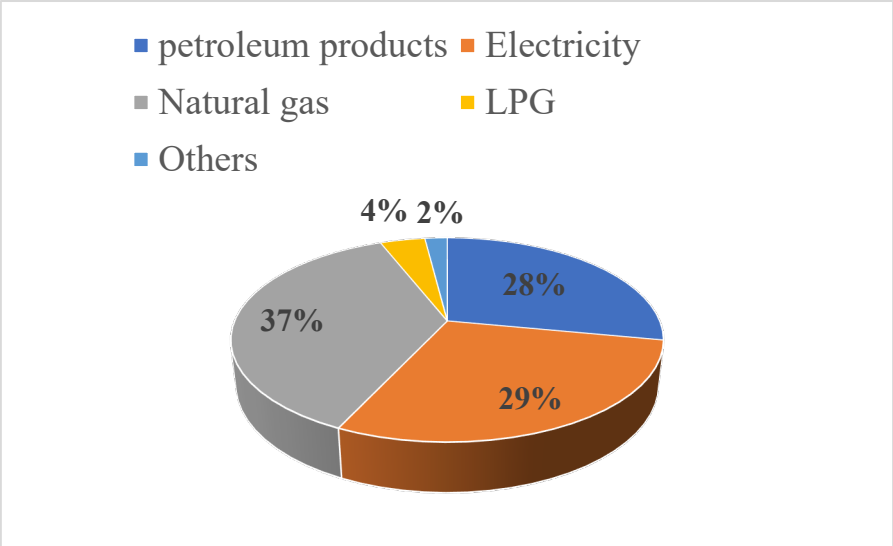

Figure 1.5. National consumption by form of energy [17].

1.3.4 Final energy consumption by sector in Algeria

In 2011, the residential and other sectors, which include the buildings sector, accounted for 41 percent of energy demand, while industry accounted for 23 percent and transportation accounted for 36 percent (Figure 1.6) [21].

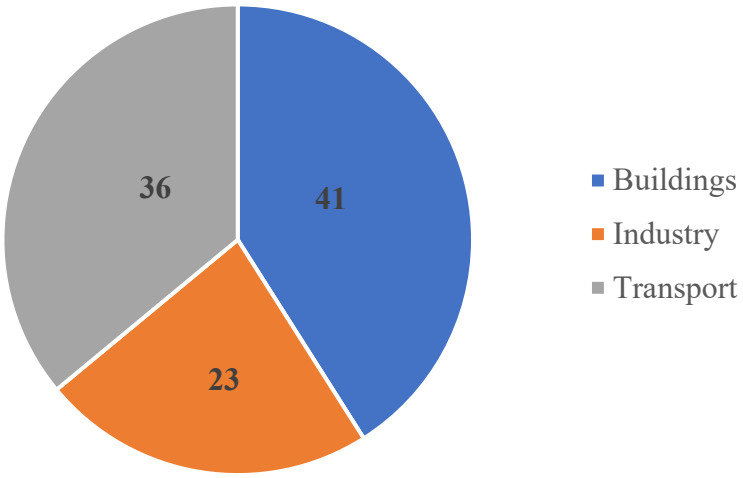

Figure 1.6. Final energy consumption in Algeria by sector in 2011[21].

In 2021, the residential sector had the highest energy demand, accounting for 47%, followed by the transportation sector at 29%, and then the industrial sector at 24% (Figure 1.7) [22]. These

statistics highlight the urgent need to rebalance energy consumption through policies aimed at reducing consumption and/or improving energy efficiency in the building sector. Compared to 2011, the residential sector remained the largest energy consumer in 2021. It is now essential to take the necessary steps to reduce this impact, similar to Canada, which in recent years has become a leader in energy efficiency. Canada has set an example for developed countries in sustainable energy management and offers developing countries an alternative path for growth, helping them avoid the same mistakes made by industrialized nations.

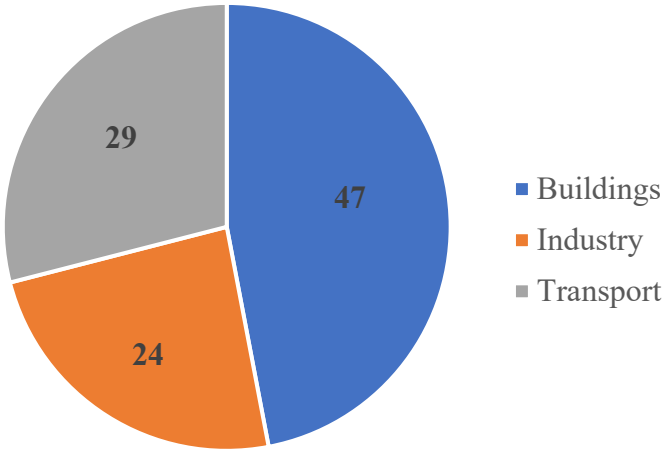

Figure 1.7. Final energy consumption in Algeria by sector in 2021[22].

It's clear that the construction industry plays a vital role in managing energy demand and improving energy efficiency. With ready access to advanced technologies and well-established methods, the building sector can significantly help address the environmental challenges facing the world today.

1.3.5 Requested service and the population in Algeria

Energy efficiency is anticipated to play a critical role in Algeria's energy outlook as demand surges, largely fueled by the expansion of the building sector, with new housing developments, public infrastructure, and industrial growth. Algeria faces a rising energy challenge linked to its increasing population, as energy demand—both fossil and renewable—grows in line with population trends, particularly impacting housing and service sectors. The ongoing population increase is one of the most significant global challenges. Algeria, specifically, saw a sharp

demographic rise from the 2000s to 2023, resulting in a population surge primarily due to higher living standards and healthcare improvements, and , as depicted in curve 1.8.

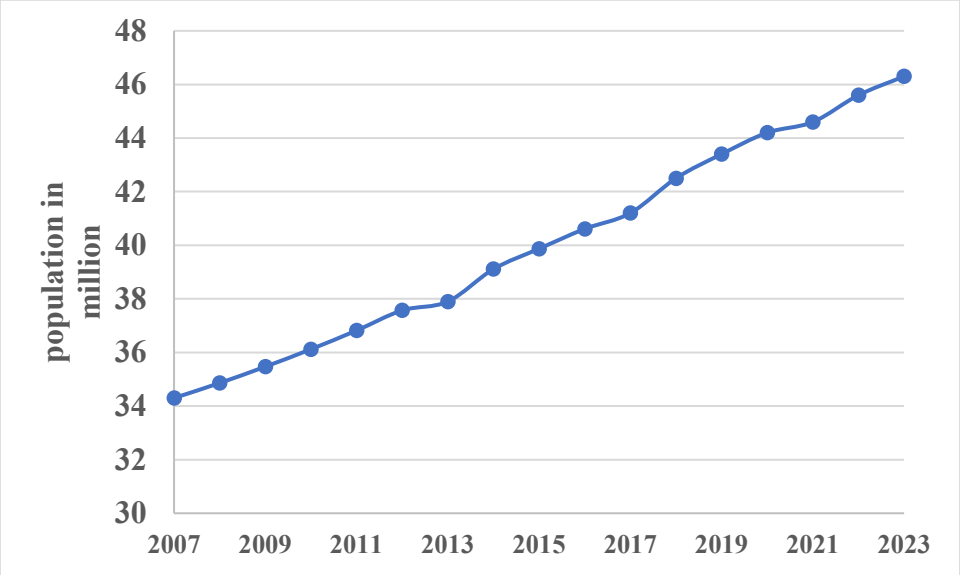

Figure 1.8. Population segmentation in Algeria.

1.3.6 Energy demand forecast by sector

The econometric approach examines trends in energy demand by extrapolating from data [15]. Its main objective is to establish a relationship between energy consumption (either total or by sector, by energy type or all types combined) and key macroeconomic indicators. The table (1.1) below summarizes the results of a previous study on final energy demand in Algeria (ktep). Energy demand is divided into three main categories, subdivided by energy service needs: the industrial sector, the transport sector, and the residential sector. By 2040, the total final energy demand of the industrial, transport and residential sectors is projected to reach 206% of the 2013 level, which itself represents an increase of 203% compared to 2001.

Table 1.1. Projected Energy Consumption by Sector in Algeria (ktep)

year	**2001**	**2013**	**2040**
Industry	4,610	8,229	17,371
transport	4,797	13,889	34,762
Household	9,588	16,425	27,210
total	18,955	38,543	79,321

1.4 Energy context of the building sector

1.4.1 Final energy consumption

Energy analysis, commonly referred to as sectoral analysis, typically divides energy consumption into four main sectors of activity, each with different patterns of energy use: industry, agriculture, transportation, and buildings. The buildings sector includes both tertiary buildings (such as shops, offices, schools, hospitals, etc.) and residential buildings (or dwellings). However, some types of accommodation are generally associated with the tertiary sector, such as university dormitories, workers' hostels, hotels, shelters (such as social housing and homeless shelters), campsites, prisons and accommodation in certain religious buildings. The residential sector can then be defined as all housing-related spaces [20]. At the national level, according to the annual energy reports published by the Ministry of Energy (ME), Algeria's final energy consumption is divided into three main sectors: industry, transport, and households (which includes residential and tertiary buildings), as well as other sectors such as agriculture. Figure 1.9 shows the evolution of household energy consumption, measured in Mtep, up to 2019.

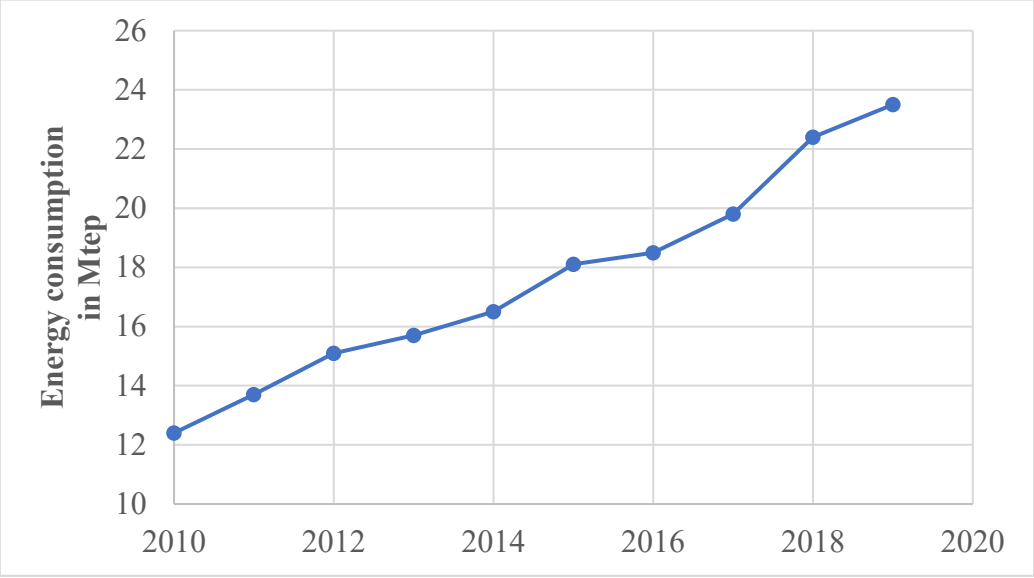

Figure 1.9. Evolution of final energy consumption in the household sector (2010-2019) [22].

Final energy consumption grew significantly from 2010 to 2019, then increased more rapidly to reach 23.5 Mtoe in 2019.

1.4.2 Nature and volume of consumptions of the Algerian resident's sector

With the residential sector's share of overall energy consumption in mind, we can now delve deeper into its specifics. The 2019 energy mix for the residential sector shows a strong reliance on natural gas and electricity, making up 57% and 33% of final energy use, respectively, with LPG at 9% and wood at 1%. This trend held steady in 2021, indicating a consistent pattern of energy consumption in residential areas. as showing in the figures 1.10 and 1.11.

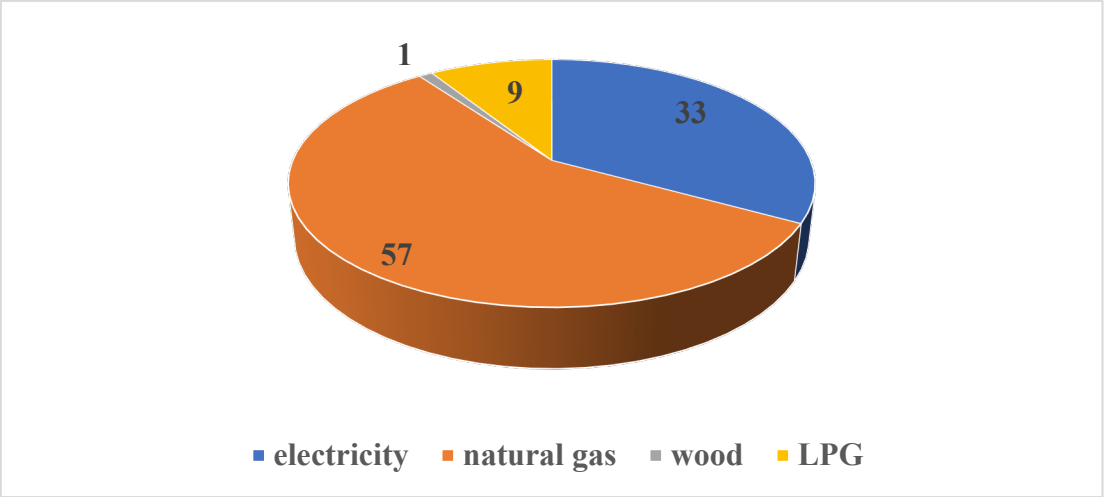

Figure 1.10. Energy mix of the Algerian residential sector 2019 [22]

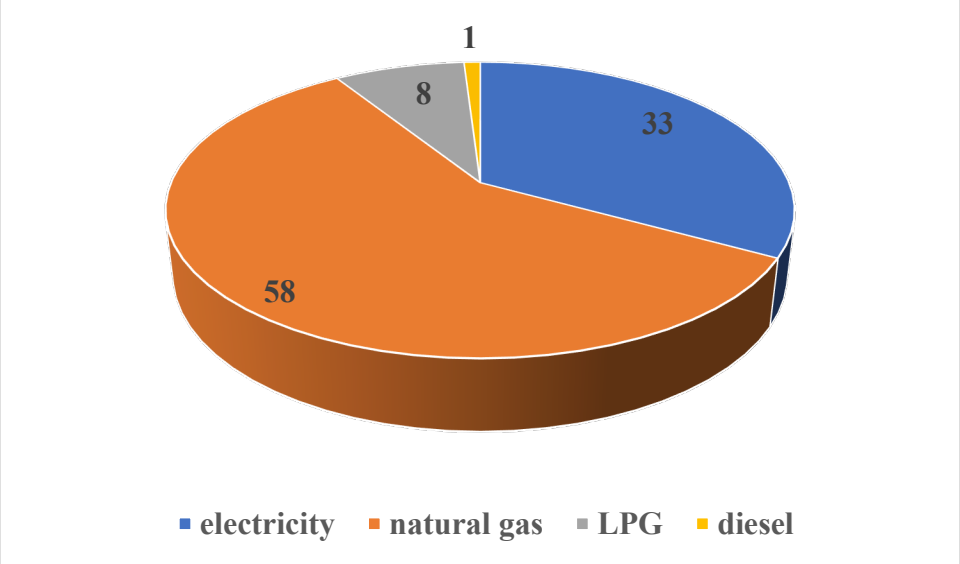

Figure 1.11. Energy mix of the Algerian residential sector 2021 [22]

1.4.3 Energy consumption in a typical home

After reviewing the types of energy consumed, the next level of analysis is to break down energy consumption by "use". This approach highlights the final energy consumption associated with the different services that households use in their homes. In a household, heating and cooling make up the largest part of energy expenses (Figure 1.12). Therefore, saving energy should focus primarily on heating. Lighting accounts for 14% of a home's electricity consumption, so it's important to find ways to manage it as well. Additionally, there are various devices, including home automation systems, electronics, and appliances, that also contribute to energy use[23].

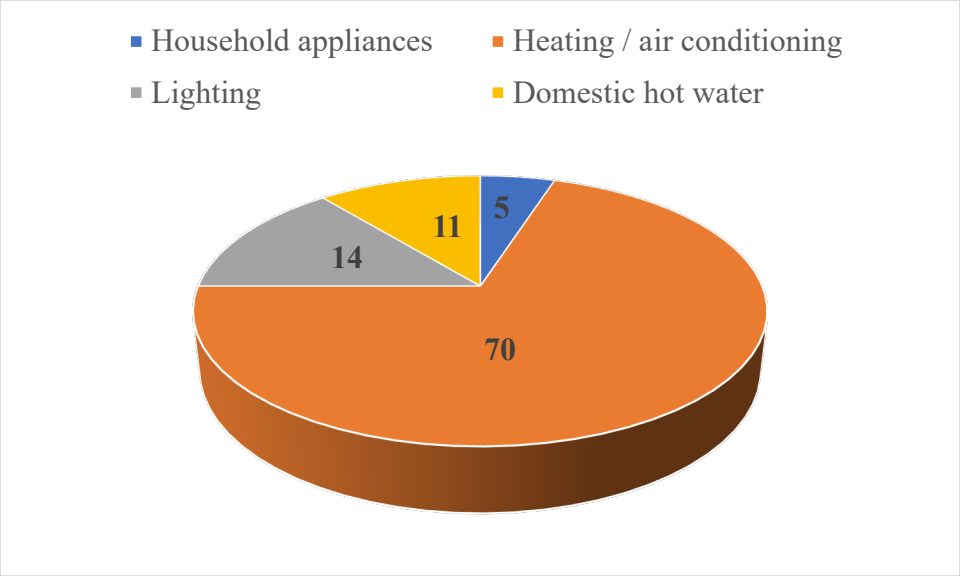

Figure 1.12. Energy expenditure in a typical household [22]

1.4.4 Heat loss in a building

A building's thermal losses represent the heat that escapes from it. These losses can also be described as the pathways through which heat exits the building in winter or enters it during summer [23]. In general, it's estimated that 50 to 75% of heat loss occurs through the building envelope, with the majority occurring through walls, windows, and ventilation. Heat loss through the floor and roof each account for up to 10% of the total losses, as shown in Figure 1.13. Heat exchange between a building and its external environment mainly depends on the outer walls. These surfaces are the primary source of significant energy loss in a building. The building envelope's effectiveness relies on architectural design, material properties, the age of the structure, and construction techniques used. Designing an effective thermal envelope is crucial for ensuring comfort while saving energy. Ignoring this aspect can lead to indoor

discomfort. Building materials play a key role in the building envelope, and their selection—whether based on specific standards or personal preferences—directly affects the thermal quality of the envelope. The thermal properties of these materials can either enhance or reduce energy performance.

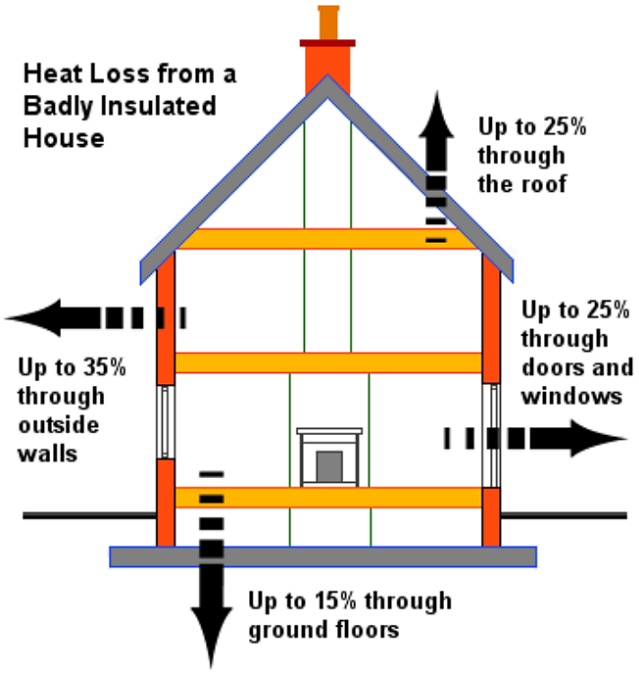

Figure 1.13. Energy loss paths in a residential building

1.5 Conclusion

This chapter outlines the current energy landscape on both global and national levels, covering resources, production, and consumption, and highlights the significant role buildings play in energy demand—particularly through electricity and gas connections and their environmental impacts. It shows that Algeria faces several energy challenges ahead and underscores the need for a comprehensive approach to rethink energy issues, emphasizing the potential for energy savings. With growing energy demand, various scenarios can be explored, given that buildings are the largest energy consumers in Algeria, with heating and ventilation as the primary household demands. Therefore, the building envelope plays a critical role in reducing energy use, and the components of Algeria's building envelope must be reconsidered.

Chapter 2

Heat Transfer and Insulation Performance in Buildings: Conventional and Earthen Materials

2.1 Introduction

Thermal insulation is one of the key elements in modern building design, playing a crucial role in reducing energy consumption and improving indoor thermal comfort. Buildings are exposed to various climatic factors such as solar radiation, heat, cold and wind, so it is essential to use materials with appropriate thermal properties that minimise heat loss in winter and reduce heat gain in summer. The efficiency of thermal insulation depends on the heat transfer mechanisms, including conduction, convection and radiation, which requires the selection of insulation materials based on their physical and mechanical properties.

2.2 Need for thermal insulation

The two essential criteria for thermal building design are the automatic and passive protection of occupants from climatic factors such as rain, wind, radiation, heat and cold through various surfaces, and the optimization of energy consumption. The designer must ensure that heating and cooling energy use remains within regulatory limits and within the financial means of the occupants, while maintaining the level of comfort defined by the project owner.

Thermal insulation, integrated into various components of the building envelope, is a key factor in energy efficiency. It helps minimize heat loss, lower heating costs, reduce greenhouse gas emissions, and improve overall occupant comfort.

A variety of thermal insulation materials are used in the construction industry today. Traditional materials such as glass wool, rock wool, expanded polystyrene (EPS) and extruded polystyrene (XPS) require a thick building envelope to achieve sufficiently low thermal transmittance. When renovating older buildings, factors such as limited space and protected facade elements must be considered to optimize energy use. In the near future, high-performance insulation materials and components will provide architects and engineers with new opportunities to design energy-efficient buildings.

The building sector is one of the largest consumers of energy, primarily to maintain thermal comfort. However, effective insulation strategies can significantly reduce energy consumption in residential, commercial and industrial buildings. Insulation helps minimize the need for cooling in the summer and heating in the winter, resulting in lower energy demand and reduced dependence on fossil fuels such as oil and gas. As a result, it also helps to slow resource depletion and reduce greenhouse gas emissions [24].

Thermal insulation works by limiting heat transfer through materials with high thermal resistance. In buildings, energy loss occurs through various elements, including walls, ceilings, floors, and windows. Since walls represent the largest surface area, they play a critical role in heat gain and loss. Therefore, proper insulation can have a significant impact on the energy efficiency of a building [25].

A variety of insulation materials are used to improve thermal performance, including fiberglass, mineral wool, foam, and polystyrene. These materials help maintain stable indoor temperatures and reduce heat exchange between the indoor and outdoor environments.

In addition to energy savings, insulation provides other benefits. It improves fire safety, enhances personal comfort by reducing temperature swings, and helps control condensation, preventing moisture buildup and mold growth. In addition, insulation contributes to soundproofing, making indoor spaces quieter and more comfortable [26].

Overall, thermal insulation is an essential component of energy-efficient building design, providing environmental, economic, and comfort benefits.

2.3 Heat transfer in insulating materials

The function of insulating materials is to minimize heat transfer through the building structure. Heat transfer is typically divided into three components: conduction through the solid, conduction through the gas phase, and radiation through the pores, as shown in Equation (2.1):

$$\lambda_T = \lambda_{ga} + \lambda_{so} + \lambda_r \tag{2.1}$$

Where λ_T $\lambda_{ga}, \lambda_{so}$ and λ_r represent the total thermal conductivity, the thermal conductivity of gas conduction, the thermal conductivity of solid conduction, and the thermal conductivity of radiation, respectively.

Typically, the dominant factor in heat transfer is conduction through the solid. To counter this, insulating materials are highly porous, containing only a small amount of solid material.

In materials with very little solid content, radiative heat transfer becomes more significant, this leads to an optimal balance for insulation, where the combined effects of radiation and solid conduction reach a minimum. This minimum value is then added to gas conduction, which remains nearly constant in conventional insulating materials.

As a result, the total thermal conductivity remains low, with a minimum value of around 30 mW/m·K, which is comparable to the thermal conductivity of air, estimated at 25 mW/m·K.

Typical materials in this category include mineral wool, expanded or extruded polystyrene, loose-fill cellulose fiber, and cellular glass. Their thermal conductivities are listed in Table 2.1.

Table 2.1. Thermal conductivity of some common insulating materials

Insulating materials	**Thermal conductivity** [*mW/(mk)*]
Mineral wool	33-40
expanded polystyrene	30-40
cellulose fiber	39-42
expanded polystyrene	39-45

- *Conduction in the Solid*

For different materials, there is also some variation in solid state conduction. This means that the choice of solid material and its physical properties play an important role in determining heat conduction through the solid phase.

To minimize solid conduction, an appropriate material must be selected, reducing the density of the material reduces the solid conduction. While the effective thermal conductivity of the solid itself remains unchanged, the cross-sectional area of the solid phase within the porous

material decreases. This reduction in solid area results in less heat conduction per square meter of material.

However, as mentioned earlier, a decrease in density also increases radiative heat transfer, which offsets the decrease in solid conduction to some extent.

- *Radiation*

Heat transfer by radiation occurs through electromagnetic waves emitted by all surfaces. The net radiation is the difference between the radiation emitted by the hot surface and the radiation emitted by the cold surface.

The rate of radiative heat transfer depends on the surface temperature and can be described by equation (2.2).

$$\lambda_r = \frac{16n^2\sigma T^3}{3K} \tag{2.2}$$

where n is the refractive index, σ ($J \cdot K^{-4} \cdot m^{-2} \cdot s^{-1}$) is the Stefan-Boltzmann constant, and k (m^{-1}) is the extinction coefficient.

As temperature increases, radiative heat transfer rises rapidly. This effect can be countered by adding an opacifying agent to the material. Examples of such agents include titanium dioxide (TiO_2), which scatters radiation, and carbon black, which absorbs radiation. While these additives reduce thermal conductivity, they also decrease the transparency of the material.

2.3.1.1 Gas Conduction

Gas conduction depends on the type of gas and its ability to transfer heat. To achieve low thermal conductivity, the gas can either be replaced with a low conductivity gas or modified to limit its heat transfer capability.

Examples of gases, along with their thermal conductivity and molecular weight, are shown in Table 2.2.

Table 2.2. conductivity and molar mass of some common gases

Insulating materials	Thermal conductivity [*mW/(mK)*]	Mass
Air	25.5	29
Nitrogen	24.1 (0°C)	28
Argon	16.2 (0°C)	40
Carbon Dioxide	16.2 (25°C)	44
Trichloro Monofluoromethane	8.3 (30°C)	137

A common gas exchange solution is found in windows, where argon or krypton is used between panes of glass. Another example is polyurethane foam, where low-conductivity reactive gases are trapped in a closed-pore system. The thermal conductivity of the gas can be reduced by reducing the pore size of the material. Collisions between gas molecules and solid surfaces are elastic and transfer small amounts of energy compared to collisions between gas molecules. Smaller pores increase the likelihood that gas molecules will collide with the pore walls rather than with each other.

2.3.2 Convection in porous materials

Convection in porous materials can be divided into two types: pore convection and macroscopic convection through the material. For closed pore systems,there is no macroscopic convection, and for small pores, convection within the pores can often be ignored, in part because of the small temperature differences along the walls of the cells. This means that heat transfer by convection can usually be neglected for materials with a closed pore structure. However, for materials with open cells, large-scale macroscopic convection can have a significant impact and cannot be ignored. Large-scale macroscopic convection can be caused by either natural or forced convection. In natural convection, air movement is driven by density differences resulting from temperature differences, while forced convection occurs due to a pressure difference, such as that caused by wind or an air extractor.

2.4 Thermal insulation terminology

Thermal insulation is a material or combination of materials designed to reduce the transfer of heat between two environments or surfaces. Its primary function is to slow the flow

of heat, either by retaining heat in a warm space (such as a building in cold weather) or by preventing heat from entering a cooler space (such as a building in hot weather)[27].

Thermal insulation is effective because it reduces heat transfer through three main mechanisms:

Conduction - the direct transfer of heat through a material.

Convection - the transfer of heat through the movement of air or liquid.

Radiation - the emission and absorption of infrared heat waves.

By minimizing these heat transfer processes, thermal insulation plays a critical role in energy efficiency and indoor comfort.

2.4.1 Thermal Conductivity

Thermal conductivity is a measure of a material's ability to conduct heat. It represents the heat flow through a material 1 meter thick when there is a temperature difference of 1 Kelvin between its opposite surfaces. This property is expressed in ($W.m^{-1}.K^{-1}$).

A lower thermal conductivity indicates that the material is a better insulator because it allows less heat to pass through. Conversely, materials with high thermal conductivity are better conductors of heat and are less effective as thermal insulators.

2.4.2 Thermal Resistance

Thermal resistance (R) is a measure of a material's insulating ability for a given thickness (e). It is expressed in $m\mathrm{I}.K.W^{-N}$and indicates how effectively a material resists heat flow. A higher thermal resistance means better insulation because it reduces heat transfer through the material. This property is particularly important in thermal insulation applications, where increasing R-values improves energy efficiency and thermal comfort in buildings.

2.4.3 Thermal Diffusivity

Thermal diffusivity is a dynamic property of a material that plays a key role in transient heat transfer processes. It quantifies how quickly a material can transfer heat when subjected to temperature changes. This property is expressed in $m^2.s^{-1}$ [38]. A material with a high thermal diffusivity responds quickly to temperature changes, while a material with a low thermal diffusivity heat or cools more slowly.

2.4.4 Thermal Effusivity

Thermal effusivity measures the ability of a material to exchange thermal energy with its environment. It reflects how a material absorbs and releases heat when in contact with another surface. A high thermal effusivity indicates that the material adapts quickly to the ambient temperature, while a low thermal effusivity indicates slower thermal interaction.

2.5 Earth as a Building Material

Earth has been used as a building material for centuries due to its abundance, sustainability and thermal performance. It is a natural and environmentally friendly material that provides good thermal insulation, high thermal mass, and moisture regulation, making it suitable for energy efficient buildings.

Various construction techniques use earth, including rammed earth, adobe, cob, and compressed earth blocks (CEB). These methods rely on locally available soil, often mixed with water, fibers, or stabilizers such as lime or cement to increase durability and strength.

One of the key advantages of earth-based construction is its thermal inertia, which helps regulate indoor temperatures by absorbing and slowly releasing heat. This characteristic reduces the need for mechanical heating and cooling, contributing to energy efficiency. In addition, earthen materials are biodegradable, recyclable and require little energy to produce, making them an excellent choice for sustainable architecture.

2.6 Evolution of Thermal Insulation

Throughout history, people have sought ways to keep their homes warm in the winter and cool in the summer. In ancient times, nomadic groups used materials such as animal skins, wool, and plant fibers such as straw and reeds to insulate their temporary shelters. However, these materials were not very durable. As humans transitioned to a sedentary agricultural lifestyle, they began to construct homes from more robust materials such as stone, wood, and earth. Earth-sheltered dwellings, including caves, became popular because of their affordability and natural insulating properties. The dense nature of the earth slowed temperature changes inside homes, a phenomenon known as thermal lag, helping them stay warm in the winter and cool in the summer. One of the earliest known examples of earth-sheltered housing is the Neolithic village of Skara Brae in Scotland, which dates back nearly 5,000 years.

In the late 19th century, construction methods changed significantly with the introduction of new materials such as steel, concrete, glass, and cast iron. While these materials allowed for more advanced structures, they also posed thermal challenges as they expanded and contracted with temperature changes, causing cracks and requiring additional insulation. Unlike traditional thick-walled adobe or brick buildings, these modern materials had lower insulating properties, resulting in greater heat loss and increased heating requirements. As energy consumption increased and the price of fossil fuels rose, the need for effective thermal insulation became more pressing. Engineers began studying heat loss and gain in the 1880s, laying the foundation for modern building physics and insulation theories [28].

Although synthetic insulation has greatly improved the energy efficiency of buildings, concerns about fossil fuel depletion and climate change have highlighted its drawbacks. Burning fossil fuels releases carbon dioxide, a major greenhouse gas.

2.7 Algeria's rich tradition of earthen architecture

Algeria is home to many traditional earthen buildings, known as ksour, which have significant cultural and historical value. These structures have been an integral part of the country's architectural heritage for centuries. In 1943, architect Michel Loix designed a provincial hospital in Adrar, demonstrating the potential of earthen construction for public buildings.

Earth has been a reliable building material for thousands of years, and when combined with modern techniques, it remains a sustainable choice for contemporary, environmentally friendly construction. Today, nearly half of the world's population still lives in earthen homes. While these structures are more common in developing countries, they can also be found in developed countries such as Germany, France and the United Kingdom, where there are over 500,000 earthen buildings [29].

In recent years, earthen construction has seen a resurgence in places such as Iran, the United States, Europe and the Middle East, driven by a growing interest in environmentally friendly building practices [30].

2.8 Earth Building Techniques

Earth has been used as a building material for thousands of years and is still widely used today. Various traditional techniques have evolved, including rammed earth, wattle and daub,

cob, adobe, and compressed earth blocks. It is estimated that over two billion people currently live in earthen structures, and approximately 10% of World Heritage sites are earthen.

2.8.1 Adobe

Adobe is one of the oldest and simplest earthen building techniques, which is why many ancient structures were built using this method. A wooden form is filled with damp earth and allowed to dry naturally in the sun. The word "adobe" comes from the Arabic word attob, which means sun-dried brick. Traditionally, adobe bricks were made entirely of earth, but in modern applications, straw is often added to improve thermal insulation [31]. Figure 2.1 shows the ease and simplicity of making this traditional type of brick.

Figure. 2.1. Production Method of Molded Adobe Bricks [32].

Other earth building techniques include :

- *Rammed earth*: Layers of moistened earth are compacted in forms to create strong walls.
- *Wattle and daub*: A wooden frame is filled with an earth-fiber mixture to provide structural support.
- *Cob*: Wet earth mixed with fibers is shaped by hand or foot to form uniform walls.
- *Compressed earth blocks*: Earth is pressed into block molds by hand or hydraulic methods, providing a more uniform and durable alternative to adobe.

2.9 Methods for Stabilizing Earthen Materials

Earth is an affordable, renewable and environmentally friendly building material. However, its durability can be compromised by water absorption and limited mechanical strength. To improve its performance, stabilizers such as lime, cement, or a combination of both are commonly used.

Stabilization methods are generally divided into three main types:

- *Mechanical stabilization:* Improving soil density and strength through compaction.
- *Physical stabilization:* Improving properties using techniques such as fiber reinforcement.
- *Chemical stabilization:* using additives such as lime or cement to increase water resistance and structural integrity.

2.10 The use of natural fibers (Date Palm Fibers) in clay blocks

The date palm (Phoenix dactylifera L.) has been cultivated for thousands of years, particularly in the Middle East and North Africa. It generates a significant amount of agricultural waste, with nearly 2.6 to 2.8 million tons discarded annually. Algeria, as one of the world's largest producers of dates, plays a key role in this industry [33].

A study in the Biskra region estimated that each date palm tree produces approximately 47.57 kg of residues per year, including fibers from leaves, rachis, petioles, and other parts. These fibers are comparable to jute, flax, ramie, hemp and sisal, which are widely used as reinforcements in construction materials [34].

The use of date palm fiber in construction materials is relatively new, but has great potential. Each tree can yield approximately 35 kg of raw palm fiber per year, with a lifespan of up to 100 years, contributing to an estimated annual fiber production of 4,200 tons. Research suggests that date palm fiber production significantly exceeds that of many other natural fibers, making it a promising material for sustainable construction.

2.11 The commonly used building insulation materials

Here is a brief overview of some of the most commonly used building insulation materials today, known for their relatively low thermal conductivity.

Mineral wool

Mineral wool includes both glass wool (fibreglass) and rock wool. These materials are usually made into mats or boards, although they're sometimes used as loose-fill insulation. The lighter, softer types are often used in timber-framed buildings and other structures with cavities. In contrast, denser and more rigid boards are used where the insulation needs to support weight, such as on floors or roofs. Mineral wool can also be used to fill gaps and cavities. Its thermal

conductivity depends on several factors, including temperature, moisture content and the density of the material [35].

Figure. 2.2. Mineral wool used as thermal insulating into building.

Expanded Polystyrene (EPS) and Extruded Polystyrene (XPS)

Expanded polystyrene (EPS) is made from small beads of polystyrene, a material derived from crude oil. These beads contain an expanding agent, such as pentane (C_6H_{12}), which causes them to expand when exposed to steam. As they expand, the beads fuse together at their points of contact. EPS is usually moulded into rigid sheets or produced continuously on a production line. It has a partially open cell structure. The typical thermal conductivity of EPS is in the range of 30 to 40 milliwatts per metre Kelvin [mW/(mK)]. The thermal performance of EPS can be affected by temperature, moisture content and density. EPS panels can be perforated, trimmed or shaped in the field without reducing their insulating properties.

Extruded polystyrene (XPS), on the other hand, is produced by melting polystyrene and injecting an expanding gas - such as HFCs, CO_2 or pentane (C_6H_{12}) - during the process. XPS has a closed cell structure and also offers thermal conductivity values typically between 30 and 40 mW/(m-K).

Figure. 2.3. Expanded polystyrene beads used to make clay bricks [36].

Cellulose

Cellulose insulation is made from recycled paper or wood fibers. Certain additives are included to enhance its performance and durability. It is commonly used as a loose-fill material to fill gaps and cavities in buildings, but it's also available in the form of boards and mats. The typical thermal conductivity of cellulose insulation ranges from 40 to 50 [mW/(mK)].

Figure. 2.4. Cellulose used as thermal insulating into building.

Vacuum insulation panels

Vacuum Insulation Panels (VIP) consist of a porous core, typically fumed silica, surrounded by multiple layers of metallised polymer laminate (see Figure 2). These panels provide excellent thermal insulation, with initial thermal conductivity values as low as 3 to 4 [mW/(m-K)] when new. Over time, however, air and water vapour can slowly penetrate through

the outer layers and into the open-pored core, leading to a gradual increase in thermal conductivity. After about 25 years, the thermal conductivity typically increases to about 8 mW/(m-K). Depending on the type of barrier used in the VIP envelope, the values may increase further after 50 or 100 years. This inevitable ageing effect is one of the main disadvantages of VIP.

2.12 Conclusion

Thermal insulation is a critical factor in improving the energy efficiency of buildings, helping to reduce the consumption of conventional energy sources and lowering carbon emissions, thereby promoting environmental sustainability. Insulation materials vary in their properties based on heat transfer mechanisms, so the selection of the right material depends on several factors such as density, porosity and thermal conductivity. The integration of phase change materials (PCMs) into thermal insulation systems can significantly improve indoor temperature stability, reducing the need for artificial heating and cooling

Chapter 3

Phase Change Materials (PCMs) – Fundamentals, Classification, and Building Integration Strategies

3.1 Introduction

This section of the chapter provides basic information for this research and provides a general understanding of the use of phase change materials (PCMs) in buildings. The main goals are to improve thermal comfort and reduce reliance on excessive heating and cooling systems, which in turn reduces energy consumption and improves overall energy efficiency.

The chapter focuses on several key aspects, including heat storage, an overview of PCMs, their characterization, encapsulation, and selection, and measurement techniques for thermal characterization. It also explores the concept of thermal comfort in buildings.

3.2 Thermal Storage in Buildings

Heat storage in buildings can be divided into two main techniques:

Sensible heat storage, where the temperature of the storage material changes in proportion to the amount of heat stored. Based on the storage medium, this technique is further divided into two categories: liquid-based storage and solid-based storage.

Latent heat storage, in which thermal energy is absorbed or released during a phase change of a material, such as solid-to-liquid or liquid-to-gas transitions. This method allows for efficient heat storage without significant temperature fluctuations.

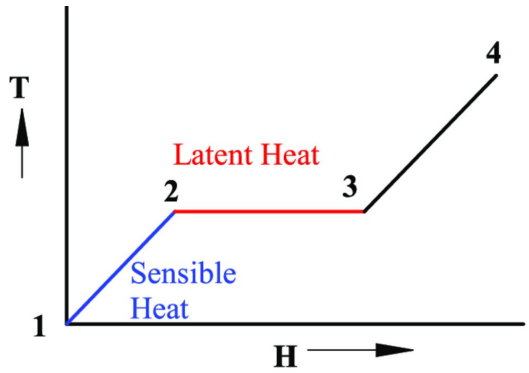

Figure 3.1. Evolution of the temperature of a pure homogeneous body with phase change.[37]

3.2.1 Sensible Heat Storage

Sensible heat storage refers to the accumulation of energy by heating or cooling a material without a phase change. This process occurs when the temperature of the material increases or decreases, storing or releasing heat accordingly. The amount of energy stored by this method depends on the enthalpy change resulting from the temperature changes in the material, which also takes into account its mass and specific heat capacity.

This storage method is cost effective and is one of the most technically advanced and widely used thermal storage technologies. Its main advantage is its high thermal capacity, which makes it particularly suitable for applications such as space heating and domestic hot water storage.

The amount of heat stored in a material using this method can be expressed mathematically as:

$$Q = \int_{T_1}^{T_1} m \cdot Cp \cdot dT \qquad (3.1)$$

Where :

- Q is the heat stored (Joules),
- m is the mass of the material (kg),
- C_p is the specific heat capacity (J/kg·K),
- T_1 and T_2 are the initial and final temperatures of the material (K).

3.3 Definition of phase change materials

Any material capable of absorbing, storing and releasing heat in the form of thermal energy can be a PCM. In PCMs, thermal energy is stored during the melting process and released during the solidification process [38]. These materials have a high energy storage density and the ability to maintain a constant temperature while absorbing heat during melting and releasing it during solidification. When the ambient temperature rises above the melting point of the PCMs, the chemical bonds in the PCMs begin to break down and the PCMs absorb heat in an endothermic (melting) process. When the ambient temperature falls below the melting point of the PCMs, they release the heat in a thermal process and return to a solid state. The properties of PCMs can therefore be used to maintain indoor comfort, particularly in buildings with low thermal mass [39]. The use of PCMs to improve the thermal energy performance of buildings has received increasing attention in recent years [40]. Due to the sun's rays and high temperatures during the day, heat waves penetrate the walls of buildings. The

PCM absorbs the excess heat through the melting process, delaying the heat wave inside the building. During the day, the ambient temperature remains comfortable and less energy is consumed. At night, when temperatures drop, the PCM releases the heat stored in the ambient air inside the building, as shown in Figure 3.2 [41]. Thermal storage in buildings can be divided into two main techniques: Sensible heat storage, where the temperature of the storage materials varies with the amount of heat stored. Latent heat storage, where thermal energy is stored or released when a body changes state (from solid to liquid).

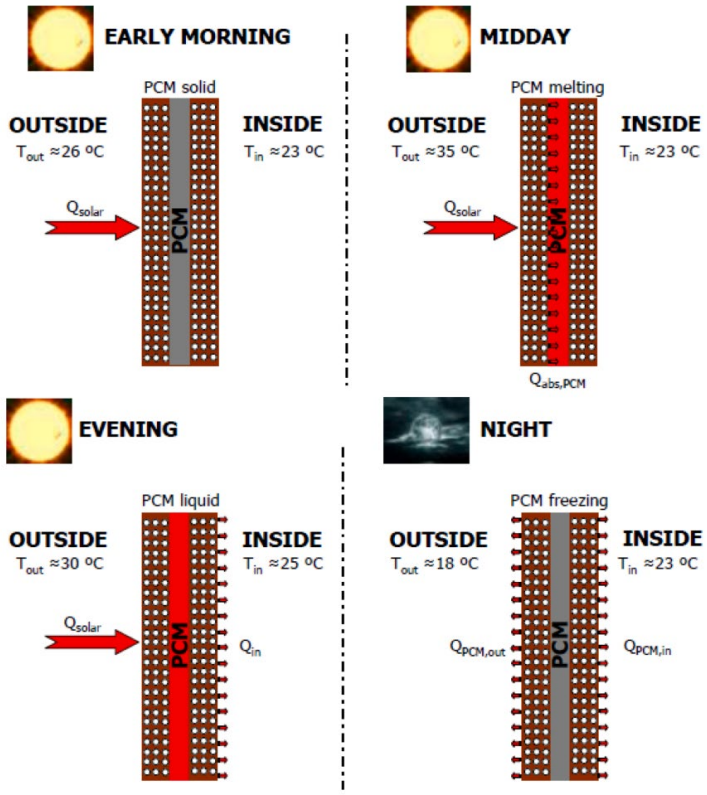

Figure 3.2. Schematic diagram of how the PCM works [41].

3.3.1 Latent heat energy storage in PCMs:

Latent heat storage (LHS) systems work by absorbing or releasing latent heat during a phase change, such as from solid to liquid or vice versa. Depending on the phase change process, latent heat storage can occur through solid-solid, solid-liquid, gas-solid, or liquid-gas transformations. Each of these options has its own advantages and disadvantages.

Of these, the solid-liquid phase change (melting and solidification) is particularly effective for storing large amounts of heat, provided an appropriate material is selected. During the melting process, as heat is absorbed by the storage material, its temperature remains constant at the

melting point, also known as the phase change temperature. Once the material has completely melted, any further heat transfer will result in sensible heat storage. The heat absorbed during melting is called latent heat and is calculated using the equation:

$$\Delta Q = m \times \Delta h \tag{3.2}$$

where:

- m is the mass of the phase change material (kg).
- Δh is the latent heat of fusion (J/kg).

3.4 Classification of PCM

Depending on their state, PCMs can be divided into three groups: solid-solid, solid-liquid and liquid-gas. Of these, solid-liquid PCMs are more suitable for thermal energy storage, while solid-liquid PCMs can be divided into organic, inorganic and eutectic compounds [42]. Several types of PCM are available on the market and can be used in buildings with a wide range of characteristics, which can be divided into three groups according to their components. As shown in Figure 3.3 [43].

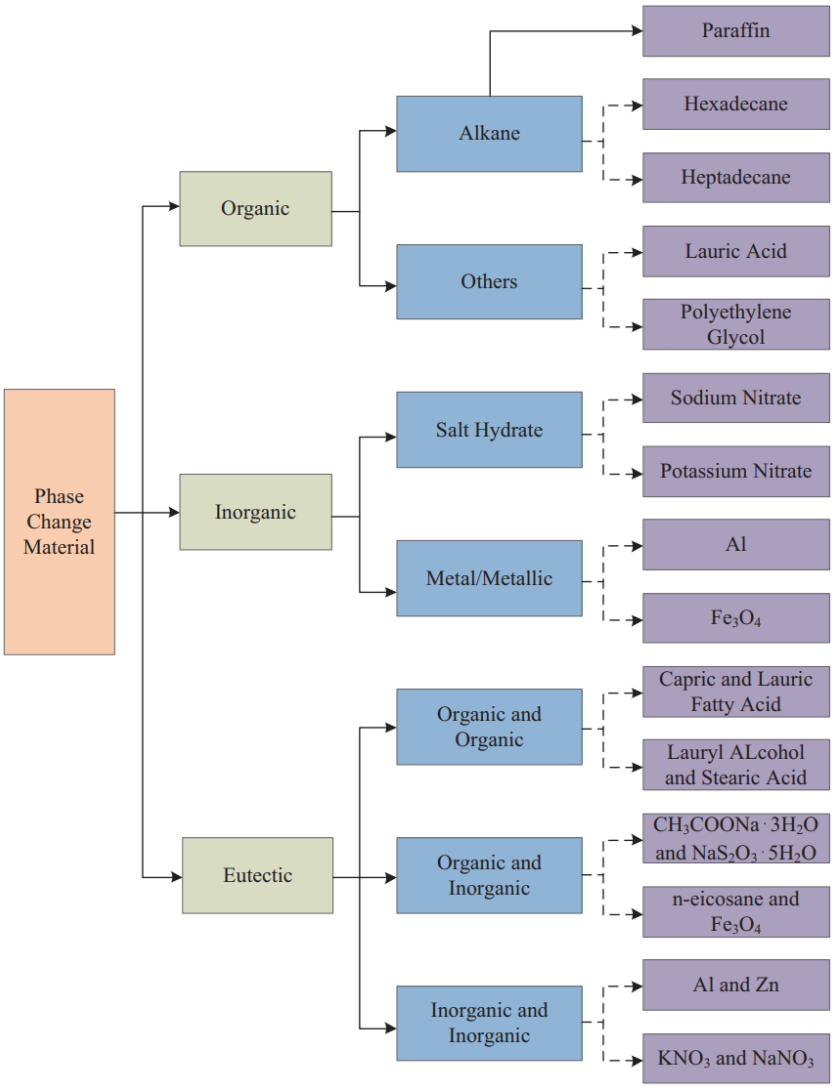

Figure 3.3. Classification of PCM [43].

3.4.1 Organic PCM

This type of PCM can be divided into paraffin and non-paraffin types. Its main advantages are that it is chemically and thermally stable, non-corrosive, recyclable and does not undercool. On the other hand, the disadvantages of using organic PCMs are their flammability, low thermal conductivity and low phase change enthalpy compared to other types of PCMs. The most commonly used types are paraffin and fatty acids [44]. In general, organic PCMs offer numerous advantages, including a wide operating temperature range, chemical stability, non-corrosive and non-toxic nature, minimal subcooling, no segregation, high latent heat of fusion, and a high nucleation rate. However, despite these benefits, organic PCMs have some significant drawbacks. These include low thermal conductivity, which slows the charging and discharging rates, supercooling effects during solidification cycles, and leakage from containers. Overcoming these challenges remains a priority in their application [38].

***Paraffin*:** This chemical is produced as a by-product of petroleum refineries and is composed of carbon and hydrogen atoms and is known by the general formula: CnH2n+2 as shown in Figure 3.4, where n is the number of carbon atoms (C). If the C is between 20 and 40, this material is called paraffin wax [44]. Paraffin has different empirical properties because it is a mixture of different alkanes [45]. Table 3.1 presents examples of paraffins along with their thermophysical properties [46].

Table 3.1. Thermo-physical properties of Paraffins

	Paraffins			
	Hexadecane	**Tetradecane**	**Eicosane**	**Octadecane**
Formula	$C_{16}H_{34}$	$C_{14}H_{30}$	$C_{20}H_{42}$	$C_{18}H_{38}$
Enthalpy of fusion [kJ/kg]	237	226	247	244
Melting temperature [°C]	16.7	5.5	36.7	28
Thermal conductivity [W/m.°C]	0.15	0.15	0.15	0.15
Specific heat capacity [kJ/kg. °C]	2.11	2.07	2.21	2.16
Solid density [kg/m3]	835	825	856	814

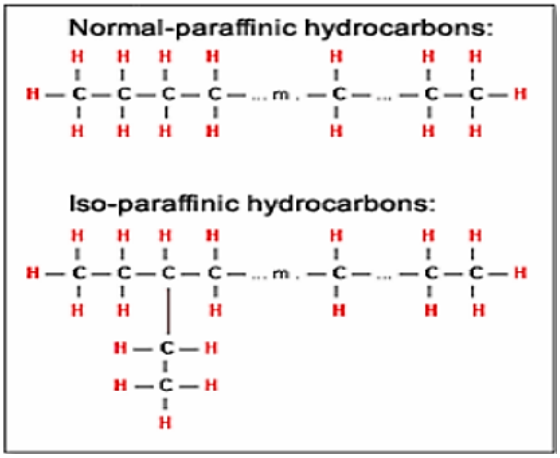

Figure 3.4. Chemical structure of paraffins

***Fatty Acids**:* It is a carboxylic acid with a long hydrocarbon chain of carbon atoms (from 10 to 30) and hydrogen atoms, with the general formula $CH_3(CH_2)2nCOOH$. Recently, fatty

acids have gained interest due to thermophysical properties such as high energy capacity, congruent melting and congruent melting, solidification behaviour and good chemical and thermal and thermal stability[47]. In addition, they are non-toxic, toxicity, no corrosivity, little or no undercooling, little volume change during phase and are easy to produce from vegetable and animal oils. Only a few of these fatty acids have a melting temperature in the range of thermal comfort (15 to 30 °C) [1]. As shown in table 3.2. However, the melting temperature of the PCMs can be adjusted to this climatic by preparing eutectic mixtures of fatty acids.

Table 3.2. Chemical formula and melting point of fatty acids [48].

PCM	Formula	Melting temperature (°C)
Capric acid	$C_{10}H_{20}O_2$	31.4
Lauric acid	$C_{12}H_{24}O_2$	43.8
Myristic acid	$C_{14}H_{28}O_2$	54.1
Palmitic acid	$C_{16}H_{32}O_2$	62.4
Stearic acid	$C_{18}H_{36}O_2$	69
Arachidic acid	$C_{20}H_{40}O_2$	75
Methyl palmitate	$C_{17}H_{34}O_2$	29
Methyl stearate	$C_{19}H_{38}O_2$	37.8
Methyl eicosanoate	$C_{21}H_{42}O_2$	46.3

3.4.2 Inorganic PCM

It is classified as hydrates, salts and minerals. It has a high latent heat storage capacity and is non-flammable. On the other hand, it has the problem of supercooling and significant volume changes [44].

3.4.3 Eutectic

They are easily produced by mixing organic/organic, inorganic/inorganic or inorganic/organic PCMs. They result from a light melt mixture of two or more components that are capable of melting and solidifying simultaneously during the melting and solidification process. However, it lacks physical thermal properties [49]. In recent years, extensive research has been carried out on eutectic mixtures of fatty acids and fatty alcohols [50]. Numerous studies have shown that the incorporation of phase change materials (PCMs) for latent heat

storage is a highly effective strategy for improving thermal capacity, energy efficiency and indoor comfort in buildings [51]. Binary mixtures of stearic acid (SA) and lauric acid (LA) are commonly used for PCMs with low eutectic temperatures. Their structures, morphologies and thermal properties have been extensively studied. Differential scanning calorimetry (DSC) analysis showed that under optimum conditions, the synthesised PCMs had melting and solidification temperatures of 27.9°C and 28.3°C, respectively, with latent heat values of 170 kJ/kg for melting and 155 kJ/kg for solidification [52].

Eutectic organic PCMs consist of two or more organic components that behave as a single substance and undergo uniform phase transitions. Their main advantage is that they can be tailored to achieve specific thermal properties. Some eutectic blends of fatty acids have higher melting points than individual PCMs, while retaining the favourable properties of organic materials. Consequently, these eutectic PCMs serve as innovative thermal energy storage solutions [53]. By adjusting the mixing ratios, it is possible to fine-tune the melting temperatures of these materials. High latent heat capacity, together with appropriate melting and solidification temperatures, are crucial factors in the development of efficient organic PCMs [54]. DSC analysis was used to evaluate the energy storage performance of a eutectic mixture of LA and 1-tetradecanol, revealing a phase transition temperature of 24°C and a fusion enthalpy of 161 kJ/kg. Accelerated thermal testing further demonstrated the excellent thermal stability and energy storage potential of the binary eutectic [55]. Fatty acids, including SA, capric acid (CA), LA, and palmitic acid (PA), were used to produce ternary eutectics with varying weight ratios. The thermal characteristics of these new PCMs were evaluated using DSC. The melting point ranged from 14 to 21°C, and the latent heat varied from 150 kJ/kg to 175 kJ/kg, rendering them useful for various low-temperature thermal energy storage applications [56]. Various binary and multiple eutectic mixtures of fatty acids were produced using five types of fatty acids: LA, CA, SA, PA, and MA. The melting points of the tested materials were observed to be in the range of 15 and 53°C [57]. The table 3.3 represent Advantages and Disadvantages of PCMO, PCMIO and PCME.

Table 3.3. Advantages and Disadvantages of PCMO, PCMIO and PCME [58].

PCM Type	Benefits	Disadvantages
	- No segregation - Non-reactive - Non-toxic	- Liquid leakage during melting

PCMO	- Low volume change - Compatible with conventional building materials - Low vapor pressure - Recyclable - Low price	- Low thermal conductivity (about 0.2 W/m.K) - Flammable
PCMI	- High volumetric latent heat storage capacity - Non-flammable - High thermal conductivity compared to PCMO	- supercooling problem - Segregation - Not melting congruently - High volume changes - Corrosive to metal - Phase separation on repeated phase change cycles
PCME	- Very small melting range - Properties can be customized to meet specific requirements	- High cost - Lack of data on thermophysical properties

3.5 Properties of PCMs

The key functions of PCMs vary from manufacturer to manufacturer. The economic, chemical, physical and thermal properties listed in Table 3.4 play a critical role in enabling PCMs to be used as efficient thermal storage systems [59].

Table 3.4. General characteristics of PCMs

Thermal properties - Suitable phase change temperature - High specific heat capacity - High latent heat during phase change - High thermal conductivity in liquid and solid phase	*Physical properties* - High density - Negligible subcooling effect - Low vapor pressure - Small volume variation - Sufficient crystallization rate
Chemical properties - Prolonged chemical stability	*Economic Properties* - Abundant

- Compatibility with container materials - Non-toxic, non-flammable and non-explosive - No phase separation	- Inexpensive

3.6 Commonly Used PCMs

Several PCMs and their properties related to their specific applications have been listed in many publications [42]. Table 3.5 showcases several commercially available PCMs designed for temperature ranges between 10°C and 118°C [60]

Table 3.5. Commercially available PCMs for the temperature range (10°C to 118°C)

Name	**Melting temperature (°C)**	**Density (KJ/kg)**	**Latent heat (KJ/kg)**	**Manufacturer**
E 21	21	1480	150	EPSLtd. (www.epsltd.co.uk)
E 13	13	1780	140	EPSLtd. (www.epsltd.co.uk)
C 32	32	1450	302	Climator (www.climator.com)
C 24	24	1480	216	Climator (www.climator.com)
A 22	22	770	220	EPS Ltd. (www.epsltd.co.uk)
S 27	27	1470	207	Cristopia (www.cristopia.com)
RT 20	22	870	172	Rubitherm (www.rubitherm.com)
RT 26	25	880	131	Rubitherm (www.rubitherm.com)
RT 42	43	880	174	Rubitherm (www.rubitherm.com)
STL 27	27	1090	213	Mitsubishi Chemical
STL 47	47	1341	221	Mitsubishi Chemical
TH 58	58	1290	226	TEAP (www.teappcm.com)
TH 25	29	1540	188	TEAP (www.teappcm.com)

3.7 Choice of PCM

The main factor determining the type and quantity of PCM is the weather, while the optimum location of PCM in the building envelope is close to the heat source, according to numerous studies [61]. Phase change materials are available in different types and properties,

but not all PCMs can be used in buildings. Table (3.6) shows the required properties of phase change materials that are commonly used and incorporated into buildings [58].

Table 3.6. *Selection criteria for PCM* [58].

Economic properties	Low cost. Availability
Kinetic properties	High nucleation rate, no supercooling, no overheating, high crystal growth rate.
Chemical properties	Chemical stability, No degradation, Non-corrosive, Full reversible cycle, Non-toxic, No degradation.
Thermodynamic properties	Suitable melting temperature, High latent heat, High specific heat, High density, Thermal conductivity.

The selection of phase change materials (PCMs) for effective use as thermal energy storage materials is based on many criteria [48],[62]:

3.7.1 Thermodynamic properties:

Transition temperatures within the desired range: The phase change temperature of the PCM should fall within the required temperature range for the target application. For thermal comfort applications, this range is typically between 25°C and 40°C, which is suitable for regions in southern Algeria [63].

- The PCM should have a high latent heat of fusion per unit volume to store a significant amount of energy.
- High density is essential so that the material takes up less space.
- It should also have a high specific heat capacity to allow effective storage of sensible thermal energy.
- Good thermal conductivity is critical for efficient heat absorption and release, even with small temperature changes.
- The PCM must melt and solidify completely and uniformly to ensure that both phases remain homogeneous. This is essential to prevent density differences between the solid and liquid states that could cause material segregation and change its chemical composition.

3.7.2 Chemical properties:

a) The PCM should be able to melt completely and freeze repeatedly without problems.

b) It must remain chemically stable under all conditions.

c) The material must be able to withstand many cycles of melting and freezing without degrading, ensuring a long service life.

d) It must not cause corrosion or damage to building materials.

e) The PCM must be safe to use, i.e. non-toxic, non-flammable and non-explosive.

Table 3.7 shows the physical and thermal properties of PCMs that have recently been used by researchers in many countries around the world.

Table 3.7. Brief comparative analysis of the various (experimental) studies examined in several countries.

Year	Country	PCM	Melting Temperature (°C)	Thermal conductivity (W/k.m)	Density (kg/m3)	Cp [J/(kg·K)] Solid	Cp (J/kg·K) liquid	Latent heat (kJ/kg)	REF
2023	Iraq	Paraffin wax	40–44	0.21	930	2100	2100	190	[64]
2022	Malaysia	EnFinit 35	32–35	0.08	400	1000	3200	180	[65]
2022	China	PCM	18-26	0.25	1300	1785	1785	216	[66]
2022	Mexico	Infinite R29	29	0.54	1433.58	3140	3140	200	[67]
2021	India	OM 30	23-32	0.16	950	2040	2780	230	[68]
2021	China	Paraffin wax	18	0.2	880	4810	3110	236	[69]
2021	Iraq	Paraffin wax	44	0.21	930	2100	2100	190	[70]
2021	Iraq	Paraffin wax	38-43	0.2	880	2000	2000	174	[71]
2020	China	Paraffin wax	26-28	0.36	850	2150	2300	231.2	[72]
2020	India	OM 35	35	0.16	900	2310	2710	160	[73]
2020	India	Eicosane	36-38	0.15	815	1920	2460	247.3	[73]
2020	India	OM 37	35-40	0.16	960	2141.8	2180.8	218	[74]

2018	Tehran	RT35	33-38	0.2	815	2000	2000	160	[75]
2017	Italy	RT28	28	0.14	800	2000	2000	250	[76]

3.8 Thermal characterization measurement techniques

The performance of a thermal energy storage system is directly related to the phase change properties of the PCM (phase change material). These properties are typically provided by the manufacturer, but can sometimes be inaccurate, unreliable, or overly optimistic [77]. Therefore, it is essential to perform measurements to obtain accurate phase change properties of the PCM. Before being used in real applications, the thermal performance of PCMs incorporated into building materials must be tested. This ensures their suitability, evaluates the actual benefits of the building system, and assesses the dynamic thermal properties of the composites and their effectiveness in reducing indoor temperature variations in buildings. Several measurement techniques are available to determine latent heat, melting temperature, and specific heat, including differential scanning calorimetry (DSC) and differential thermal analysis (DTA). Accurate knowledge of thermal conductivity is another critical thermal parameter needed for proper design of latent heat storage systems or accurate simulation of dynamic models with PCMs. During a DSC (Differential Scanning Calorimetry) test, the sample and a reference material with known thermal properties are kept at the same temperature throughout the experiment. By measuring the difference in heat supplied to the sample and the reference, various thermal properties of the sample can be determined, such as the heat of fusion, heat capacity, and melting/solidification temperatures. In a Differential Thermal Analysis (DTA) test, the same amount of heat is applied to both the sample and the reference (unlike in a DSC test, where the temperature is kept constant). Phase changes and other thermal properties can then be analyzed by observing the temperature difference between the sample and the reference.

3.9 Integrating PCM into the building envelope

The three most promising methods for incorporating PCM into conventional building materials were direct incorporation, immersion and encapsulation [78]. Incorporating PCMs into building envelopes is an effective technology for improving thermal performance in different climates, reducing energy consumption and reducing carbon dioxide emissions. It is necessary to know the appropriate technology for each climate (type of PCM, method of integration) and therefore the appropriate method for each climate. This choice depends on a number of factors such as climate, location and building type. It is advisable to study and

simulate the feasibility of this technology throughout the four seasons with simulation programmes (TRNSYS or ANSYS or COMSOL ...etc.) and it is recommended to use more than one type of PCM in areas with weather variations [26].

3.9.1 Direct incorporation:

A cost-effective method where PCM is mixed directly into building materials such as cement, concrete and wallboard during production [79]. However, it has certain disadvantages, it reduces the bond strength between the aggregate and the binder paste, affects the hydration process and reduces the mechanical properties and durability [80]. Figure 3.5 illustrates the production process of an advanced concrete-based PCM.

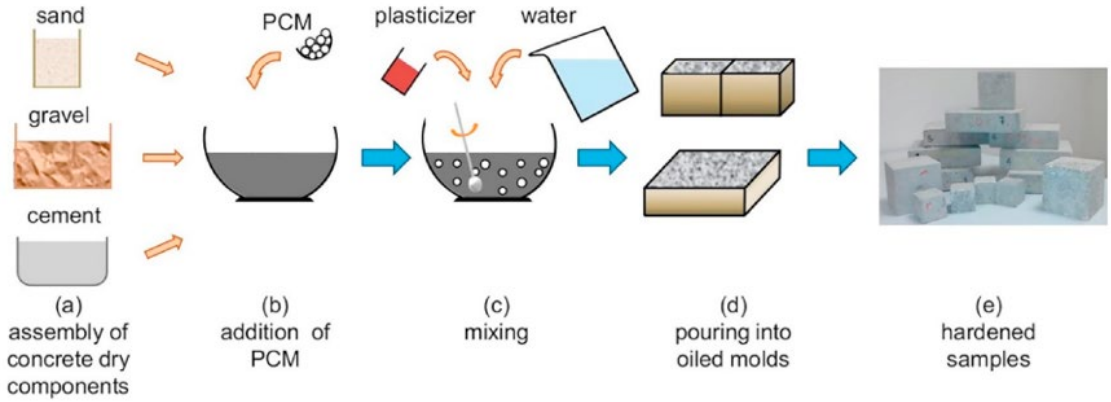

Figure 3.5. The production process of an advanced concrete-based PCM.

3.9.2 Immersion:

In this technique, plaster, concrete or bricks (components of the building structure in general) are immersed in the molten PCMs. Thanks to capillary action, the building materials absorb the PCMs into their internal pores [24]. These two methods of incorporating PCM directly into the building material suffered from a number of critical drawbacks [81].

3.9.3 Encapsulation of PCMs:

Most PCMs designed for building applications are solid and therefore pass through the liquid phase, at which point encapsulation is required to avoid certain problems such as PCM leakage to the surface and liquid diffusion [82]. PCM must be encapsulated before it can be used in components. In general, there are two methods of PCM packaging, macro-encapsulation and micro-encapsulation [83].

a. Microencapsulation of PCM: Microcapsules are particles containing a core material surrounded by a layer or shell, with a diameter of 1 to 1000 µm. This process is used in

construction and is widely used in commercial applications including textiles, adhesives and pharmaceuticals [84]. The shell material must be compatible with the environment and the PCM, as it plays an essential role in improving the thermal performance of the PCM. The majority of materials suitable for microcapsule manufacture are made from synthetic and natural polymers [44]. Figure 3.6 shows the production method Micro encapsulation of PCMs.

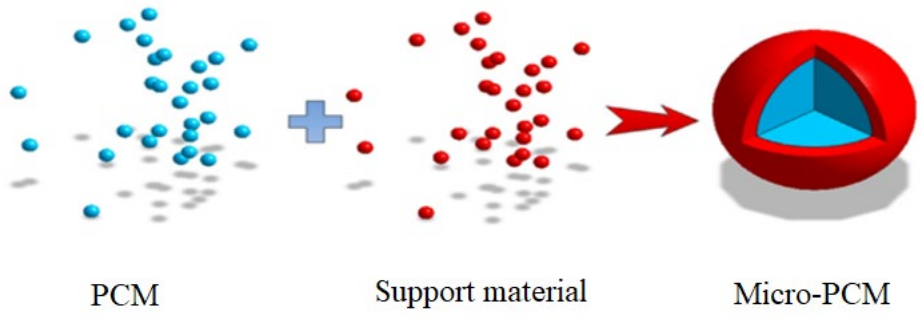

Figure 3.6. Shows the production method Micro-encapsulation of PCMs [85].

b. Macro-encapsulation of PCM: Macro-encapsulation is the best known method of encapsulating PCMs in specific forms of packaging such as tubes, bags, spheres, plates or other containers of various sizes and shapes, generally with a diameter greater than 1 mm [86] . Total encapsulation is the most commonly used technology in buildings due to its low manufacturing cost. However, this technology suffers from a low heat transfer rate [87]. Figure 3.7 summarises the common forms of macro-encapsulation used in building envelopes.

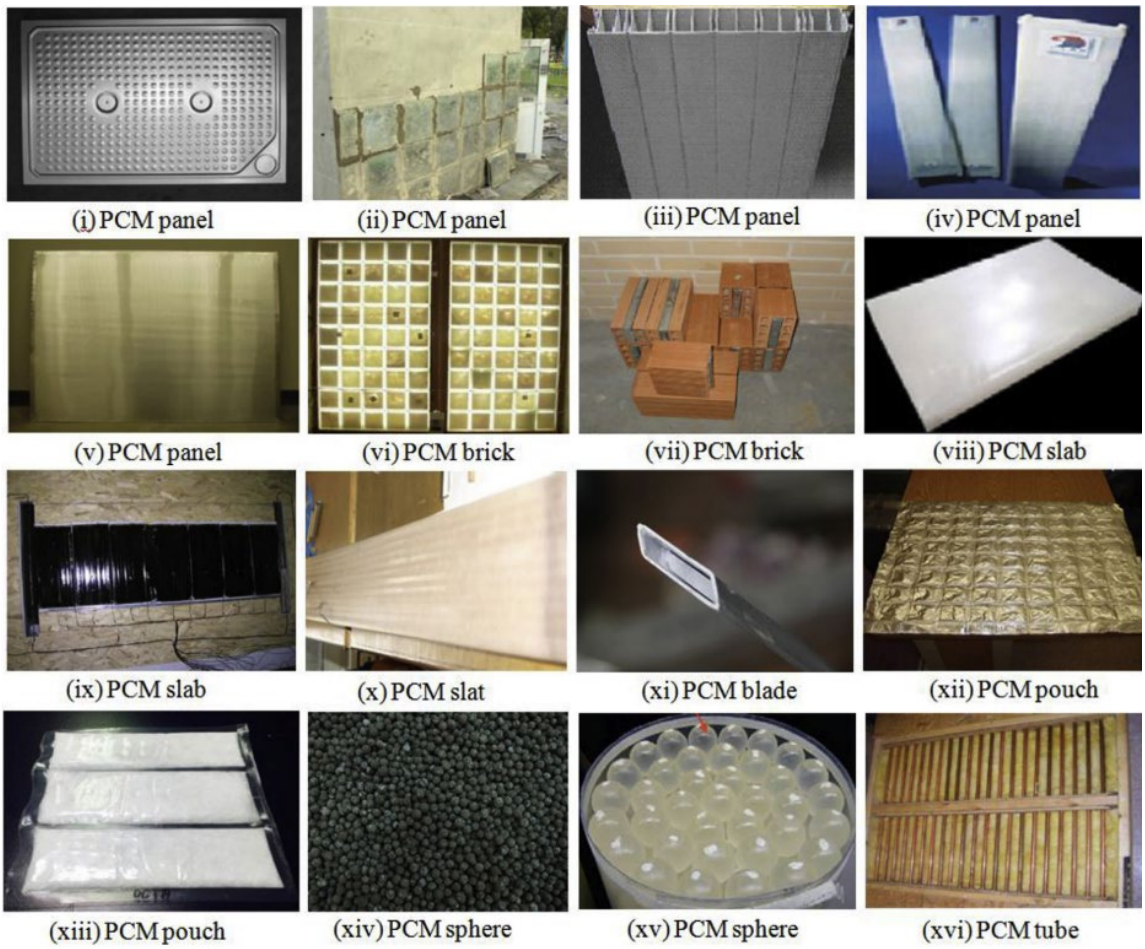

Figure 3.7. Common forms of macro-encapsulation used in building envelopes [88].

Micro-encapsulation and macro-encapsulation have the advantages and disadvantages shown in the table 3.8.

Table 3.8. Advantages and disadvantages of microencapsulation and macroencapsulation [80].

	Microencapsulation	**Macroencapsulation**
Benefits	- Prevents leakage of PCM during phase transition by creating a barrier that enhances its incorporation into various building materials. - Ensures high heat transfer due to increased surface area per unit volume.	- Easier to handle. - Can be designed to suit specific applications. - Improves PCM's compatibility with the environment by acting as a barrier. - Reduces external volume changes of the capsule, which is important for building applications.

	- Resists volume changes during phase transitions. - Improves chemical stability.	
Disadvantages	- The rigidity of the capsule prevents natural convection and therefore reduces the rate of heat transfer. -Microencapsulation can affect the mechanical properties of building materials. - Investment costs for microencapsulation are high.	- Poor thermal conductivity. - Must be protected from destruction (drilling holes or nails into walls) when the building is in use. - More work on site to integrate into the building structure.

3.10 Influence of PCMs on the thermal behaviour of the building envelope

The use of phase change materials (PCM) in the building sector aims to increase the thermal inertia of buildings and reduce the energy consumption associated with heating and cooling systems that maintain indoor comfort conditions. This approach enhances the thermal storage capacity of various building envelope configurations by integrating PCMs. These materials are particularly effective due to their ability to exchange significant amounts of heat isothermally through phase change. By harnessing latent heat storage, they provide thermal insulation for buildings, helping to mitigate the effects of outdoor temperature fluctuations.

The main role of the building envelope is to provide effective thermal resistance so that external heat waves do not easily propagate into the interior. This role is enhanced by the incorporation of phase change materials. Numerous studies have been carried out on this subject. The use of PCM in buildings has many advantages: PCM reduces energy consumption, reduces the need for cooling energy, reduces temperature fluctuations [89]. The first PCM house was built in 1947 by Dr. Maria Telkes in Dover, Massachusetts, USA. Since the 1980s, numerous studies have been carried out on the use of phase change materials (PCMs) in buildings. These studies have led to the development and integration of PCMs into building envelopes [41]. In this section, an overview of the uses of PCMs in buildings will be presented, first experimentally and then numerically.

To study the evaluation of the internal thermal behaviour of the building fitted with macro PCM capsules in an outdoor tropical environment and to determine the reduction in the cooling

load. Two identical cabins measuring 1.12 m 1.12 m 1.12 m were erected in concrete and cement mortar. To ensure that stored heat could be removed during the night, the cells were fitted with a window (0.15 m 0.15 m) and a door (0.15 m 0.46 m), as shown in Fig 3.8.

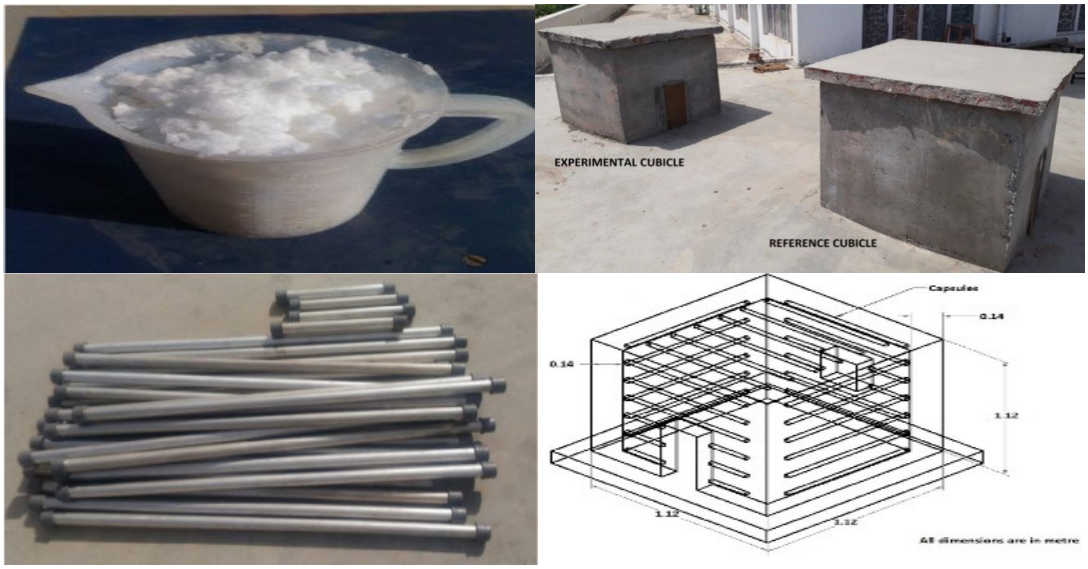

Figure 3.8. Steps for installing PCM in pipes and then in the building envelope [74].

The cabins were prepared using building materials that are commonly used in the construction of residential and commercial buildings in India, such as cement, concrete, river sand, etc. ..... One cabin is made of concrete only, while the other cabin has an encapsulated macro PCM embedded in the walls and roofs (the incorporation of the PCM with the building materials had good results as shown in Figure 3.9).

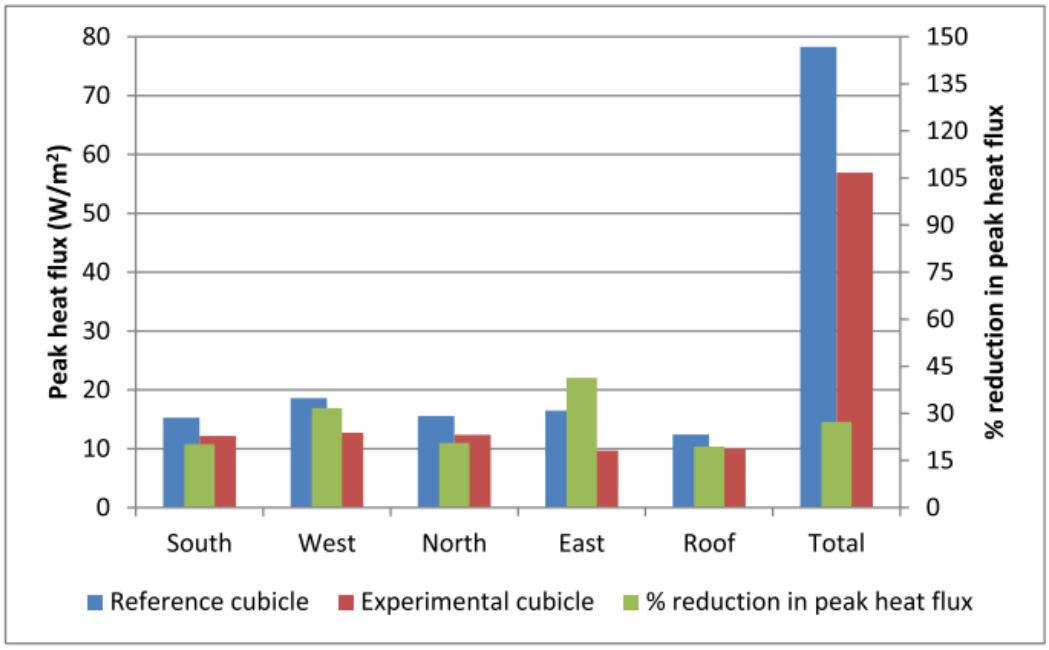

Figure 3.9. Maximum heat flux and corresponding percentage reduction of the two cells.

The building structure with PCM shows a reduction in peak temperature ranging from 3.8°Cto 5.8°Cwith a reduction in indoor temperature compared to the building structure without PCM. The integration of PCM into the concrete structure results in an average annual cost saving of 0.34$/day, cost savings on the electricity bill [74].

To assess the real effect of PCM capsules embedded in hollow brick cavities, two identical chambers were built to test two walls with and without PCM. The PCM was encapsulated in small identical tubes and inserted into the cavities in the rows of hollow bricks in one wall. The results showed that encapsulating the PCM in the wall reduced the temperature inside the chamber by approximately 4.7°C, reduced the temperature fluctuation by 23.84% and increased the time delay by 2 hours [71]. In order to improve the internal temperature of the buildings, two chambers were built in warm climatic conditions in Iraq (latitude: 31.84 and longitude: 47.14), paraffin wax was used as the phase change material as its melting temperature varies from (40 to44) °C. In which the phase change materials were encapsulated by the macro encapsulation method, then the PCMs were combined in the first chamber (the second chamber without PCMs), the completion steps are shown in Figure 3.10.

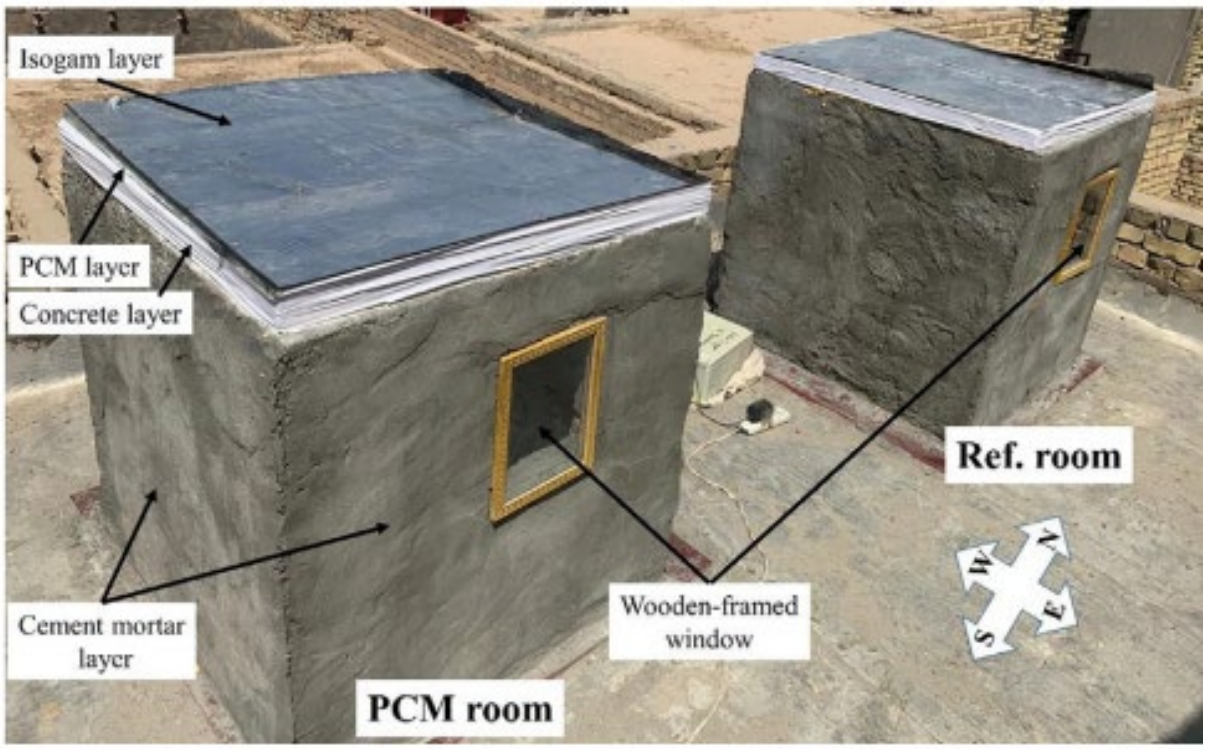

Figure 3.10. Building structure developed with PCM and without PCM [64].

Tested for three consecutive days in unventilated conditions (windows completely closed). The indoor temperature was reduced by 2 degrees Celsius, equivalent to a reduction in convection of approximately 8.71%. As a result, 80.64 Iraqi dinars/day were saved [64]. Under summer climatic conditions in Italy, experimental and numerical analyses have been carried out on a roof surface divided into three parts: the first part contains (PCM), the second part contains a different type of (PCM), i.e. with a different melting temperature, while the third part is without (PCM). Continuous monitoring is carried out to assess the thermal performance of each part. The results showed a reduction in the maximum thermal load of between 13% and 59% for each type of PCM [76].

Kong et al [90] developed a shape-stabilized composite PCM wallboard (CPCMW) made of paraffin and expanded perlite, which was installed on the interior walls and ceiling of a test room. To assess its impact on the thermal performance of the building, they compared the indoor temperature variations between two rooms - one with CPCMW and one without - under summer conditions in Tianjin. The results showed that the incorporation of CPCMW helped to passively regulate the indoor temperature and increased the thermal mass of the building envelope.

Figure 3.11. Composite PCM wall panel and the experimental room [90].

Kong et al [91] presented an innovative hybrid PCM wall design for winter heating. This hybrid PCM wall panel integrates a solar thermal system with a shape-stabilised PCM panel (Figure 3.12). To evaluate its performance, two test rooms (1.7 m × 1.7 m × 2 m) were constructed - one with the hybrid system and one without. Three experimental tests were carried out, measuring indoor air temperature and daily energy consumption. The results showed that incorporating this system into the building walls significantly improved thermal comfort and reduced daily energy consumption by around 44% compared to a conventional building without PCM. Although the system showed promising results, further techno-economic analysis is required.

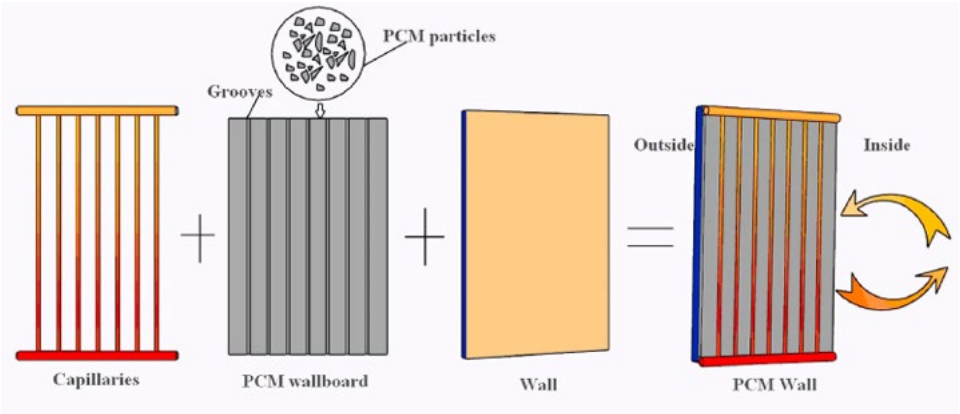

Figure 3.12. Hybrid PCM wall [91].

More recently, Cabeza et al [92] investigated the long-term thermal performance of a test cell with PCM-integrated walls, a decade after its construction. They compared its performance with a reference test cell without PCM under summer conditions. The results were also compared with data recorded in the summer of 2005, which showed a similar thermal

response. This study confirmed that PCM integrated into building walls maintains its effectiveness over time without degradation and continues to reduce indoor temperature variations even after 10 years.

The PCM wall panel is seen as an efficient and cost-effective alternative to traditional thermal mass for storing solar heat in buildings. In this system, the PCM is embedded in materials such as plasterboard, gypsum or other substrates. The thermal properties of the PCM wall panel are very similar to those of pure PCM and, due to the diffusion process, a higher concentration of PCM tends to accumulate in the outer third of the panel thickness near each surface. Kuznik et al (2011) used DuPont de Nemours PCM wall panels in the renovation of a commercial building and found them to be highly effective, especially when outdoor temperatures fluctuated around the melting point of the PCM [93].

As part of a European Union project, Cabeza et al. (2007) carried out experimental research to analyse the main effects of microencapsulated PCMs mixed with cement. Their aim was to evaluate the thermal performance of a small test cabin (Figure 14) in a Mediterranean climate and to develop a material capable of significantly reducing energy consumption in buildings. For this study, they used a commercial PCM from MicronalPCM (BASF) with a phase change temperature of 26°C and a phase change enthalpy of 110 kJ/kg. Compared to a conventional wall, the results showed that the PCM-concrete mix provided better thermal inertia, resulting in more stable indoor temperatures by reducing fluctuations [94].

Figure 3.13. Experimental cabin (dimensions: 2.4 m × 2.4 m × 2.4 m)[94].

Castell et al (2010) carried out studies on the integration of PCMs in brick constructions. To analyse the impact of PCMs, they built five test cabins with different construction materials and envelope types. Three of these cabins were made of perforated bricks, while the other two

were made of cellular bricks. The PCM RT-27 was applied to the perforated bricks, while SP-25 A8 was used with the cellular bricks [95]. The tests were divided into two categories: one involved free temperature variation without any cooling system, while the other was conducted in a controlled environment with a cooling system to maintain a constant indoor temperature of 24°C. The results were similar to those obtained by Cabeza et al. (2007), confirming the thermal benefits of integrating PCMs into brick structures.

An experimental and numerical evaluation of the effect of incorporating a PCM layer into the square holes of an external red brick wall has already been discussed by Necib et al. (2013). The model was tested under the climatic conditions of Ouargla, Algeria, making this study an important reference for those interested in PCM applications in arid regions. The numerical model was successfully validated by experimental results. The results showed that PCMs can significantly increase the thermal inertia of bricks, and that the reduction in heat gain through the wall is strongly influenced by both the amount of PCM used and its placement within the holes [96].

PCMs are incorporated into the plaster either by microencapsulation, immersion or direct addition during manufacture. Most studies evaluating the passive performance of plasterboard use a comparative approach, typically analysing one panel with PCM and one without (Figure 3.14) [97].

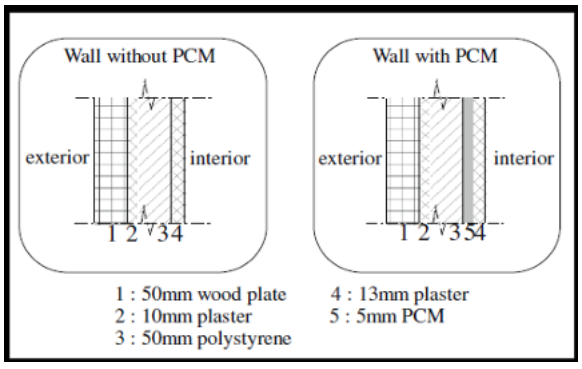

Figure 3.14. Plasterboards with and without PCMs

The main objective of incorporating PCMs into concrete materials is to improve heat storage in heavy building materials [98]. Direct incorporation of PCMs into concrete has shown promising results, mainly due to reduced thermal conductivity and increased thermal mass at certain temperatures. However, PCM-enhanced concrete also exhibits some undesirable

properties, such as reduced mechanical strength, uncertain long-term stability and reduced fire resistance [99]. Several studies on PCM concrete have shown positive effects, particularly in reducing indoor temperatures in hot climates.

Four test cells were built at PUGVERD LLEIDA, Spain, to evaluate the impact of PCMs on thermal performance in a continental climate with significant temperature variations. The study included a hollow brick reference cell, a polyurethane insulated cell and two PCM enhanced cells using RT27 paraffin and SP25 A8 salt hydrate (Figure 16) [100].

Two experimental setups were carried out: one with free temperature variation and one with controlled temperature using a heat pump set at 24°C. In the free temperature setup, the PCM cells showed a temperature reduction of 1°C and more stable conditions, especially in the alveolar brick cell due to higher thermal resistance. However, there were problems with night-time solidification due to the lack of ventilation. In the controlled temperature setup, energy consumption was significantly lower in the PCM cells. The RT27 + PU cell reduced energy consumption by 15% compared to the PU-insulated cell, while the SP25 A8 + alveolar brick cell achieved a 17% reduction compared to the reference. The study highlighted the need for appropriate cooling strategies to improve PCM performance.

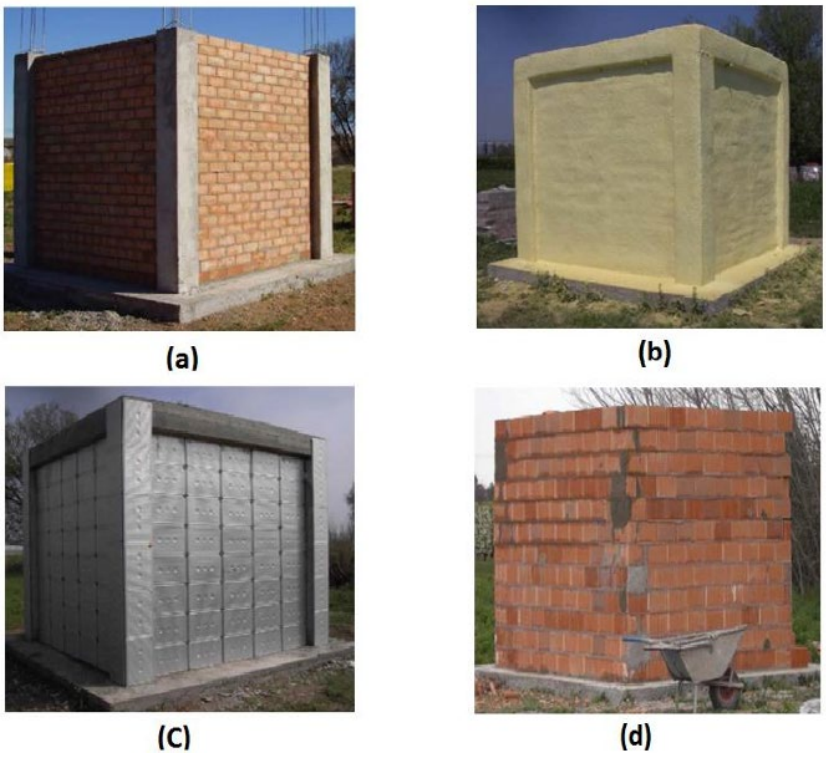

Figure 3.15. four test cells

Gowreesunker and Tassou [101] conducted an experimental study of the thermal performance of PCM wall panels during the summer months. Their results showed that the maximum indoor temperature could be reduced by up to 3°C compared to conventional plasterboard, effectively minimising overheating in summer.

Izquierdo-Barrientos et al [102] carried out a numerical analysis of the transient heat transfer in an external building wall containing a PCM layer over two separate periods (six days in summer and six days in winter). They investigated the effects of phase transition temperature, PCM layer position and wall orientation to identify optimal parameters for reducing energy fluctuations. Their results showed that there is no single optimal transition temperature that minimises heat loads, as it varies between 5°C and 35°C depending on the season, wall orientation and PCM placement. In addition, the study found that PCM layers had little effect on reducing total heat loss in winter, regardless of wall orientation or transition temperature. In summer, however, significant differences in heat gain were observed due to high solar radiation. The high thermal inertia of the wall meant that the PCM layer increased the heat load during the day and reduced it at night.

Numerical modelling and simulation of PCM-integrated building walls (PCMIWB) has become increasingly important for system design and optimisation over the last decade. Two widely used methods for modelling the phase change process in PCMIWB are the effective heat capacity method and the enthalpy method [103]. Most numerical studies use commercial software such as EnergyPlus [104], TRNSYS[105], MATLAB/Simulink [106], COMSOL [107], [108],[109]. and ANSYS Fluent to solve the energy governing equations and simulate the thermal behaviour under varying weather conditions. These studies primarily focus on the effects of PCM integration into walls, its placement, thermophysical properties (such as melting temperature and thermal conductivity), and its thickness. This section provides an overview of key numerical studies on PCMIWB, highlighting prominent research in this area.

Li et al [110] conducted a numerical study of the thermal performance of PCMIWB in the Isfahan (Iran) climate, analysing thirteen different PCMs in three wall designs. They investigated the effects of PCM position, thickness and melting temperature. While PCM selection is typically based on melting temperature, their results suggest that thermal conductivity should be prioritised instead. A PCM with a lower thermal conductivity can better reduce heat transfer into the interior, resulting in lower energy consumption. If two PCMs have similar conductivities, the melting temperature should be closer to the indoor temperature. In

terms of PCM placement, the study recommends that PCMs should be placed closer to the exterior wall to improve thermal performance in the Isfahan climate.

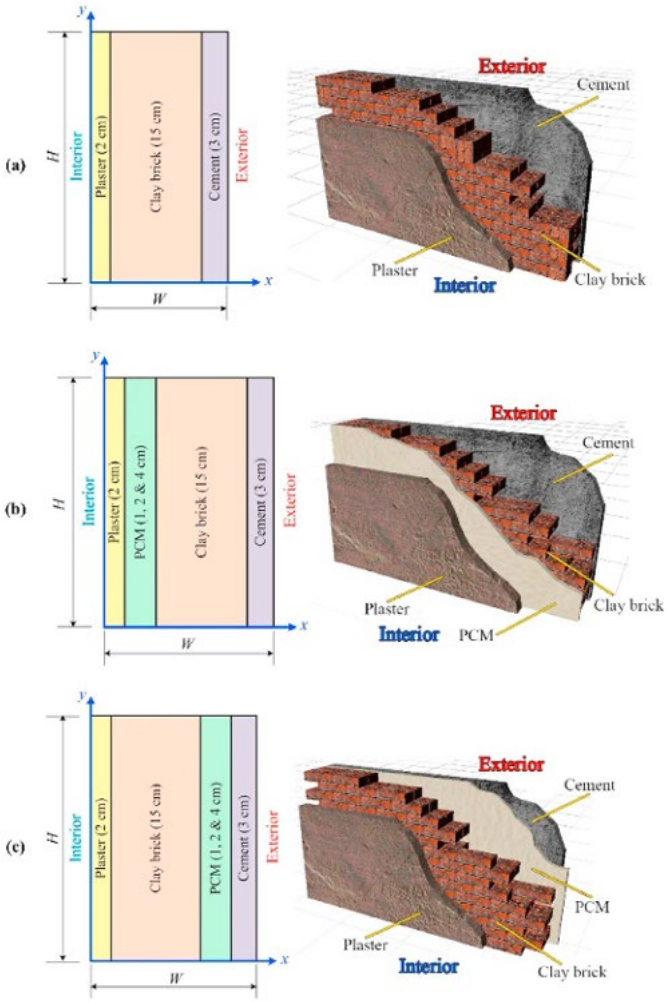

Figure 3.16. Studied wall configurations [110].

Arıcı et al [111] conducted a numerical study of PCMIWB to analyse the effect of design and operational parameters on thermal performance. They modelled the heat transfer within the PCM and wall components using the unidirectional conduction transfer equation. Their optimisation study, carried out for three cities in Turkey, investigated PCM position, thickness and melting temperature. The results showed that the optimal PCM placement depends on the climate and building location. In heating conditions, they recommended placing the PCM close to the outside, while in cooling conditions, placing it closer to the inside proved more effective.

Wang et al [112] conducted a parametric study of PCMIWB to evaluate its effectiveness in reducing heating loads in the Shanghai climate. They used a two-dimensional heat equation to simulate heat transfer in a wall with a PCM layer and concrete. Their results showed that

adding PCM to the wall helps reduce surface temperatures and slows down heat transfer, especially in summer. For optimal performance in this season, they determined that the ideal thickness for RT-42 PCM is about 20 mm, with the best placement on the outside of the wall.

Jiang et al [113] have developed a simplified analytical model to determine the optimum phase transition temperature and latent heat of a PCM integrated into the interior surfaces of walls. Their model is based on key factors such as the lower limit of the comfort temperature range, ventilation rate, building envelope characteristics and outdoor temperature. Their numerical results showed that the optimal PCM melting temperatures in different climatic regions in China are relatively similar, typically exceeding the lower limit of the comfort temperature range by about 1.1 to 3.3°C.

Erlbeck et al [114] carried out a detailed study to determine the optimal thermal performance of PCM integrated into concrete blocks. They analysed different PCM container shapes, including plate-shaped, cuboidal, cylindrical and spherical shapes, positioned in different orientations (Figure 20). The results showed that the thin plate-shaped PCM container was the most effective design, as it provided superior heat transfer during both melting and solidification, regardless of its placement or orientation.

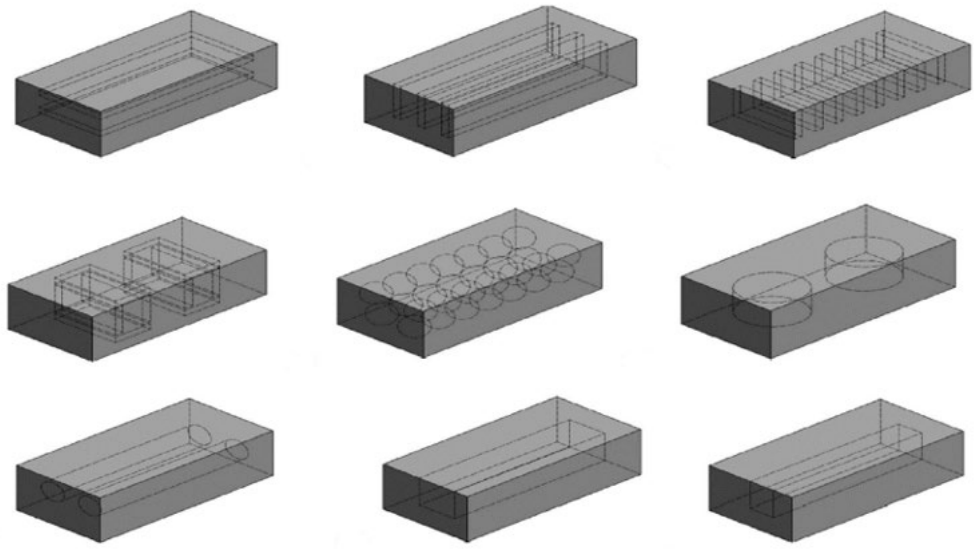

Figure 3.17. Possible designs for PCM enclosures integrated into concrete blocks [114].

Tunçbilek et al [115] conducted a numerical study to evaluate the seasonal and annual performance of bricks with PCM, focusing on energy savings from latent heat storage for heating and cooling in Marmara, Turkey. They analysed different brick models with PCM-filled voids (Figure 3.18), considering factors such as PCM position, melting temperature and

quantity, and compared them with traditional air-filled void bricks. The results showed that model D, with the PCM placed close to the inside, provided the highest energy savings. The optimal melting temperature varied by season, ranging from 18°C to 26°C, while an annual analysis identified 18°C as the ideal temperature, resulting in a 17.6% reduction in heat demand. The study highlighted that PCM integration improved thermal performance more in winter than in summer. In addition, careful selection of the PCM melting temperature is critical to avoid overheating, which could significantly increase cooling loads.

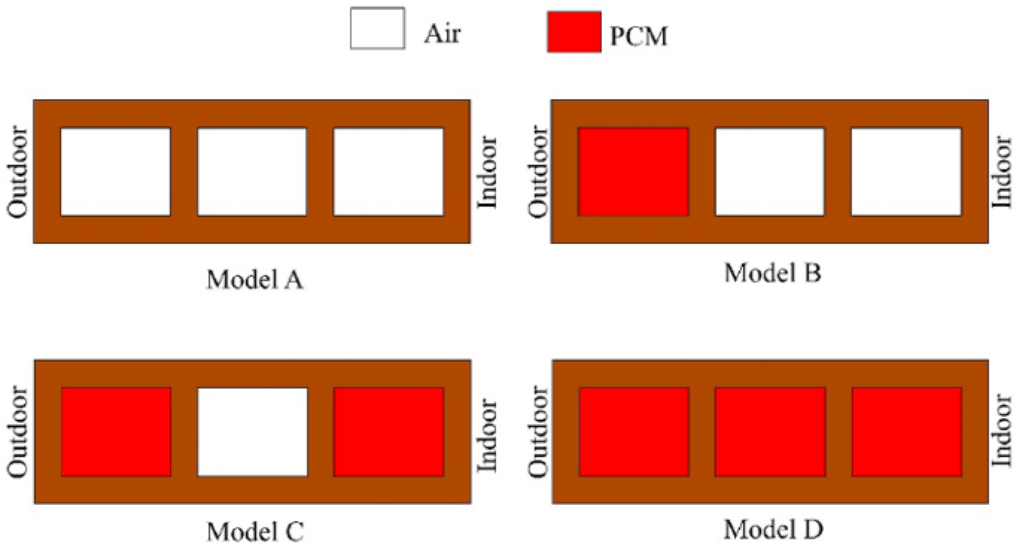

Figure 3.18. Suggested brick designs [115].

Bricks are the most widely used building material in many countries. It has many advantages, including ease of manufacture and low cost. However, traditional bricks have poor thermal performance, resulting in an uncomfortable indoor thermal environment. It is therefore necessary to improve the thermal performance of these bricks. An effective technique for improving the thermal performance of bricks is to increase their heat storage capacity by incorporating PCMs. A numerical heat transfer analysis of hollow bricks containing PCM has been carried out, as shown in Figure 3.19.

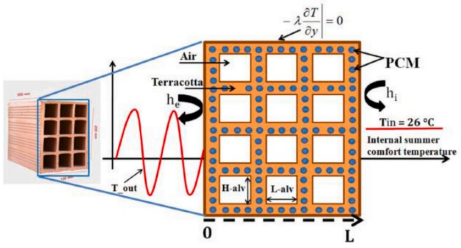

Figure 3.19. Distribution of PCM in hollow bricks used in construction [116].

The results indicate that the incorporation of PCM in bricks improves the thermal energy storage capacity, thus improving the thermal comfort due to the incorporation of PCM [116].

3.11 **Conclusion**

This chapter has provided an overview of thermal energy storage in buildings, highlighting the advantages of latent heat storage using phase change materials (PCMs). The discussion covered different types of PCMs, their integration into building materials, factors affecting storage efficiency, techniques for measuring thermal properties, and the impact on thermal comfort. The reviewed studies confirm that PCMs have significant potential to improve energy efficiency and indoor comfort by reducing reliance on heating and cooling systems. Their integration into building envelopes represents a promising approach to improving thermal performance and sustainability in construction.

Chapter 4

Development and Characterization of a Bio-Based PCM Eutectic Mixture for Clay Brick Enhancement

4.1 Introduction

The phase change materials (PCM) sector is largely dominated by paraffins and hydrated salts, with paraffins recently gaining more popularity than hydrated salts. However, bio-based compounds are starting to reshape the market, especially in the construction industry. Despite the advantages of paraffinic PCMs, they come with high costs and flammability concerns. Additionally, their reliance on crude oil makes their prices vulnerable to seasonal changes and geopolitical factors, creating challenges for manufacturers. As a result, research is needed to develop alternative, non-petroleum-based PCMs, particularly bio-based options. These bio-based PCMs are especially promising, as they come from renewable and environmentally friendly sources.

Currently, bio-based phase change materials (PCMs) are the focus of extensive research, especially those derived from natural sources due to their renewable nature and fully eco-friendly properties [48]. Many innovative studies have been conducted to develop smart, sustainable materials for energy storage, particularly for regulating heat exchange in building envelopes [107] Bio-based PCMs are made from animal fats and vegetable oils, such as fatty acids, plant-based waxes, soybean oil, and coconut oil. These materials offer great potential for energy storage in buildings, contributing to more sustainable and efficient thermal management.

To achieve these goals, we focused our study on developing a new model—an innovative phase change material based on fatty acids. This material is designed with environmental, economic, and energy-efficient considerations in mind, making it suitable for integration into building materials to enhance their thermal inertia. This study aims to improve the energy efficiency of buildings through the use of environmentally friendly materials. Date palm fibers (DPF) and phase change materials (PCM) were incorporated into clay bricks. First, a eutectic mixture of fatty acids sourced from the Algerian market was prepared and effectively incorporated into date palm fibers. This modified material was then incorporated into clay bricks. The resulting bricks were subjected to mechanical, physical and thermal tests to assess their performance.

4.2 Development of a bio-based phase change material

4.2.1 PCM selection

To be effectively used as thermal storage materials, PCMs are selected based on the following criteria [48],[62]: a) Transition temperatures within the desired range of comfort: For thermal comfort applications, this range is typically between 25 °C and 40 °C, which is suitable for regions in southern Algeria [63]; b) High thermal conductivity; c) System compatibility and integrity: PCMs must be compatible with the overall system and nontoxic, noncorrosive, nonflammable, nonexplosive, and minimally harmful to the environment to ensure safe and reliable operation[117] and d) Use of abundant and economical viable materials.

These selection criteria are essential when choosing PCMs for specific energy storage applications. They ensure the system's efficiency, reliability, and safety while optimizing its design and cost-effectiveness. Fatty acids and their derivatives, given their intended uses, are cost-effective materials. They exhibit storage properties comparable to those of paraffin and are available with melting temperatures ranging from −23 °C to 78 °C [118]. Compared with paraffin, they offer competitive thermal capabilities, with latent heat ranging from 100 to 300 kJ/kg. Furthermore, they offer favorable specific temperatures and are safe to use because they are non-flammable, non-corrosive, and non-toxic.

4.2.2 Prepared samples

As part of our efforts to protect the environment and promote sustainable solutions, it is essential to emphasise the use of environmentally friendly materials to help reduce global warming. This approach contributes significantly to improving the efficient use of various energy sources.

By choosing bio-based materials for construction, industry and other sectors, we can reduce carbon dioxide emissions, reduce dependence on non-renewable energy sources and encourage the transition to more sustainable practices.

In this work, we have developed a new environmentally friendly phase change material (PCM) that is natural, non-toxic and non-flammable. The prepared samples consist of a simple mixture of myristic acid and stearic acid, whose melting temperatures are shown in Table 4.1. Myristic (MA, $C_{14}H_{28}O_2$, analytical reagent) and stearic (SA, $C_{18}H_{36}O_2$, analytical reagent). Myristic acid (MA) has melting temperature of 54 °C as stearic acid (SA) has melting temperature of 68 °C. Both acids are available in Algeria (fig 4.1).

Table 4.1. Properties of fatty acids used

Fatty acid	**Formula**	**Melting Temp [°C]**	**Latent heat [kJ/kg]**	**Price [$/kg]**
Myristic acid	$C_{14}H_{28}O_2$	54	210	6.6
Stearic acid	$C_{18}H_{36}O_2$	68	258	6.6

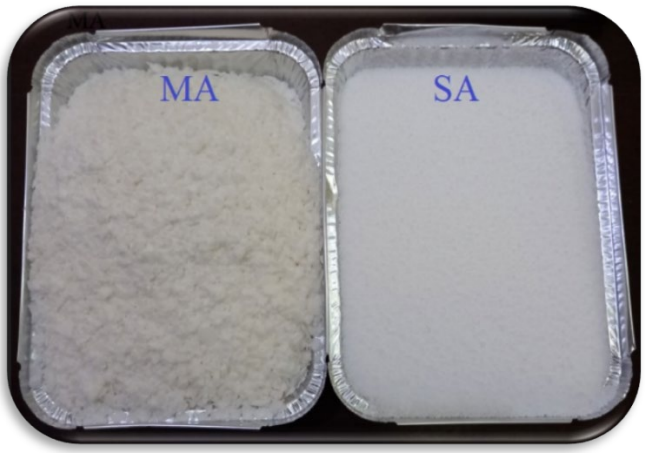

Figure 4.1. Both acids used.

The development of a bio-based PCM using these components, especially fatty acids, has been the focus of several research projects [119] ,[120] [121]. Due to their ability to store energy through phase transition. In general, myristic acid melts at a temperature above 54°C, while stearic acid has an even higher melting point. This is considered a disadvantage when used as a PCM in buildings. Therefore, both acids are mixed to achieve a lower melting point, making them more suitable for thermal energy storage applications.

4.2.3 Sample preparation methodology:

The materials, namely, MA ($C_{14}H_{28}O_2$) and SA ($C_{18}H_{36}O_2$), used in this study were directly utilized without any pretreatment. MA, commonly known as tetradecanoic acid, is a saturated fatty acid found in coconut oil, palm kernel oil, and butterfat. SA, also known as octadecanoic acid, is a saturated fatty acid mainly derived from animal fats. This organic acid is readily available in the Algerian market and are cost-effective. These are among the least expensive PCMs used in buildings [48].

Components are blended in low to high weight ratios at 10 mass ratios ranging between 0 to 100 %. For this step we use a precision balance (up to a thousandth of a gram) to weigh the quantity necessary for our sample (fig4.7). Additional molar ratios have been prepared around the eutectic point in order to understand the thermal properties of this point. The specific experimental steps for creating the binary eutectic mixture of MA–SA were as follows: a given mass ratio of MA to SA was mixed in a test tube. The test tube was heated in a constant water bath at 80°C and stirred with a magnetic stirrer at 400 rpm for 1 hour to ensure homogeneity. The eutectic composition of the PCM was determined according to the theory of the lowest eutectic point [120]. Figure 4.2 summarizes the preparation process.

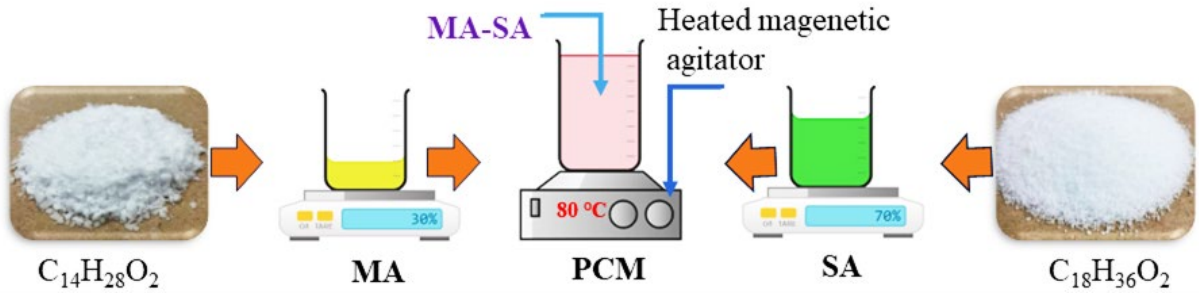

Figure 4.2. The method used to prepare and mix fatty acids.

4.2.4 Binary mixture selection

Fatty acids like MA and SA consist of long carbon chains with a carboxyl group (-COOH) at the end, as shown in **Figure 4.3**. When mixed, the difference in chain lengths disrupts the molecular arrangement, making it less organized. This disruption reduces the energy required for the transition from solid to liquid, resulting in a lower melting point [122]. The eutectic composition of the PCMs was determined based on the theory of the lowest eutectic point (Experimentally). On the other hand, it was possible to rely on the lowest melting point equation used in many studies such as Ruiqi et al [123]. Based on the stepwise cooling curve for DSC analysis, MA/SA mass ratios of 70% and 30% were chosen. The measurement results are presented in **Figure 4.4**. The lowest melting point obtained was 35°C when the weight ratio of MA/SA was 70% or 30%. However, the melting temperatures of the other ratios were high, indicating that they were outside the previously defined range.

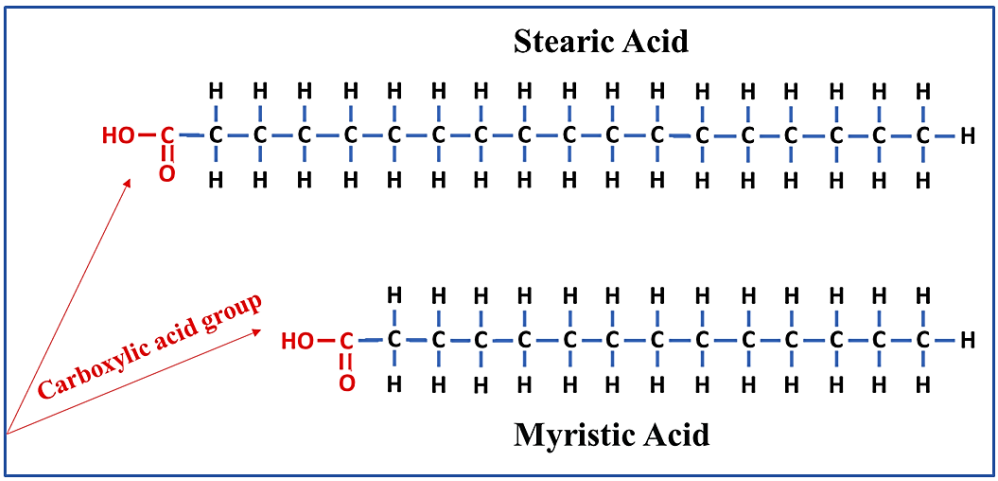

Figure 4.3. Chemical structure of myristic and stearic acid

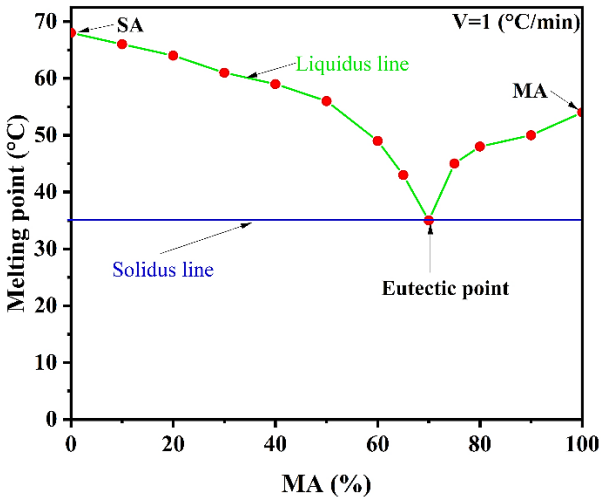

Figure 4.4. Experimental phase change temperatures of mixtures of MA and SA with different proportions of MA by mass

4.3 Characterization of the MA–SA eutectic mixture (70% and 30%).

4.3.1 Introduction

Energy storage in thermal energy storage (TES) systems using phase change materials (PCM) offers high energy storage capacity due to the latent heat associated with phase transition. To ensure optimal performance when integrating PCM into building envelopes and solar energy systems, careful selection of the appropriate material is essential.

In order to evaluate the energy storage performance of PCM, it is crucial to study the heat transfer during its operation. This requires the determination of all thermo-physical properties of the PCM, including phase change range, phase transition peak, latent heat, heat capacity, thermal conductivity and density.

4.3.2 Thermal characterization (DSC/ATG)

The thermal properties and stability of the materials were analyzed using Differential Scanning Calorimetry DSC (fig4.5) (Q20, TA Instruments, operating temperature range: -90 to 550 °C) and Thermogravimetric Analysis TGA (fig4.6) (Q600, TA Instruments). DSC was used to evaluate the thermal energy storage capacity by examining the fusion and solidification properties of the prepared PCM composites. It measures the heat flow released by the materials being tested, as well as the change in mass during the tests. The DSC technique measures the difference in heat flow between a sample and a reference material. This is done while the temperature of the crucible changes at a constant rate over time. The measurement records the difference in heat flow. The DSC was calibrated using two reference standards, indium and aluminum, to ensure accurate measurement over the selected temperature range. Before conducting measurements, preliminary verification was performed to correct the initial reference. The measurements were then carried out cyclically, with a heating/cooling rate of 1 °C per minute, covering a temperature range of 5 °C to 60 °C during the heating phase and 60 °C to 5 °C during the cooling phase. (**Figure 4.8**) [48]. Each sample, weighing between 9 and 12 mg, was placed in an alumina crucible. The initial masses, measured using a highly sensitive electronic balance (Figure 4.7). To ensure accuracy, each sample was tested in triplicate.

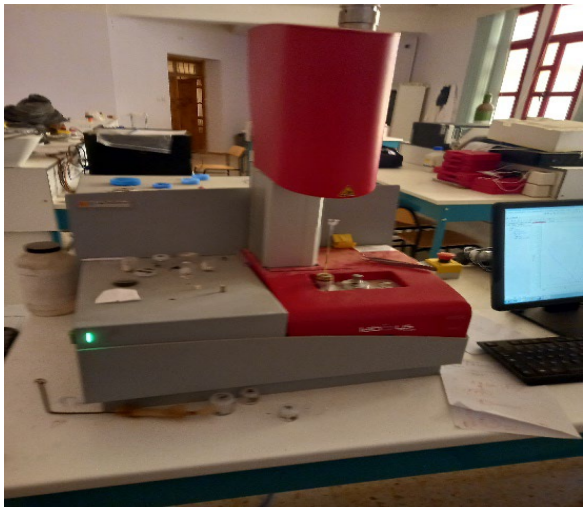

Figure 4.5. Thermogravimetric analysis (TGA) (University of M'sila).

Figure 4.6. Used differential scanning calorimeter (DSC).

Figure 4.7. highly sensitive electronic scale used.

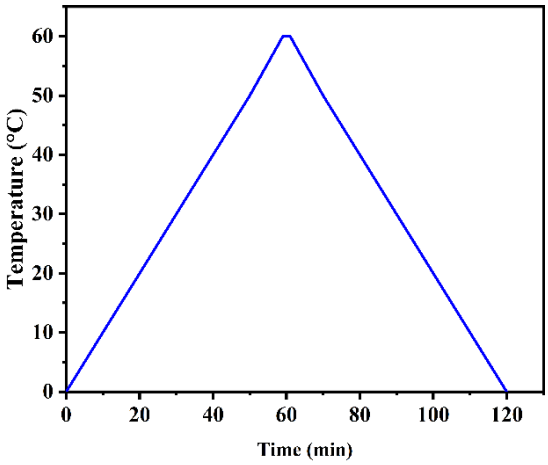

Figure 4.8. Heating/cooling program for DSC measurements

Thermogravimetric analysis (TGA) is a tool used to assess the stability of a material over the temperature ranges encountered in building applications. In TGA, the changes in mass of a material are measured relative to temperature (or time) under a defined atmosphere. **Figure 4.9** shows the weight loss curve of the PCM from 20 to 160 °C. The curve indicates that the PCM primarily degrades between 90 °C and 160 °C, with the onset of degradation occurring at approximately 70 °C. By identifying the temperatures at which these transitions occur, it can be inferred that the formulated PCM exhibits good thermal resistance below 85 °C, with a mass loss of less than 0.5%. This makes it suitable for use in the building industry, where temperatures rarely exceed 60 °C.

The results of the thermogravimetric analysis (TGA) tests are shown in Figure 4.9. The curves obtained indicate that the mass loss is minimal as the temperature increases. This indicates that there is no significant mass loss in the sample crucibles within the range of our study.

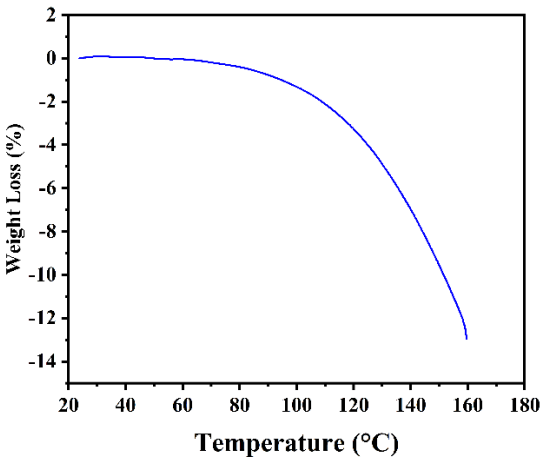

Figure 4.9. TGA curve of the MA–SA eutectic mixture (70% and 30%)

4.3.3 *Identifying the phase change intervals*

The selection of a phase change material (PCM) for a specific application depends primarily on several factors, the most important of which are the phase change temperature, the phase transition range, the latent heat, and the thermal capacities in both the liquid and solid phases. Various methods are used to characterize phase change materials, either through experimental setups or differential scanning calorimetry (DSC). By analyzing the heat flow curve obtained, it is possible to determine the specific heat capacities of the solid and liquid phases, the initial (T_{onset}) and final (T_{endset}) melting temperatures - representing the points at which the PCM begins and ends to melt - and the peak melting temperature (Tpic). These properties are typically determined using differential scanning calorimetry (DSC) [124], [125], [126], [127].

- **DSC**

DSC, which analyzes the fusion/solidification properties of the fabricated PCM composite, was used to measure the thermal energy storage capacity. Studies have employed slow scanning speeds when investigating PCMs to ensure precise thermal measurements [48]. Consequently, this study used a scanning rate of 1 °C/min to characterize bio-based PCMs comprising 70% MA and 30% SA. The DSC curves of the PCM composites are shown in Figure 4.10. The fusion and solidification temperatures, along with the enthalpy of the PCMs, are shown in Table 4.2. DSC analysis of the MA–SA mixture revealed that the sample with 70% MA and 30% SA exhibited a phase transition interval suitable for incorporation into building walls. This result has been confirmed by numerous studies on the MA–SA eutectic mixture [128]. The fusion point of the obtained eutectic mixture was closer to those reported in previous studies (Table 4.3). The slight discrepancy could be attributed to variations in the purity level of each acid or differences in the measuring equipment used. Additionally, at high scanning speeds, the melting peak of the MA–SA mixture increases [129] . We observed that the supercooling phenomenon, where a liquid remains in its liquid state below its freezing point, did not occur due to the presence of sufficient crystalline nucleation centers [130]. In our experiment, we employed a slow cooling rate of 1 °C/min, which provided enough time for the crystalline nucleation centers to form naturally. Furthermore, the presence of impurities in the mixture acted as crystallization nuclei, promoting the crystallization process and preventing supercooling.

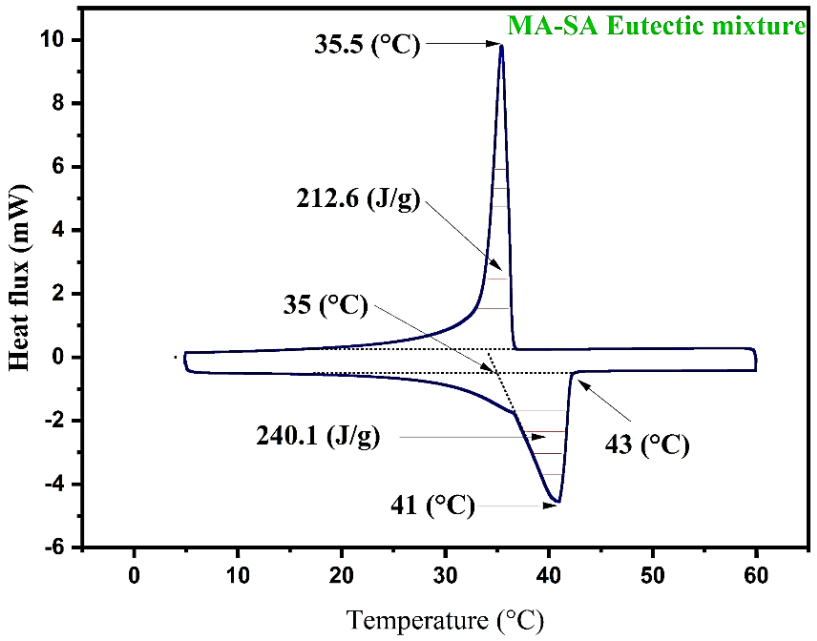

Figure 4.10. DSC curves of the MA–SA eutectic mixtures (70% and 30%): temperatures of interest and enthalpies

Table 4.2. Thermal properties of the selected binary system of fatty acids with eutectic compositions measured by DSC

PCM	Melting temp. (onset) [°C]	Melting peak temp. [°C]	Endset melting temp. [°C]	Solidification temp. (onset) [°C]	Solidification peak temp. [°C]	Endset melting temp. [°C]	Latent heat of fusion [J/g]	Latent heat of solidification [J/g]
Eutectic mixture	35.0	41.0	43.0	37.0	35.5	33.0	240.1	212.6

Table 4.3. *Melting temperature of different MA–SA mixtures*

Myristic acid [%]	**Stearic acid [%]**	**Melting temperature [°C]**	**Scanning rate [°C/min]**	**Ref.**
65.7	**34.3**	**44**	**10**	[121]

70	**30**	**35.8**	**-**	[120]
66	**34**	**39.54**	**5**	[128]
64	**36**	**44.13**	**5**	[119]
70	**30**	**35**	**1**	**Present study**

4.3.4 *Heat capacity (Cp)*

The calculation of the heat capacity (Cp) of PCMs depends on factors such as the type of product and the desired level of accuracy, which influence the selection of an appropriate measurement technique [107]. In this study, the Cp of the eutectic MA–SA mixture was precisely determined using DSC, taking advantage of its effectiveness and reliability in characterizing thermal responses within a specified temperature range. DSC measures the heat flow (J/s) in response to time changes (**fig 4.10)**, as expressed by the following equation:

$$heat\ flux = \frac{q(J)}{t(s)} \quad 4.1)$$

Heating rate (°C/s), which refers to the rate at which the temperature increases over a given period of time as follows:

$$Heat\ rate\ = \frac{\Delta T(^\circ \mathrm{C})}{t(s)} \qquad (4.2)$$

Thus, the heat capacity equation is obtained by dividing equation 4.1 by equation 4.2 over the mass.

$$C_p\left(J/^\circ C.g\right) = \frac{q(\mathrm{J})}{\Delta T(^\circ C).(g)} \qquad (4.3)$$

Where q is the DSC measured energy and ΔT the temperature difference.

Using Eq. (3) and the data provided in **Figure 4.11**, which illustrates the variation in heat flow measured by DSC for various samples at a scan rate of 1 °C/min, the curves showing the variation in Cp with temperature for the eutectic MA–SA mixture whether in the liquid, solid, or phase-change state were obtained, as shown in **Figure 4.12**. Approximately 9,500 data points

were collected from the sample analysis over a temperature range of 5 °C to 60 °C. Based on the trends observed in **Figure 4.12**, the results are summarized in Table 4.4.

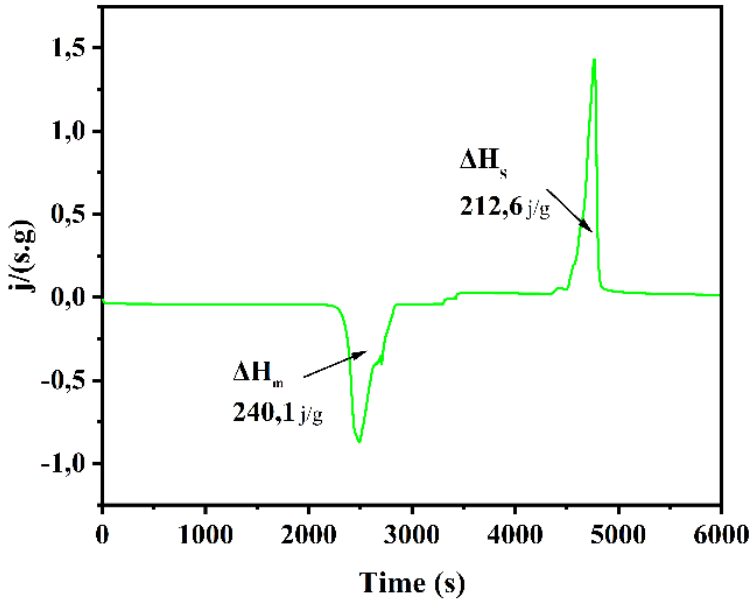

Figure 4.11. DSC curve showing the enthalpy of melting and solidification

Table 4.4. Thermal capacities of the MA–SA eutectic mixtures in various states

	Solid-state temp. (°C)		**Melting temp. (°C)**	**Peak temp. (°C)**	**Endset melting temp. (°C)**	**Liquid state (°C)**	
Temperature (°C)	7	20	35	41	43	50	55
Heat capacity [J/g °C]	0.84	2.30	6.92	21.31	2.15	2.07	2.06

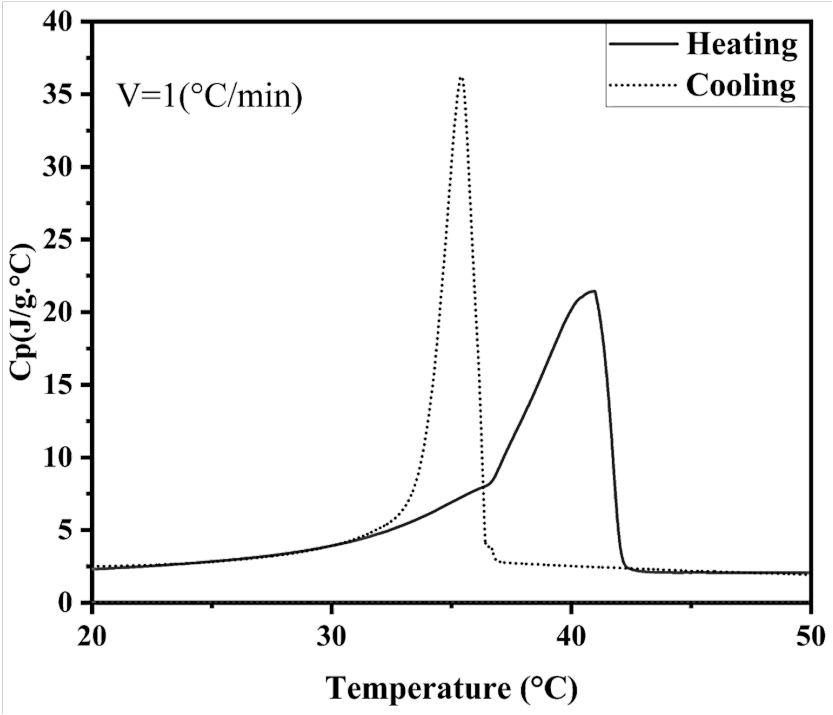

Figure 4.12. DSC curve of the heat capacity of the new PCM

The equivalent heat capacity can be written under the following form:

$$C_{p_{eq}} = \begin{cases} C_{p_s} & T < T_s \\ C_{p_{in}} & T_s < T < T_l \\ C_{p_l} & T > T_l \end{cases} \qquad (4.4)$$

Based on the heat capacity changes observed in the DSC of the new PCMs, we derived the analytical formulas for the heat capacities in the different states of the PCMs. This method was also employed by Kravvaritis et al. [131]. By solving the linear equations for the different states of the PCMs using the data presented in Table 4.4 and **Figure 4.12**, we obtained the thermal capacity variations with temperature for the novel PCMs, as shown in the correlation expressions below:

$$C_{p_s}(\mathrm{T}) = 0.1637T - 0.6136 \quad (4.5)$$

$$C_{p_l}(\mathrm{T}) = 0.0517T + 4.5239 \quad (4.6)$$

4.3.5 The densities

The densities of the MA–SA eutectic mixtures in both the liquid and solid states were determined using the following formula [132]:

$$\rho_{MA-SA} = \frac{\rho_{MA} \times \rho_{SA}}{\rho_{MA} \times X_{SA} + \rho_{SA} \times X_{MA}} \quad (4.7)$$

where ρ_{MA} and ρ_{SA} are the densities of MA (824(l), 860(s) kg/m^3) and SA (848(l), 840(s) kg/m^3), and X_{MA} and X_{SA} are their weight fractions, respectively, with [X_{MA} +X_{SA} = 1].

4.3.6 Characterization of thermal conductivities of the MA–SA eutectic mixtures (70% and 30%).

The TCi Thermal Conductivity Analyzer is used to measure the thermal conductivity of various materials. It is based on the Transient Plane Source (TPS) technique, which uses a thin wire or film as a sensor. This sensor is heated to a specific temperature and placed in contact with the sample. As heat flows through the material, the temperature change in the sensor is recorded. By analyzing how the temperature changes over time, the TCi determines the thermal conductivity of the material. Figure 4.13 illustrates the changes in thermal conductivity with temperature for the bio-based PCMs. The thermal conductivity curves show three distinct regions corresponding to the solid, mushy and liquid states of the samples. In the solid state, the thermal conductivity is high and then decreases more rapidly during the phase transition. This decrease continues until it reaches values that decrease slowly with temperature as the liquid phase progresses.

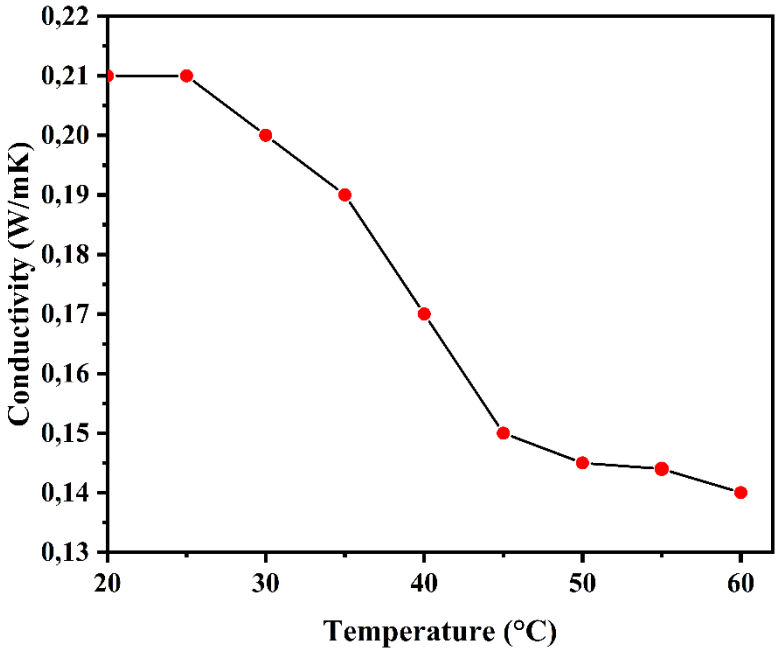

Figure 4.13. Experimental thermal conductivity of the MA-SA eutectic mixture (70%, 30%).

The high thermal conductivity of the MA-SA eutectic mixtures (70% and 30%) in their solid state is due to the strong bonds between the molecules in this phase. In solids, atoms or molecules are tightly packed together to form a uniform lattice structure. These particles vibrate around their equilibrium positions, creating coordinated vibrations throughout the material. This uniform arrangement enhances thermal conductivity by allowing thermal energy to be efficiently transferred between adjacent atoms or molecules.

During the phase transition, the thermal conductivity of these MA-SA eutectic mixtures (70% and 30%) changes due to structural changes and variations in particle mobility. In the liquid state, the thermal conductivity is lower than in the solid state. This difference is explained by the increased molecular mobility and reduced structural order in liquids. Because the molecular arrangement is less organized, heat transfer between particles is less efficient than in solids. The irregular motion and weaker interactions between molecules in liquids further reduce the efficiency of thermal energy transfer, resulting in a lower thermal conductivity than in the solid state.

4.4 Manufacture of clay bricks with phase change materials

4.4.1 Traditional building materials (Soil, sand and lime)

This research goals to utilizing local resources such as soil, sand, and palm fibers from the cities of Adrar and Ouargla situated in the southwest and southeast of Algeria respectively. These regions are renowned for their high temperatures, surpassing 55 °C.

4.4.1.1 Clay soil

The clay was assessed based on its chemical composition, with a focus on key oxides such as SiO_2, Al_2O_3, and Fe_2O_3, while the presence of CO_2 and $CaCO_3$ was found to be minimal (Table 4.5). From an industrial perspective, the Al_2O_3/FeO_3 ratio is less than 5.5, indicating a high iron content, making this clay suitable for the production of building materials such as bricks and tiles [133]. This soil has been used in many studies [134], [135], [136].

4.4.1.2 Dune Sand and lime

Dune sand from the Adrar region of Algeria is used in the production of all brick mixes. The chemical composition of this sand and soil is given in Table 1. Quicklime from the lime unit in Saida, Algeria, was utilized. The figure (4.14) below shows a sample of the soil and sand used.

Fig 4. 14. The soil and sand used.

Table 4.5. Chemical properties of the soil and dune sand used in the present study

Component (%)	**SiO_3**	**CaO**	**Al_2O_3**	**FeO_3**	**$CaCO_3$**	**CO_2**
Soil	82.10	1.96	3.33	4.41	0.93	0.41
Sand	87.1	6.3	0.01	1.35	4.55	2.03

4.4.1.3 Date palm fibers

Date palm natural fibers (DPF) were obtained from Touggourt Oasis and had an absolute density of 1300 ÷ 1450 Kg m^{-3}, length L = 10 ± 1 mm, diameter ϕ = 0.14 ÷ 1.7 mm, the tensile strength and moisture content in the range of 170 ÷ 290 MPa and 9.5 ÷ 10.5 %, respectively [137]. The density of 610 ± 40 kg m^{-3} is in the same range as that determined for date palm (Phoenix dactylifera L.) from the Biskra Oasis in Algeria. The figure() below shows a sample of used date palm fiber remains.

Figure 4.15. Date palm fibers used.

4.4.1.4 Water

The water used in the mixture is potable, with a temperature between 20°C and 22°C. It meets the quality requirements of the NFP 18-404 standard for drinking water.

4.4.2 Preparation and characterization of shape-stabilized phase change material (SS-PCM)

The SS-PCM composites were produced using the vacuum impregnation method, which offers the advantage [138] of enhancing PCM (liquid phase) absorption into the support's pores by eliminating the air trapped within them.

To obtain the MA-SA/DPF stable form composite, the vacuum impregnation technique has been used (Figure 4.14). Date palm fiber is weighed (m_1) and mixed with the pre-weighed liquid MA-SA. Both the date palm fibers and the eutectic mixture were placed in the conical flask, which was placed in a water bath at 60 °C, that temperature remains higher than the melting one of the PCM. Then, the vacuum pump was connected and vacuumed. The air from the porous of DPF was evacuated. The vacuum process continued for 1 hour to complete the impregnation. The melted MA-SA is absorbed in the pores of the date palm fiber by capillarity and surface tension forces [139]. Finally, the vacuum process was and the samples were removed. After impregnation, the excess of liquid MA-SA is filtered out. The impregnated date palm fiber is put on a filter paper and kept in the oven at 60 ◦C to remove the MA-SA on the face of the date palm fiber. The paper was continuously changed until no leakage was observed. The final mass of the composite (m_2) is weighed and the mass ratio of MA-SA in the composite is calculated using equation (1) according to [139].

$$R = \frac{m_2 - m_1}{m_2} \times 100 \qquad (4.8)$$

The final mass ratio without leakage is 52.39%. This value is comparable with the value reported in the literature for fibers as shown in table (4.6).

Table 4.6. Comparison between the Percentage of impregnation of the prepared MA-SA/ DPF composite with that of other bio-based PCM composites.

	Biochar	**Wood flour**	**Wood fibers**	**Kapok fibers**	**Hemp shives**	**Date palm fiber**
Impregnation (%)	48.5	44	52	40.5	53	52.39
Reference	[140]	[141]	[142]	[143]	[62]	**This study**

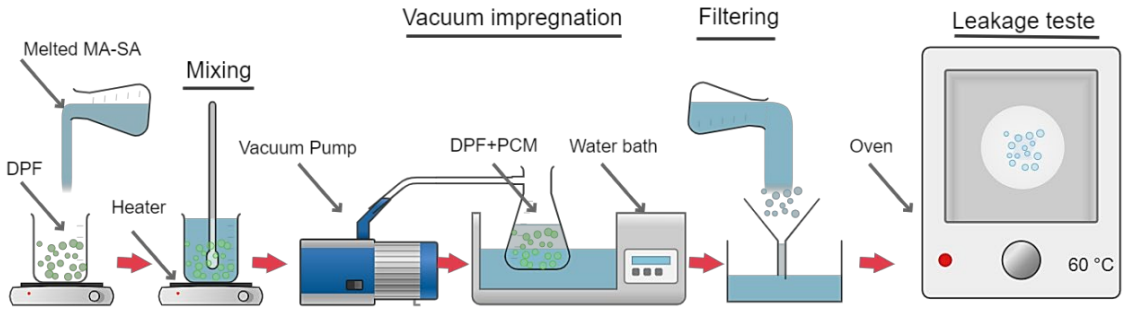

Figure 4.14. Fabrication process of the DPF/MA-SA by vacuum impregnation method.

4.4.2.1 Preparation of samples

The optimal dune sand content for compressive strength was determined to be 75% by weight, as shown in Figure 4.15. A water content of 25% by weight was selected to achieve a uniform mixture suitable for molding adobes. Mixing was done using an electric mixer for 15 minutes to ensure homogeneity. The mixtures were manually filled into cubic molds (10x10x10 cm) in two layers and left to dry in the open air for 72 hours. The blocks were then removed from the molds and air-cured. The lime content was optimized for compressive strength. After that, amount of water, relative to the total mass, is added to transform the mixture from a damp blend into a uniform paste that is ready for molding [144]. Various lime contents (4%, 6%, 8%, 10%, 12%, and 14% by weight) were tested, with 10% being the optimal value, as shown in Figure 4.16.

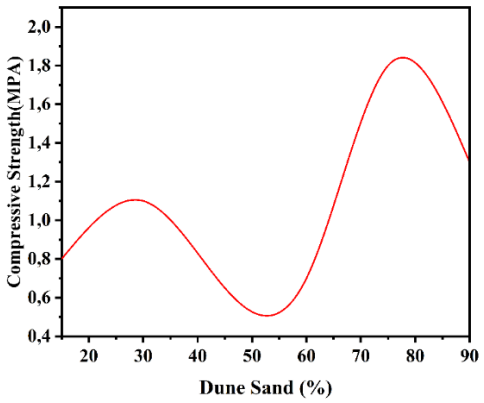

Figure 4.15. Effect of dune sand percentage on dry compressive strength of clay.

After optimizing the lime content, bricks were manufactured using a mixture of soil, sand, lime, and MA-SA/DPF. The mixing and preparation were conducted in two stages. First, the dry mixture (soil + sand + lime) was mixed for 5 minutes, then water was added and the mixture was further mixed for 15 minutes until homogenization. Finally, the required quantity of MA-SA/DPF was added gradually while continuing manual mixing. The proportions of the

different mixtures are presented in Table 4.7. It's worth noting that filling of the cubic (10x10x10 cm) and prismatic (4x4x16 cm) metal molds was done in two layers, and three test pieces were prepared for each test, as shown in Figure 4.17.

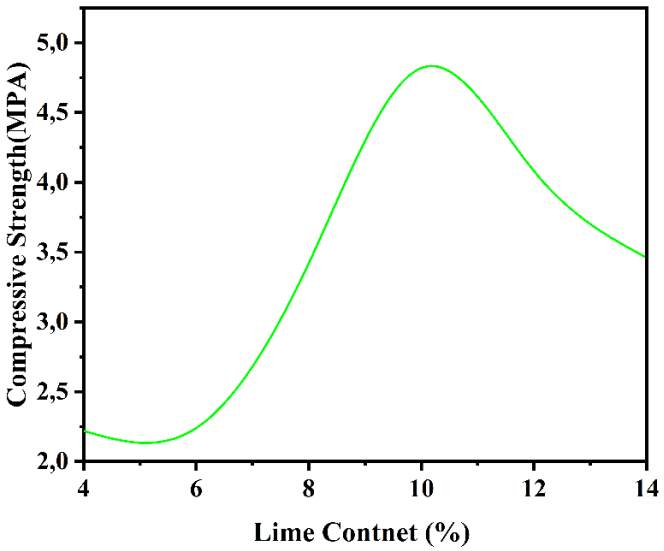

Figure 4.16. Effect of lime percentage on dry compressive strength of clay.

Figure 4.17. Compressive strength test specimens with various dimensions.

Table 4.7. Percentage of building materials in various prepared mixtures

Mixture	**Dune Sand (%)**	**Soil (%)**	**Lime (relative to the weight of sand + Soil)**	***MA-SA/DPF***
1	75	25	10	0
2	75	25	10	0,5
3	75	25	10	1
4	75	25	10	1,5
5	75	25	10	2

4.4.2.2 Mechanical characterization

According to French norm NF-EN 196-1, the dry compressive strength was determined on cubic blocks measuring (10 x 10 x 10) cm using a hydraulic press as shown in figure (5a and 5b). Employing a force sensor of 20 kN with a loading speed of 0.5 mm/min, this enabled the construction of compressive and flexural stress-strain diagrams, facilitating the observation of the material's mechanical response under dry compression and bending at various DPF contents for both natural and PCM states (solid and liquid). Each composition was tested using a three-point test configuration. The two prism halves from this test were used for compression testing.

4.4.2.3 Characterization of DPF/MA-SA composites by Differential Scanning Calorimetry (DSC)

DSC is used to assess the thermal energy storage capability by examining the melting characteristics of the prepared PCM composite. Figure 4.18 displays the DSC curve representing the eutectic MA-SA and DPF/MA-SA composite. The melting temperatures for MA-SA and DPF/MA-SA composite was identified as 35 °C and 34.5 °C, respectively. The enthalpies for melting were 240 $J.g^{-1}$ and 124 $J.g^{-1}$, respectively. Post-fabrication of the shape-stabilized DPF/MA-SA composite, melting enthalpies experienced a reduction. This decrease is attributed to the lowered mass/ratio of eutectic MA-SA within the composite and the reduced crystallinity of eutectic MA-SA. Furthermore, the phase change temperature is lower compared to pure eutectic MA-SA before impregnation, potentially due to the weak attractive interaction between fatty acid molecules and the inner surface of the porous material [145]. The measured melting and solidifying temperatures of the composite PCM are very similar to the values calculated by multiplication of the eutectic MA-SA ratio in the composite by their phase

transition enthalpy, as reported by [146]. In fact, the fusion heat ratio of pure eutectic MA-SA and DPF/MA-SA is 51,66%, which is remarkably close to the theoretical value of the impregnation rate (52.39%).

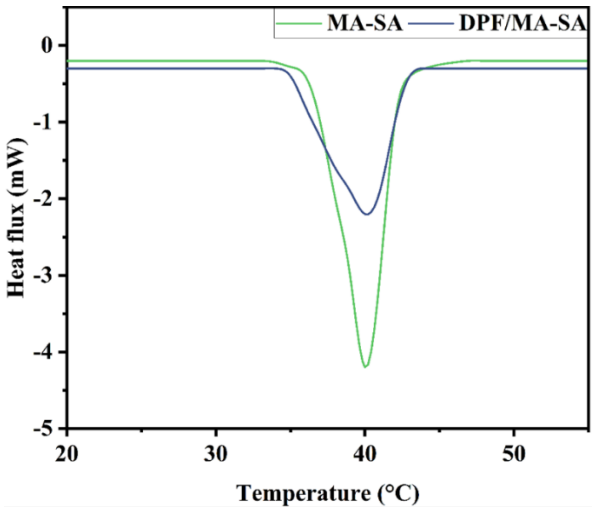

Figure 4.18. DSC curve of MA-SA, PCM only and DPF/MA-SA composite.

4.4.2.4 Thermo-Gravimetric Analysis (TGA)

Figure 4.19 illustrates the weight loss curves for MA-SA, DPF only, and the DPF/MA-SA composite from room temperature (25°C) to 350°C. From the curves, it is evident that MA-SA primarily degrades between 125°C and 180°C. For DPF alone, the TGA curve shows an initial weight loss between 75°C and 175°C, attributed to the evaporation of free water in the DPF. The MA-SA/DPF composite demonstrates good thermal stability below 125°C, with less than 1% mass loss, making it suitable for building applications where temperatures rarely exceed 60°C.

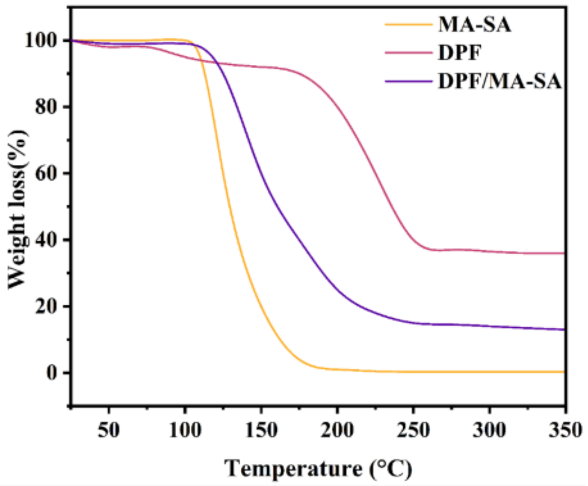

Figure 4.19. TGA curve of MA-SA, DPF only and MA-SA/DPF.

4.5 Conclusion

This chapter discusses the development and characterization of materials in a eutectic blend formulated by combining 70% myristic acid and 30% stearic acid. The objective is to create a bio-based phase change material (PCM) as an alternative to petroleum-based PCMs, with the goal of efficient integration into building envelopes to improve thermal performance.

Several techniques are used to analyze these materials. Differential Scanning Calorimetry (DSC) is used to determine the phase transition and melting temperatures, while Thermogravimetric Analysis (TGA) ensures that no significant mass loss occurs within the temperature range applicable to advanced PCMs. In addition, a TCi thermal conductivity analyzer is used to measure the thermal conductivity of the PCM under various conditions.

DSC measurements show that this bio-based PCM has great potential for energy storage applications. In particular, PCMs derived from animal and plant sources exhibit an ideal phase change temperature of 35.5°C and a latent heat of 240.12 kJ/kg, making them a sustainable and efficient alternative to petroleum-based PCMs for improving the thermal performance of building materials.

The PCM was then infused into date palm waste fibers (DPF) using a vacuum process. The melting temperatures of the eutectic mixture and the impregnated fibers were recorded at 35°C and 34.5°C respectively. To evaluate the practical use in construction, adobe bricks, commonly used in Algeria, were prepared with a mixture of 75% dune sand and 10% lime. The PCM-impregnated fibers were added to the bricks in different quantities (0.5%, 1%, 1.5% and 2%) to evaluate their mechanical and thermal properties.

Chapter 5

Numerical modeling of PCM Thermal Behavior and case studies

5.1 Introduction to Numerical Modeling

Numerical modelling generally refers to the process of using mathematical models or relationships to describe the static or dynamic behaviour of a real system. These models help in the mathematical design of a physical system. Depending on the complexity of the problem, different assumptions can be made in the numerical model. Numerical modelling is widely used for interpretative, design or predictive studies in various fields, including quantum dynamics, thermodynamics, structural analysis, geotechnical engineering and climate modelling, among others. It is essential to validate numerical models to ensure that they accurately represent physical reality. This validation follows an iterative process in which model results are compared with experimental data until the errors fall within acceptable confidence limits. Appropriate validation parameters should be used to quantify these errors and assess the accuracy of the model. Once the numerical model has been validated, simulations involve adjusting specific model parameters to analyse their effect on key variables [147].

In various applications of phase change materials (PCMs), a deep understanding of their thermal behaviour is essential for their effective integration into energy storage systems. This requires a thorough analysis, whether experimental or numerical [148], in order to optimise their performance.

5.2 Modeling heat transfer in phase change materials:

Phase change is a heat transfer process involving both sensible and latent heat within an almost constant temperature range. Based on the first law of thermodynamics, which states the conservation of energy, equation (5.1) is used to model the heat transfer process that occurs during phase change.

Energy equation:

$$\frac{\partial}{\partial t}(\rho H) = -\frac{\partial}{\partial x_j}(\rho u_j c_{pm} T) + \frac{\partial}{\partial x_j}[\lambda \frac{\partial T}{\partial x_j}] + S \qquad (5.1)$$

Where:

$\frac{\partial}{\partial t}(\rho H)$: Represents the total energy of the fluid in the control volume.

$\frac{\partial}{\partial x_j}(\rho u_j c_{pm} T)$: Accounts for energy transfer due to fluid movement in and out of the control volume.

$\frac{\partial}{\partial x_j}[\lambda \frac{\partial T}{\partial x_j}]$: Accounts for heat transfer by conduction across the surfaces of the control volume.

S : Takes into account another source of energy such as chemical reactions, electric current, etc.

In a phase change problem, a solution can be obtained by applying the boundary and initial conditions to the discretised energy equation. However, in phase change problems there are additional boundary conditions at the phase change interface, as shown in Figure 5.1 for a one-dimensional problem [147].

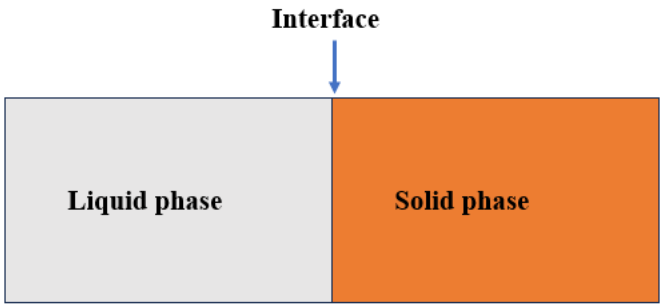

Figure 5.1. Solid-liquid interface.

For such problems it is generally assumed that heat transfer at the interface is solely by conduction, perpendicular to the interface, and that the material is homogeneous with a single melting temperature. These conditions are known as the Stefan conditions (Equation 5.2) for phase change and are expressed as follows:

$$\begin{cases} T_{sol} = T_{liq} = T \\ \lambda \frac{\partial T_{sol}}{\partial x} - \lambda \frac{\partial T_{liq}}{\partial x} = \rho L_f \frac{\partial S}{\partial t} \end{cases} \quad (5.2)$$

Where:

λ : Thermal conductivity coefficient,

ρ : Density

L_f : Latent heat of melting

∂S : Represents the position of the phase interface at time (t)

The Stefan conditions represent the conservation of energy at the phase change interface and are associated with discrete phase change temperatures. Solving the energy equation with these additional boundary conditions would describe the temperature distribution within the material. However, the challenge in this process is that the boundary conditions at the interface change continuously as the phase change progresses, meaning that they have to be determined as part of the final solution. To avoid explicitly tracking the phase change interface in numerical models, several numerical methods have been developed. While these methods have simplified phase change modelling, numerical simulations remain complex, especially when dealing with hysteresis, supercooling and nucleation. Common "non-explicit" phase change tracking models include the enthalpy method, the effective heat capacity method, the temperature transformation method and the heat source method.

5.3 Numerical formulation of heat transfer problems in phase change materials

Several numerical methods are available for modelling energy storage in phase change materials (PCM) [149], such as the enthalpy method or the source-based method. Among these, the effective heat capacity method stands out as a particularly important and widely used technique.

5.3.1 The enthalpy method:

In the enthalpy method, latent heat and specific heat are combined into an enthalpy term within the governing equation. For heat transfer primarily by conduction, the equations can be reformulated into a single equation where latent heat is included in the enthalpy term (Eq. 5.3).

$$\rho \frac{\partial h}{\partial t} = \frac{\partial}{\partial x}(\lambda \frac{\partial T}{\partial x}) \qquad (5.3)$$

From equation (5.3) it is clear that the current enthalpy depends on the current temperature (T), making the enthalpy term non-linear. As a result, the equation cannot be solved without appropriate numerical methods to deal with this non-linearity. This can be done either by using non-linear solvers based on Newton's method or by linearising the non-linear terms and using iterative methods. If a non-linear solver is chosen, an auxiliary temperature enthalpy

function is required for equation (5.3). This auxiliary function can be formulated as follows for materials undergoing phase change within a certain temperature range:

$$T=\begin{cases}\dfrac{h_p}{C_{sol}} & , \quad h_p \le C_{sol}\times(T_f-\in) \\ \dfrac{h_p+[\dfrac{C_{liq}-C_{sol}}{2}+\dfrac{L_f}{2\in}]}{[\dfrac{C_{liq}-C_{sol}}{2}+\dfrac{L_f}{2\in}]}\times(T_m-\in) & ,C_{sol}\times(T_f-\in)\le h_p \le C_{liq}\times(T_f-\in)+L_f \\ \dfrac{h_p-(C_{sol}-C_{liq})\times T_F-L_f}{C_{liq}} & ,h_p \ge C_{liq}\times(T_f-\in)+L_f \end{cases} \quad (5.4)$$

Where: C is the specific heat capacity and $\in$ is a small arbitrary value representing the phase changing temperature.

5.3.2 Heat capacity method

The term "heat capacity" in the main equation mimics the effect of enthalpy (both sensible and latent heat) by increasing the heat capacity value during the phase change. Two common approaches are used to account for latent heat release: the apparent heat capacity method and the effective heat capacity method. Although these approaches differ in how they approximate the heat capacity, their terminology is often used interchangeably in research papers [150]. The one-dimensional heat transfer equation, driven primarily by conduction and incorporating the apparent heat capacity method, can be written as follows:

$$\rho C_{p_{eq}}\frac{\partial T}{\partial t}=\frac{\partial}{\partial x}(\lambda\frac{\partial T}{\partial x}) \quad (5.5)$$

Such as:

$$C_{p_{eq}}=\begin{cases}C_{sol} & T\le T_{sol} \\ C_{in} & T_{sol}\le T\le T_{liq} \\ C_{liq} & T\ge T_{liq}\end{cases} \quad (5.6)$$

This method is useful because temperature is the only primary variable that needs to be solved in its discretised form. The key to this approach is the approximation of the heat capacity. Two common methods are used to estimate the apparent heat capacity term in equation (5.5): analytical/empirical relationships and numerical approximations.

5.3.3 Heat source method

The heat source method divides the total enthalpy in the governing equation into specific heat and latent heat, with the latent heat acting as the source term. The equation then becomes:

$$\rho C_p \frac{\partial T}{\partial t} = \lambda \frac{\partial^2 T}{\partial x^2} - \rho L_f \frac{\partial \theta}{\partial t} \qquad (5.7)$$

In this scheme the phase change front is tracked by evaluating a nodal liquid fraction field which takes a value of 0 for solid, 1 for liquid and a value between 0 and 1 for the mushy region. This approach linearises the liquid fraction and the equation can be solved iteratively as a function of temperature. The liquid fraction can be approximated by the following auxiliary equation:

$$\theta = \begin{cases} 0 & T \le T_F - \in \\ \dfrac{T - T_{sol}}{T_{liq} - T_{sol}} & T_F - \in \le T \le T_F + \in \\ 1 & T \ge T_F + \in \end{cases} \qquad (5.8)$$

5.4 The mathematical model:

The mathematical model used allows the simultaneous calculation of processes within the PCM, including conduction within the PCM, convection within its liquid phase and conduction within the building materials. In addition, the following assumptions were made in the analysis:

-The different components of the building materials are assumed to have isotropic and homogeneous properties.

-The incident solar radiation on the outer surface is uniformly distributed.

-The molten PCM inside the container is Newtonian and incompressible.

-The properties of the PCM differ between the solid and liquid phases.

-Heat transfer by convection is considered within the molten PCM.

5.4.1 Momentum equation in the PCM

The molten PCM is assumed to be Newtonian and incompressible. Based on this property, the momentum equation is modified to account for the phase transition as described in [151]. The two-dimensional Navier-Stokes equations for natural convection are expressed as follows:

The momentum equation in the X-direction is given by:

$$\rho(\frac{\partial u}{\partial t}+u\frac{\partial u}{\partial x}+v\frac{\partial u}{\partial y})=-\frac{\partial P}{\partial x}+u(\frac{\partial^2 u}{\partial x^2}+\frac{\partial^2 u}{\partial y^2})+F_a \quad (5.9)$$

The momentum equation in the Y-direction is given by:

$$\rho(\frac{\partial v}{\partial t}+u\frac{\partial v}{\partial x}+v\frac{\partial v}{\partial y})=-\frac{\partial P}{\partial y}+u(\frac{\partial^2 v}{\partial x^2}+\frac{\partial^2 v}{\partial y^2})+F_a+F_b \quad (5.10)$$

Such as:

u and v represent the direction of velocity on the two axes.

$F_b=\rho_{liq}(1-\beta(T-T_m))g$

$F_a=A(t)\times u \quad (ox)$

$F_b=A(t)\times v \quad (oy)$

$$A(t)=-\frac{C_p(1-B(T))^2}{(B(T)^3+b)} \quad (5.11)$$

Where: F_b is the buoyancy force given by the Boussinesq approximation.

The function $B(T)$ follows a linear evolution within the phase transition region and is defined by equation (5.12) [151], as is the liquid fraction.

$$\mathrm{B}(T)=\begin{cases}0 & T\le T_{pic}-\Delta T\\ \dfrac{(T-T_{pic}+\Delta T)}{2\Delta T} & T_{pic}-\Delta T\le T\le T_{pic}+\Delta T\\ 1 & T\ge T_{pic}+\Delta T\end{cases} \quad (5.12)$$

5.4.2 Energy equation:

The energy equation for a system of building materials (bricks) or a wall containing a phase change material (PCM) is formulated below, using the equivalent heat capacity method to model energy storage within the bio-based PCM.

$$\begin{cases} \rho C_{p_{eq}} \left(\frac{\partial T}{\partial t} + u\frac{\partial T}{\partial x} + v\frac{\partial T}{\partial y} = \lambda\left(\frac{\partial^2 T}{\partial x^2} + \frac{\partial^2 T}{\partial y^2}\right)\right. & \text{in } the\,PCM \\ \rho C_p \frac{\partial T}{\partial t} + \nabla(-\lambda \partial T) = 0 & \text{in construction materials} \end{cases} \quad (5.13)$$

5.5 Numerical modeling of the PCMs product effectiveness

5.5.1 Case studies:

In this section, we take a closer look at our problem through a comprehensive investigation. The mathematical model of the studied systems is detailed, along with the boundary and initial conditions associated with each specific part of our study. The definition of these bounds is essential to determine the behaviour of the systems. This section provides a detailed review of the equivalent heat capacity method, emphasising its central role in the numerical analysis of phase change materials (PCMs). We explore its frequent application in various contexts, highlighting its relevance and effectiveness in understanding the thermal behaviour of PCMs. Through this exploration, we aim to provide valuable insights into the method and present an overview of key advances in the field of phase change materials. In addition, we are investigating the decision to use experimental data-based correlations for heat capacity, specifically tailored to the new bio-based PCM, when applying the equivalent Cp method.

There are several equivalent heat capacity formulae for phase change materials (PCMs), but we will focus on the most commonly used.

The first formula uses two constants to describe the solid and liquid states of the material, together with an expression for the phase change range. This expression combines a constant with the latent heat divided by the phase change interval (L/(2ΔT)). Many researchers have used this approach to model the thermal behaviour of PCMs [152].

The second method provides a more complex expression for the equivalent heat capacity. It includes a constant term (Cp solid) and two temperature dependent functions. The first function is ((Cp solid - Cp liquid) × B(T)) and the second is (D(T) × L). Unlike the first method, in this case D(T) × L is not divided by (2ΔT). The function D(T) is zero in both the solid and liquid states and is 1 during the phase transition, which has significant implications. Therefore, this formulation needs to be validated and optimised [153].

The third formulation is an integrated model in COMSOL, which is widely used by researchers to analyse the effects of PCMs in buildings [108], [154], [155], [156].

As part of this research, various equivalent heat capacity methods have been used to model energy storage in phase change materials (PCMs) in order to assess their effectiveness. The methods used include:

Nearly 9500 experimental data points of the heat capacity of the bio-based PCM obtained by Differential Scanning Calorimetry (DSC).

A model based on the experimental data developed in this study, which describes each phase of the bio-based PCM and is formulated in equation (44). The variations in heat capacity as a function of temperature for different states of the new bio-based PCM were obtained in the development and characterisation section using the following correlation:

$$C_{p_{eq}} = \begin{cases} C_{p_s} & T < T_s \\ C_{p_{in}} & T_s < T < T_l \\ C_{p_l} & T > T_l \end{cases} \qquad (5.14)$$

Based on the heat capacity changes observed in the DSC of the new PCMs, we derived the analytical formulas for the heat capacities in the different states of the PCMs. This method was also employed by Kravvaritis et al. [131]. By solving the linear equations for the different states of the PCMs using the data presented in Table 4.4 and Figure 4.12, we obtained the thermal capacity variations with temperature for the novel PCMs, as shown in the correlation expressions below:

$$C_{p_s}(\mathrm{T}) = 0.1637T - 0.6136 \qquad (5.15)$$

$$C_{p_l}(\mathrm{T}) = 0.0517T + 4.5239\,5.16)$$

Heat transfer within the MCP is modeled using COMSOL software,the heat transfer within the PCM component is represented by the PCM index, which is modeled using an energy balance equation that incorporates the formulation of the apparent heat capacity of the PCMs. This

formulation assumes that phase change occurs with minimal temperature variation[157]. The heat transfer in the PCM components can be described by the following equations [158]:

$$C_{p_{in}} = \theta_1 C_{p_s} + \theta_2 C_{p_l} + L_f \frac{\partial \alpha_m}{\partial T} \tag{5.17}$$

$$\alpha_m = \frac{1}{2} \frac{\theta_2 - \theta_1}{\theta_2 + \theta_1} \tag{5.18}$$

where α_m represents the fraction of the mass of the solid PCM.

L_f represents the latent heat of fusion in kJ/kg.

$$\lambda_{pcm} = \theta_1 \lambda_s + \theta_2 \lambda_l \tag{5.19}$$

$$\begin{cases} \theta_1 = 1 \\ \theta_2 = 1 \\ \theta_1 = \dfrac{T_m - T_{pcm}}{\Delta T} + \dfrac{1}{2} \end{cases} \quad if \quad \begin{cases} T_{pcm} \le \dfrac{2T_m - \Delta T}{2} \\ T_{pcm} \ge \dfrac{2T_m + \Delta T}{2} \\ \dfrac{2T_m - \Delta T}{2} \le T_{pcm} \le \dfrac{2T_m + \Delta T}{2} \end{cases} \tag{5.20}$$

where θ is the fraction by volume of the PCM and varies from 0 to 1 based on the transitions of the PCM from the solid to the liquid state. There are three cases of values of θ1 and θ2, as illustrated in Figure 5.2 and can be defined as:

$$\theta_1 + \theta_2 = 1$$

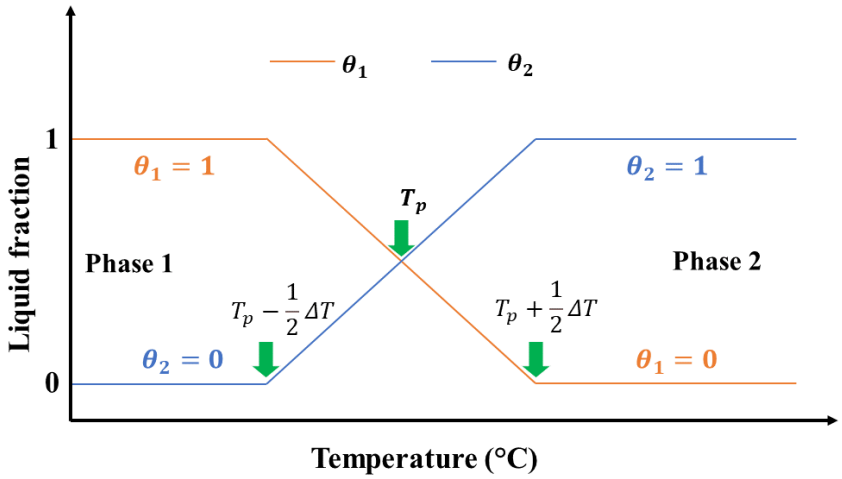

Figure 5.2. Graphical illustration of the phase change equation

5.5.2 Case study (1)

Numerical tests were conducted to evaluate the effectiveness of the proposed PCM. A two-dimensional wall was selected to analyse the thermal behaviour of walls constructed using hollow bricks packed with PCMs. The simulation was conducted under arid weather conditions for three months in the city of Adrar (latitude 27.838, longitude 0.186) in Algeria. Figure 5.3 shows the geographic location of Adrar in Algeria, known for its high temperatures, surpassing 55 °C [159].

Figure 5.3. Geographical location of the Algerian studied city (Adrar)

5.5.2.1 Description of the physical model

To evaluate the thermal properties of hollow bricks filled with PCMs, we chose two types of commercial bricks, having 12 and 8 hollow cavities, that are widely used in Algeria, as shown in Figure 5.4. When introducing the PCM, we selected five specific locations within the bricks while maintaining a consistent filling ratio of 13%. The PCM was encapsulated in aluminum to prevent mass loss. To simulate real-world scenarios of bricks filled with PCM, COMSOL Multiphysics software was used to design a model representing a typical wall. As shown in Figure 5.5**,** Model 1 serves as the reference wall with no PCM and consists of three layers: brick (15 cm) on the outside, air (5 cm) in the middle, and brick (10 cm) on the inside. Based on Model 1, Models 2–6 investigated the dynamic thermal behaviour of the wall by placing the PCMs at different positions within the reference wall (on the inside, in the middle, and outside the insulation materials). This study aimed to determine the optimal PCMs parameters and locations. The effect of these parameters on the average brick temperature is thoroughly discussed in subsequent sections. In the analysis, supercooling during solidification was disregarded. All the materials used in this study were assumed to be isotropic and homogeneous. In addition, the thermal contact resistance between wall layers was not considered [66]. Detailed information on the thermal properties of the wall materials is presented in Table 5.1**.**

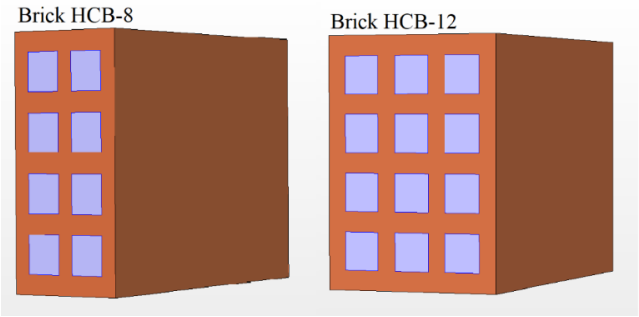

Figure 5.4. General form of the studied hollow clay bricks.

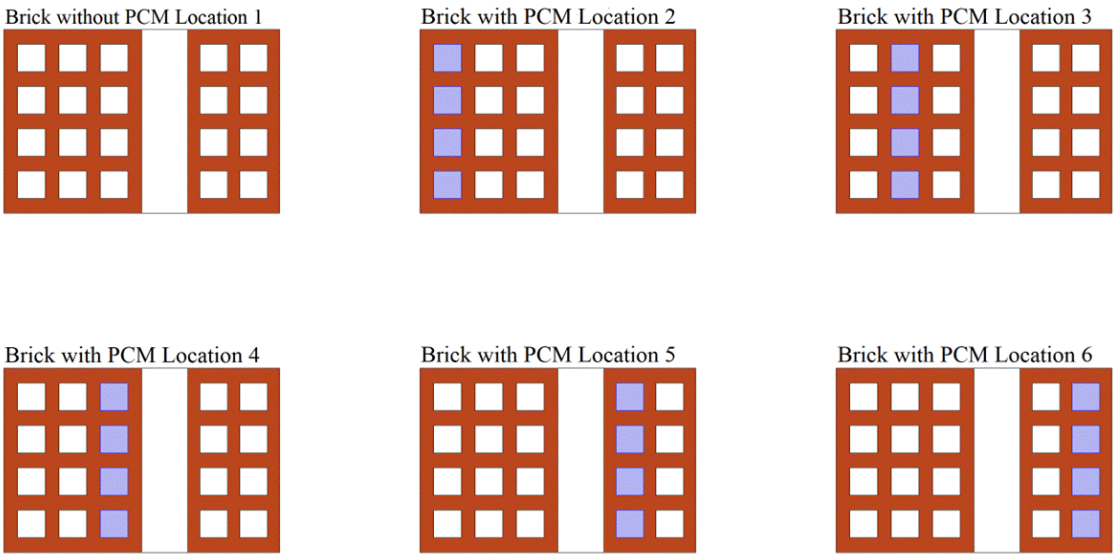

Figure 5.5. Different PCM location in hollow brick wall.

Table 5.1. Thermal properties of wall materials

Material	**ρ [kg/m^3]**	**Cp [J/kg K]**	**λ [W/m K]**	**Reference**
PCM	840(s)800(l)	$C_{p_{eq}}$	0.17(s) 0.15(l)	Present study
Clay brick	664	741	0.207	[160]
Air	1.2	1001.43	0.026	[160]
Aluminum	2700	880	210	[161]

5.5.2.2 Governing equations

This study focused on the heat transfer within a building wall made of PCMs. The primary physical assumptions are the following ones:

- The wall components are considered to have uniform and consistent properties in all directions.
- Solar radiation is assumed to be evenly spread over the exterior surface.
- The molten PCMs inside the wall is treated as a Newton's fluid with incompressible behaviour.
- The density and heat capacity of the PCMs are assumed to differ between the solid and liquid phases.
- Bricks have constant thermophysical properties

The governing equation for heat conduction in bricks can be expressed by:

$$\frac{\partial T}{\partial t} = \frac{\lambda}{\rho C_p}\frac{\partial^2 T}{\partial x^2} + \frac{\lambda}{\rho C_p}\frac{\partial^2 T}{\partial y^2} \tag{5.21}$$

The general form of the governing heat transfer equation is [157]:

$$\rho_{pcm} C_{p_{pcm}} = \lambda_{pcm}\left(\frac{\partial^2 T_{pcm}}{\partial x^2} + \frac{\partial^2 T_{pcm}}{\partial y^2}\right) \tag{5.22}$$

5.5.2.3 Boundary and initial conditions

The boundary conditions were derived from climate data in the Adrar region (Algeria), measured over three months (Figs. 5.6 and 5.7). The exterior surfaces of the blocks are heated by solar radiation, and there is a convective heat exchange with the ambient air. Eq. (5.23) computes general heat flux from exterior to the wall, denoted as $\phi_o(t)$, on the outer surface:

$$\phi_o(t) = h_o\left(T_{amb} - T_o\right) + \varepsilon_{brick}\sigma(T^4{}_{amb} - T_{brick}) + \alpha q_s(t) \tag{5.23}$$

To represent the external air temperature, q_s represents the incident solar fluxes received by the external surface of the wall. α is the solar absorption coefficient of the brick, and is assumed to be: $\alpha = 0.6$ [162]. The internal surface of the wall is maintained at a temperature of approximately 27 °C. On the outside, external convection boundary conditions were applied, with h_o = 25 W/m^2·K. On the inner face there is a free convection boundary constraint with h_i = 6.69 W/m^2·K [163]. Moreover, heat flows across the inner surface, as described by the following equation:

$$\phi_i = h_i\left(T_a - T_i\right) + \varepsilon_{brick}\sigma(T_a^4 - T_i^4) \tag{5.24}$$

The initial temperature of the entire domain was set at 25 °C.

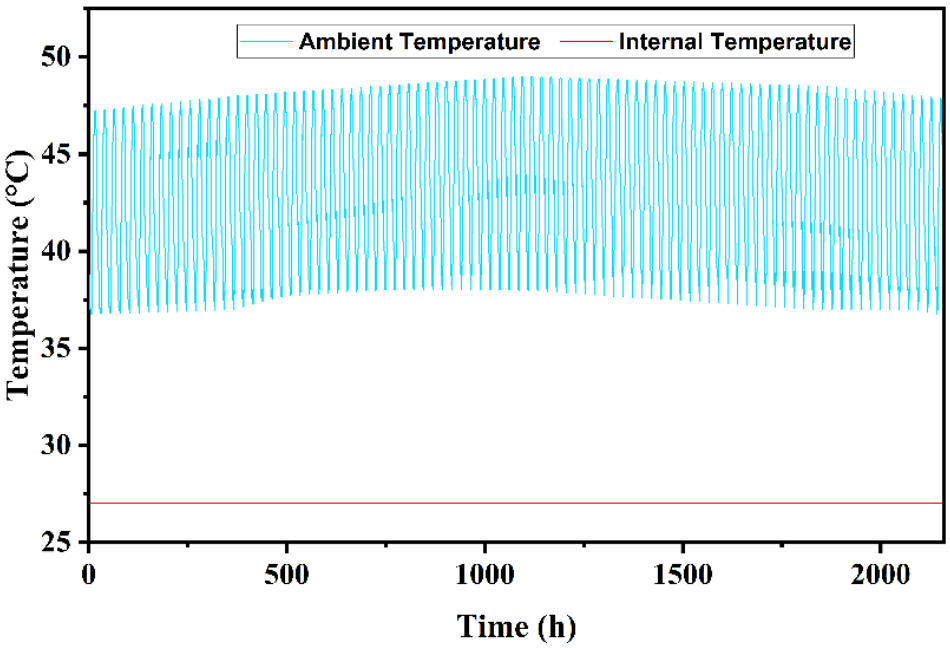

Figure 5.6. Exterior and interior temperature boundary conditions

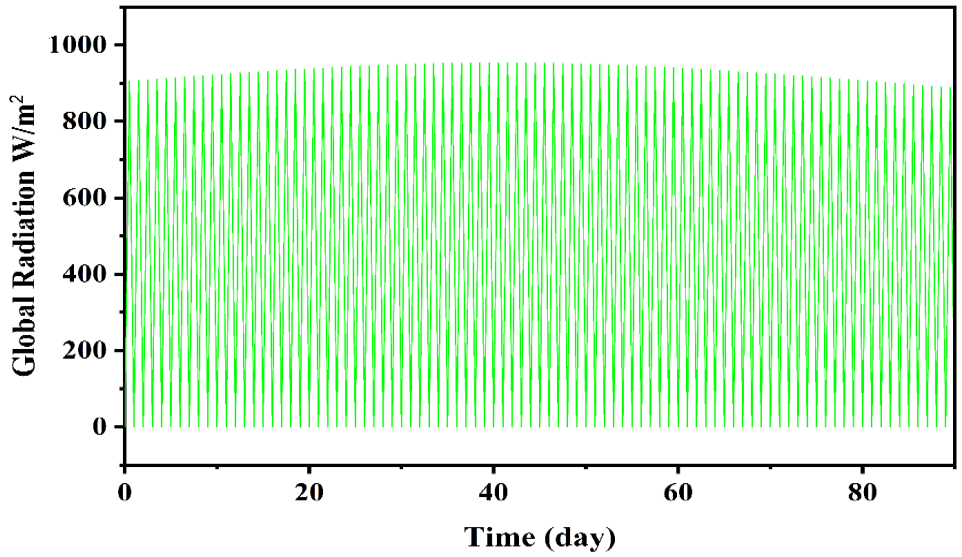

Figure 5.7. The global radiation over time during summer in Adrar city.

5.5.3 Case study (2)

5.5.3.1 Presentation of the problem

In order to assess the relevance of PCM integration in building walls, a numerical investigation was conducted on a multi-layer wall configuration consisting of a 3 cm thick concrete layer, a 15 cm thick brick layer, and a 2 cm thick gypsum layer. This wall composition is typical of Algerian construction trends. A layer of bio-based PCM was integrated into the wall, as shown in Figure 5.8. The exterior surface of the wall is exposed to heat transfer via

solar radiation and natural convection, while the interior surface experiences heat transfer through natural convection. Both sides of the wall are also subjected to infrared radiative heat transfers. For all configurations, the initial wall temperature was set to 25°C.

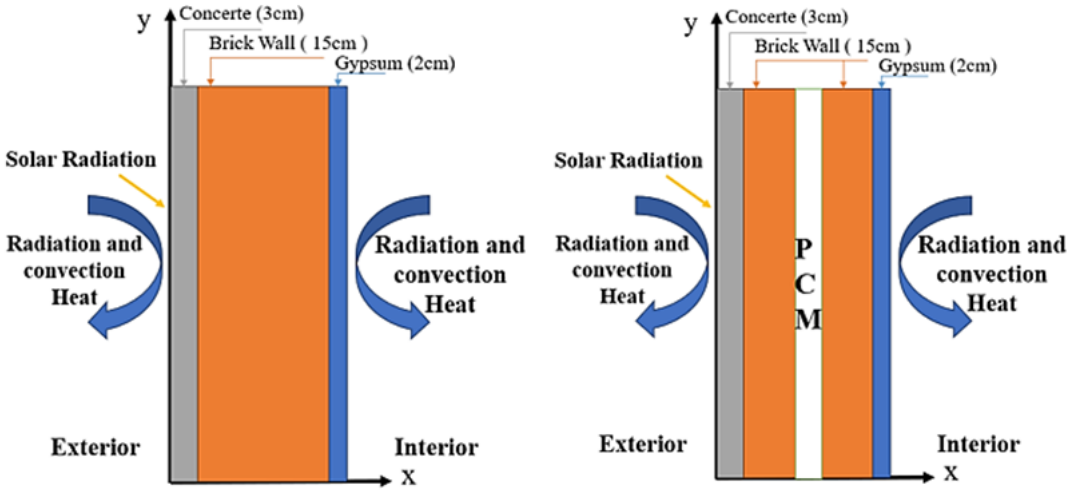

*Figure 5.8***.** Different configurations of walls and boundary conditions.

5.5.3.2 Climatic conditions

In this study, the climatic conditions of three specific cities were considered: Adrar (coordinates 27.838° N, 0.186° E), Ain Salah (coordinates 28.052° N, 9.643 ° E), and Tindouf (coordinates 27.7° N, 8.167° E). Figure 5.9 specifies the geographical position of these cities on an Algerian map. These cities are representative of the Sahara and have an arid climate, Figure 5.10 show the ambient temperature for each city (During the summer period starting from June 21st to September 21st). Ambient temperature is a major determinant of the quantity of heat transferred between the wall and the outside environment by convection.

Figure 5.9. Map illustrating the positions of selected Algerian Sahara cities.

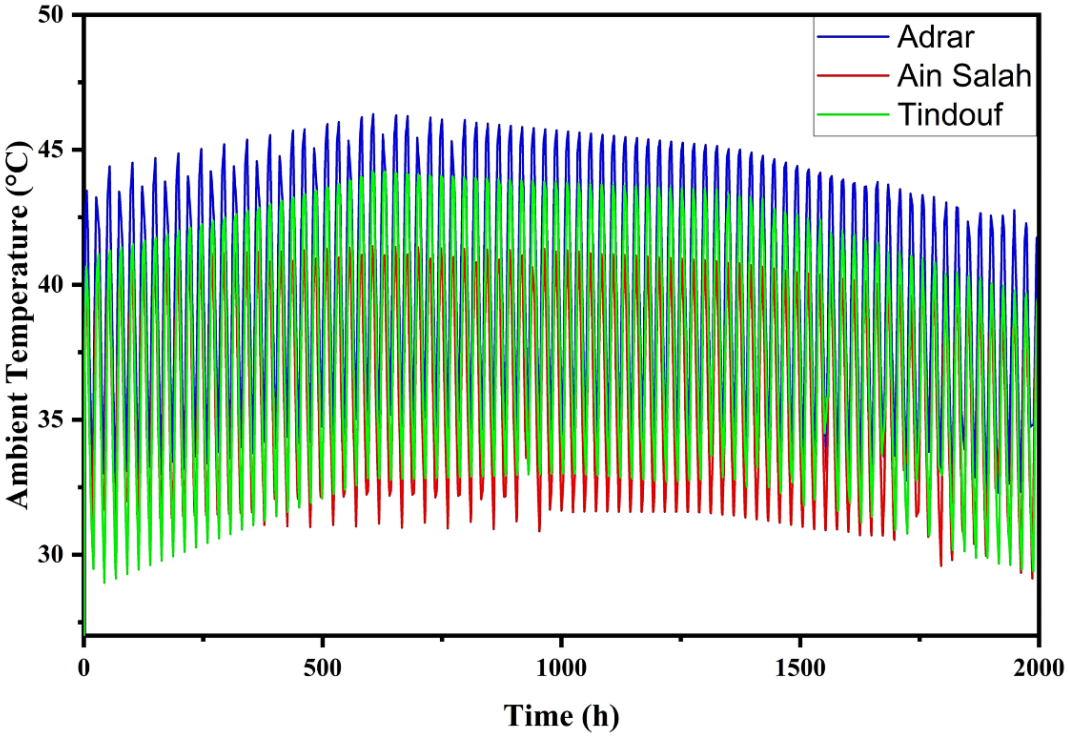

Figure 5.10. Ambient temperature as a function of time in summer for different Algerian Sahara cities.

5.5.3.3 Governing equations and assumptions

This research investigates how heat moves through a building wall that has a PCM. Here are the main physical assumptions:

• The properties of the wall components are considered uniform and consistent.

• It's assumed that solar radiation is spread evenly across the outside surface.

• The molten PCM inside the wall is viewed as a Newtonian fluid that doesn't compress.

• The PCM is assumed to have different heat capacities and densities in its solid and liquid phases.

• The thermophysical properties of brick, concrete, and gypsum stay the same.

5.5.3.4 Boundary conditions

The conditions at the two surfaces of the wall are described by Eqs. (5.25) and (5.26). Equation (11) computes the intensity of the incoming heat flux on the outer facades, denoted as $\phi_o(t)$:

$$\phi_o(t) = h_o\left(T_{amb} - T_o\right) + \varepsilon_{concrete}\sigma(T^4{}_{amb} - T_{concrete}) + \alpha q_s(t) \qquad (5.25)$$

Inside the wall, the temperature is kept around 27°C. The exterior surface of the brick experiences outer convection with a heat transfer coefficient of h_o = 25 W/m^2·K. On the interior surface, there is free convection with a heat transfer coefficient of h_i = 6.69 W/m^2·K [163]. Simultaneously, heat moves across the inner surface, and this can be expressed by the following equation:

$$\phi_i = h_i\left(T_a - T_i\right) + \varepsilon_{gypsum}\sigma(T_a^4 - T_i^4) \qquad (5.26)$$

5.6 Numerical modeling using COMSOL Multiphysics.

In our project, it is essential to solve the partial differential equations that govern the phenomena under study. This process also requires the consideration of the initial and boundary conditions associated with the given problems. For this purpose, the finite element method has been applied using the commercial software COMSOL Multiphysics version 6.0. The aim of this chapter is to present the modelling and numerical simulation process carried out using COMSOL Multiphysics.

COMSOL Multiphysics is a powerful environment for solving a wide range of engineering problems. It seamlessly transforms traditional single-physics models into multiphysics models that handle combined physical phenomena. During the solution process, COMSOL optimises and manages the workflow using a set of advanced numerical analysis tools. It performs this analysis while simultaneously generating an adaptive mesh and verifying errors through a series of numerical solvers. The process of modelling and numerical simulation with COMSOL Multiphysics involves several steps:

a) Selection of coordinate system (2D).

b) Definition of the interfaces used in our study, such as heat transfer in solids and fluids.

c) Choosing a time-dependent study.

d) Defining the geometry.

e) Setting global parameters, variables and all functions.

f) Incorporate weather conditions over time such as temperature variations and solar radiation.

g) Select and add materials

h) Define heat transfer domains in any materials

i) Modelling of the processes associated with the change of phase.

j) Apply boundary conditions for external and internal surfaces

k) Set initial conditions.

l) Specify element sizes for grids.

m) Then we use the study window.

n) Set the simulation period and time step.

5.6.1 The Newtonian method:

The Newtonian method, also known as the Newton-Raphson method, is used to solve systems of nonlinear equations. It is widely used in numerical simulation to solve complex problems, particularly in COMSOL Multiphysics where coupled equations are involved. This iterative method consists of a series of successive approximations to find a solution to nonlinear systems of equations.

In COMSOL Multiphysics, the Newton method is typically used to solve fully coupled problems where multiple physical phenomena interact. The term fully coupled indicates that all physical phenomena considered in the model are solved simultaneously.

5.6.2 Numerical validation

The COMSOL Multiphysics time-dependent solver was employed in this research, in order to solve the coupled partial differential equations developed previously in this paper. This solver uses the finite element method with Lagrange multipliers. The equations were defined using constitutive models for initial and boundary conditions. An explicit scheme with variable time stepping allowed to predefine the maximum time step, aiming to correlate with boundary conditions variations. The mathematical formulation used in this study was validated by comparison with a numerical study carried out by Bachir *et al*. [160]. Figure 5.11 shows a comparison of the temperature changes on the inner wall surface over one day. The maximum disparity between the temperatures was less than 0.779 °C. The results derived from our numerical model were consistent with those obtained by Bachir *et al*. [160], confirming the validity of our methodology.

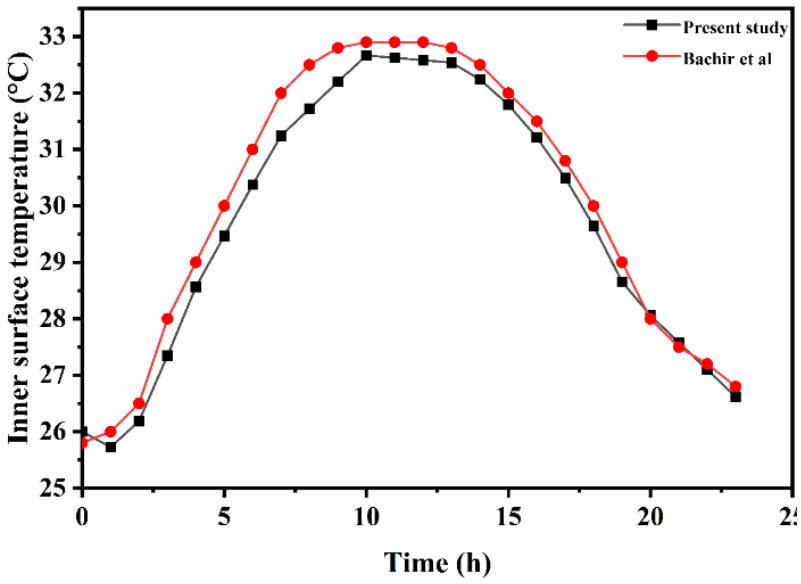

Figure 5.11. Validation of ttemperature variation in the inner surface for one day.

5.6.3 Meshing

A variety of finite element mesh configurations were tested to assess the grid independence of the results. The convergence study involved adjusting the number of finite element analysis (FEA) meshes to ensure that the results remained unaffected beyond a certain point. In this analysis, the number of elements was systematically increased through an iterative

approach, allowing the problem to be solved at each stage. When the configuration reached 27317 elements (case 1) as shown in Figure 5.12, the response stabilized, indicating convergence; further mesh refinement did not alter the results, confirming grid independence. In case 2, the mesh was made up of 3352 triangular elements, with an average element quality of about 0.8912, as shown in Figure 5.13.

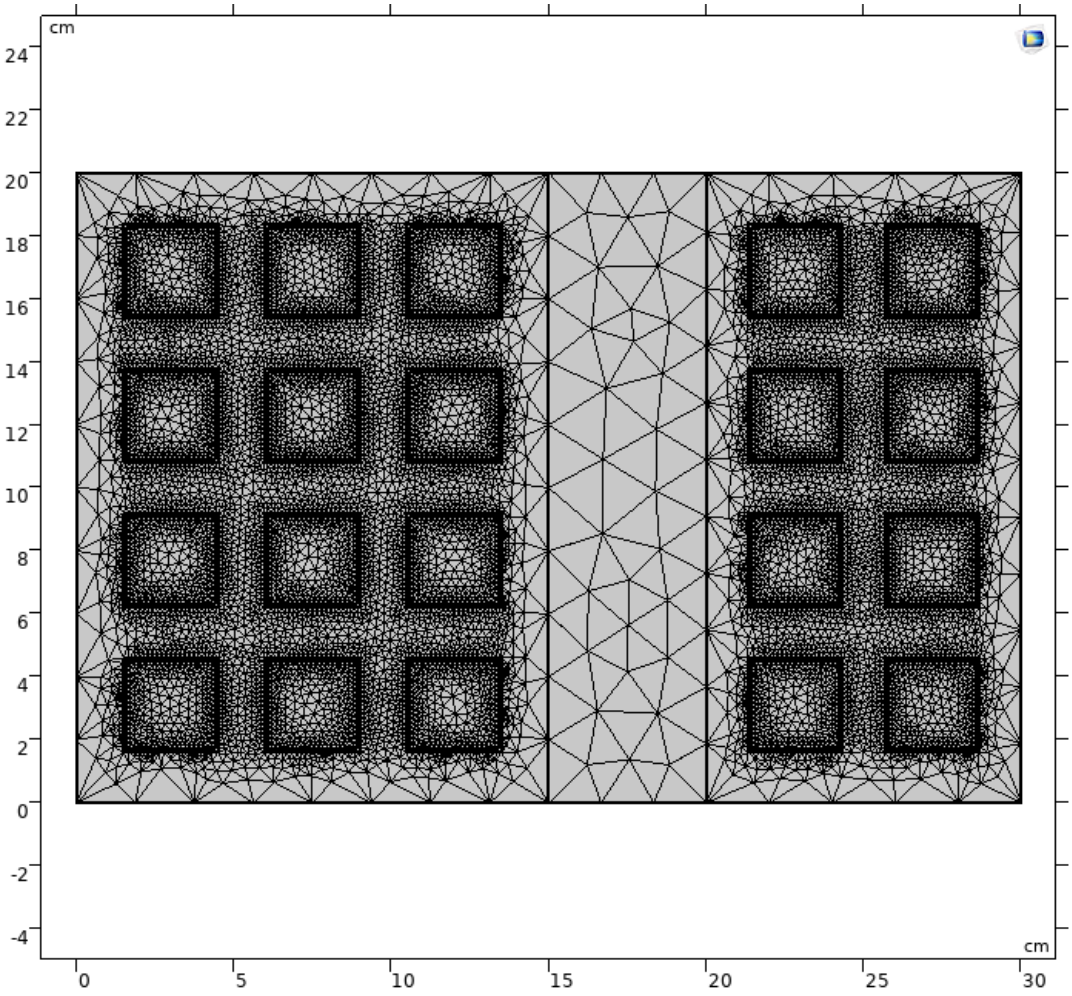

Figure 5.12. Domain geometry and Mesh of the brick-PCM assembly.

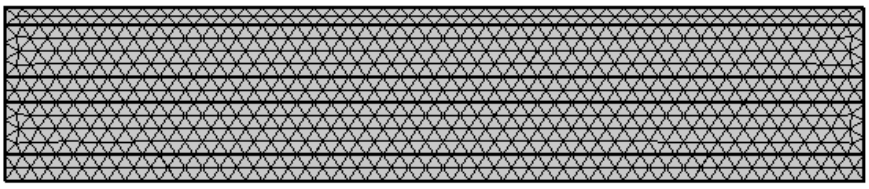

Figure. 5.13. The geometry and mesh setup of the wall-PCM assembly

5.7 Conclusion

This chapter has provided a comprehensive analysis of all aspects of our research problem, focusing primarily on the evaluation of the performance of the new bio-based PCM in energy

storage. It includes a detailed examination of the geometries of the various components, and the precise definition of boundary conditions and initial parameters for each part of the study. Given the crucial role of boundary conditions in system performance, this in-depth analysis improves our understanding of how the newly introduced bio-based PCM can improve the energy efficiency of buildings. In addition, the chapter provides an overview of commonly used methods for modelling energy storage in PCMs, with the aim of validating and refining these methods through the equivalent thermal capacity approach. This chapter has focused on the modelling and numerical simulation process using COMSOL Multiphysics. We have provided a detailed and in-depth explanation of the steps taken throughout the study.

Chapter 6

Results and discussions

6.1 Introduction

Following the development and characterisation of phase change materials (PCMs) derived from bio-based materials - myristic acid and stearic acid - and the selection of the optimal PCM for our analysis aimed at improving the energy efficiency of buildings, this chapter presents a comprehensive analysis. We will present the results of our work through an in-depth examination of three key aspects:

•Thermo-mechanical analysis of clay bricks containing date palm fibers and PCM.

•Thermal analysis of bricks used in Algeria that incorporate a new bio-based phase change material.

•Numerical study of the integration of new bio-based PCMs in building envelopes during summer in different Algerian cities.

6.2 Thermal analysis of construction bricks filled with a new eutectic mixture.

The effect of integrating the new bio-based PCM into the wall was evaluated as follows:

- Changes in the temperature and heat flow at the inner surface of the wall were assessed during a summer day.
- The overall reduction in the heat exchange rate at the inner surface of the wall was also analyzed during a summer day using the following formula:

$$THER(\%) = \left(1 - \frac{The\ quantity\ of\ heat\ exchanged\ with\ PCM}{The\ quantity\ of\ heat\ exchanged\ without\ PCM}\right) \times 100$$

6.2.1 PCM location effect on temperature distribution

The aim of this study was to achieve an optimum internal surface temperature. Figure 6.1 shows the temperature distribution along the wall at different points on 9 July at 14.00. The module at positions 5 and 6 (locations) provided less effective thermal insulation compared to the module at positions 2, 3 and 4 (locations). At locations 5 and 6, the temperature ranged from 30°C to 44°C, while at locations 2, 3 and 4, the temperature ranged from 29°C to 40°C. The better

performance of the module at locations 2, 3 and 4 can be attributed to the phase change that occurs at the corresponding external surface exposed to heat waves, as shown in Figure 6.2. The shift in the percentage of liquid phase in the centre of the PCM layer indicates that a full phase change has occurred near the outer surface of the wall, with only a small amount of liquid phase near the inner surface. This explains the lack of full phase change at the inner surface. The PCM can store significant amounts of energy within the wall during the phase change. This energy remains stored even after the phase change is complete, resulting in a temperature increase within the PCM. To facilitate the phase change process, the energy stored in the PCM needs to be released. A comparison of the five PCM-filled locations revealed noticeable differences in temperature distribution. Of the models tested, the second module had the highest efficiency and the smallest temperature fluctuation range of 9°C. On the other hand, the temperature variations for the other locations were 10°C, 10°C, 12°C and 14°C for locations 3, 4, 5 and 6 respectively.

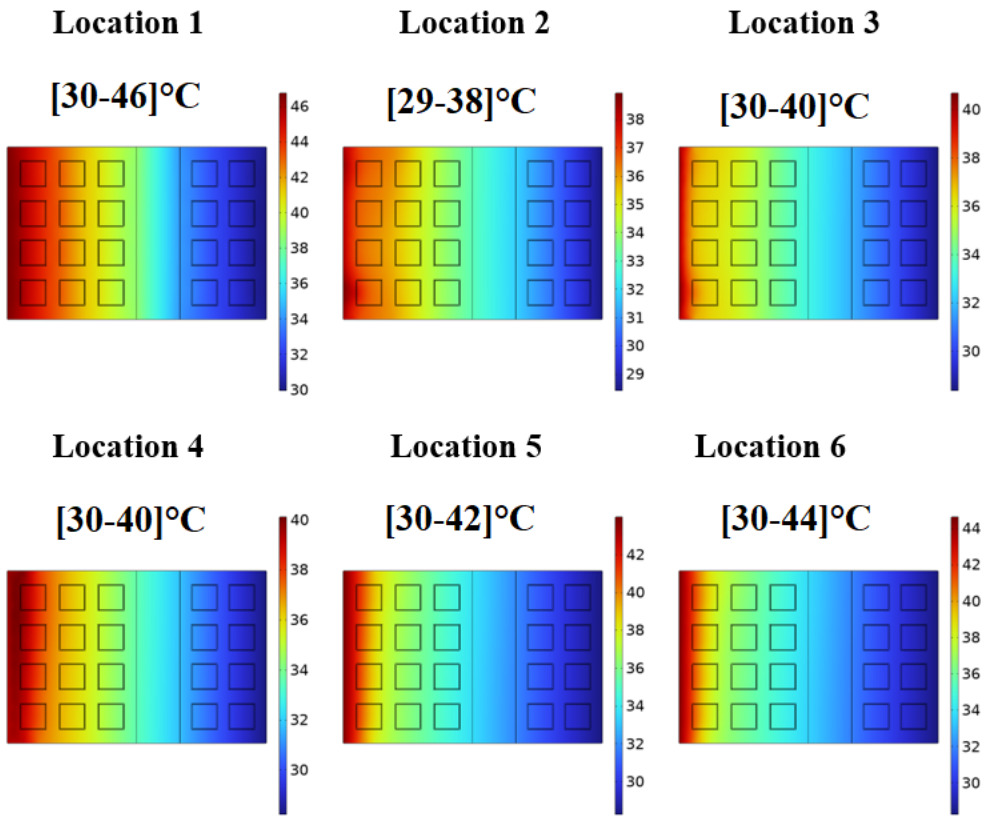

Figure 6.1. Temperature distribution along the wall, without and with the PCM (Locations 1 to 6 refers to Figure5.5)

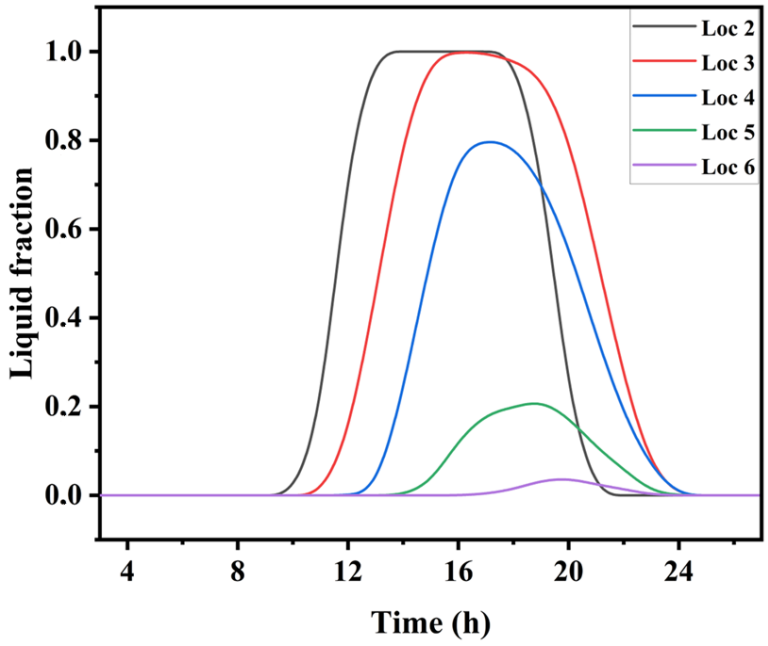

Figure 6.2. Liquid fraction variation effect for different locations in the center of the PCM layer.

6.2.2 Effect of the presence of Eutectic mixture in the hollow brick

After identifying the optimal location for the PCM, it was compared with the reference model, which consisted of a brick without PCM. Both the air and PCM layers in the bricks offered clear benefits. The air layer acted as an insulating barrier, reducing heat flow throughout the process. However, the PCM layer proved to be a more effective insulator than the air layer over a longer period of time. Combining the PCM and air layers can be beneficial as it reduces the amount of PCM required in the bricks. Temperature changes were tracked over two days (9 and 10 July) at both Loc 1 and Loc 2, as shown in Figure 6.3. The brick with PCM had a minimum temperature of 28°C and a maximum temperature of 29°C. In comparison, the brick without PCM had a minimum temperature of 28.7°C and a maximum temperature of 31.8°C. This resulted in a temperature variation of 2.8°C due to the phase change process, which was considered satisfactory as one of the main objectives was to maintain stable internal temperatures. This also delayed the peak temperature by two hours. The highest temperature for the reference wall was recorded at 3 pm, while for the wall with PCM it was recorded at 5 pm, indicating that the brick with PCM was a more effective insulator than the reference brick. Comparing these results with a recent study conducted in similar environmental conditions (a barren desert in Iraq), where paraffin wax (a petroleum-based PCM) was incorporated into the

building wall, the temperature was reduced by 2°C [64]. In contrast, the results of our study with fatty acids were promising.

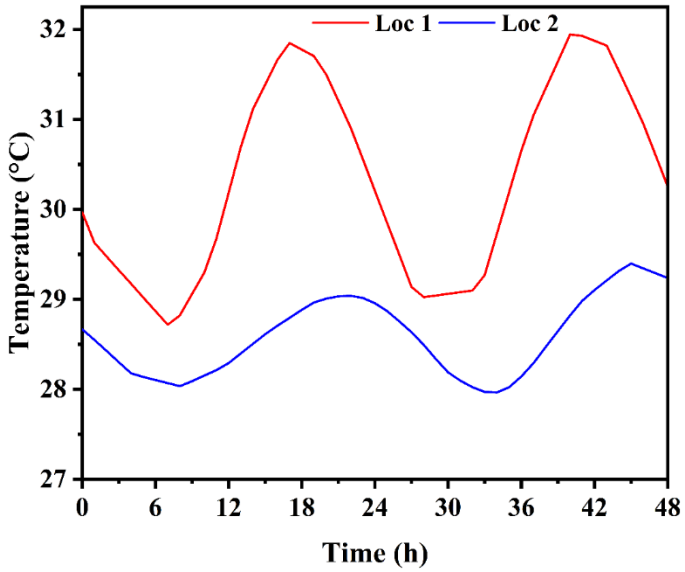

Figure 6.3. Internal surface temperature variations for the wall without PCM (orange) and the wall with PCM (blue)

6.2.3 PCM location effect on heat flux

Figures 6.4 and 6.5 illustrate the effects of placing the PCMs in different positions on the internal heat flow. The results showed that placing the PCM closer to the outside of the bricks significantly reduced the internal heat transfer compared to placing it closer to the inside. When PCMs were placed in the cavities closest to the outer surface (position 2), the heat flux at the inner surface decreased by approximately 58% compared to a conventional clay wall. This use of PCMs to fill brick cavities improves the thermal efficiency of clay bricks by minimising fluctuations in internal heat waves and reducing the total heat flow through the bricks. This reduction can be attributed to two factors: firstly, the increased thermal resistance due to the reduced thermal resistance of the PCM, and secondly, the storage of energy within the PCM voids during the fusing process, which prevents heat from passing through the bricks. These results confirm the selection of the fatty acid mixture, as they are in line with a previous study conducted in the hot regions of Algeria, which tested three different phase change materials and identified fatty acid as the most effective [160].

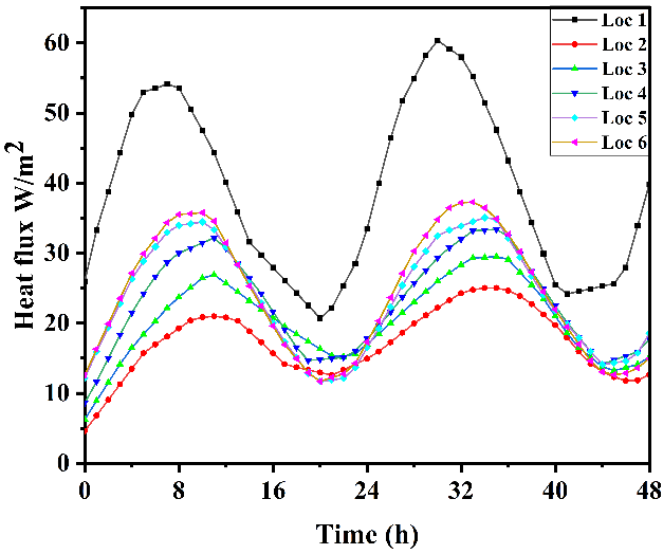

Figure 6.4 .Heat flow on the inner surface for various PCM placements.

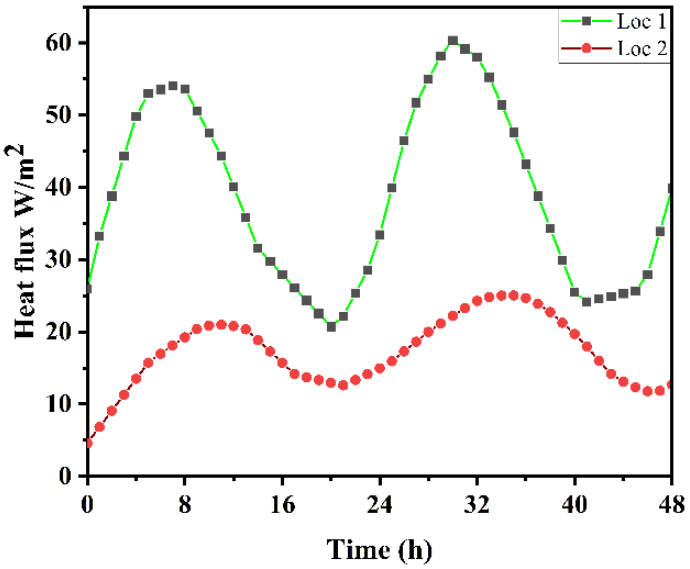

Figure 6.5. Heat flow on the inner surface of the wall without PCM and with PCM (Loc 2).

Figure 6.6 shows the overall reduction in summer heat transfer for the different positions of the PCM in the wall. In addition, Table 6.1 presents a comparison of the results obtained using a 2.8 cm thick bio-based PCM at the optimal position in the wall for Adrar, with those of previous studies aimed at improving building performance in hot environments. The results show that the current PCM effectively regulates the internal temperature of the building, leading to a significant reduction in the energy consumption of the air conditioning system. These results demonstrate the effectiveness of integrating a bio-based PCM layer to manage heat

transfer at the building surfaces and maintain a comfortable indoor temperature in the hot climate of Adrar.

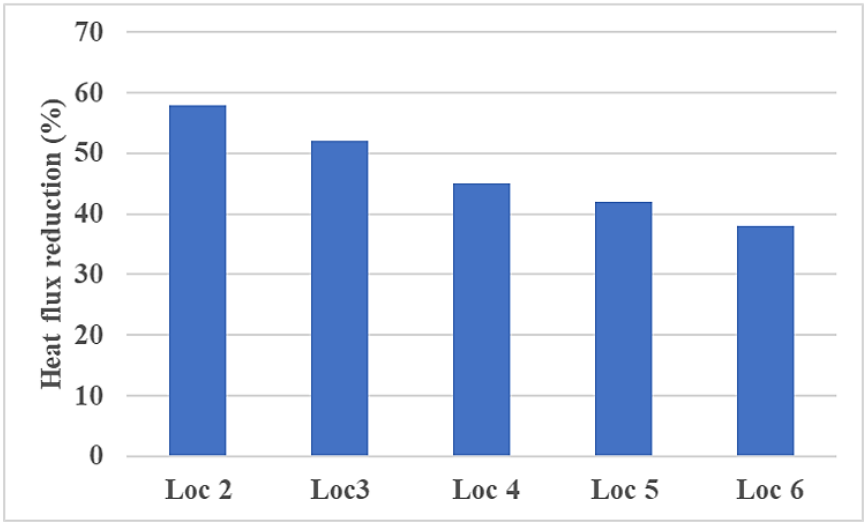

Figure 6.6. Reduction in heat transfer in summer for the city of Adrar, for various PCM locations.

Table 6.1. Comparison of the maximum reduction obtained in this study with interior temperatures in hot climates from existing studies

PCM	**Melting range [°C]**	**Thickness [cm]**	**Max ΔT [°C]**	**REF**
Bio-PCM	30–34	2	2.04	[164]
Bio-PCM Q23	23–25	2.8	3.3	[165]
Paraffin	22–28.5	2	1	[166]
Bio-PCM	27–38.3	3	3.95	[107]
Bio-based PCM	35–43	2.8	2.8 (Loc 2) 2.4 (Loc 3) 2.1 (Loc 4) 2 (Loc 5) 1.8 (Loc 6)	Present study

6.2.4 Cooling electricity cost saving

Electricity cost savings are an important economic factor in evaluating the viability of the technology. Daily electricity cost savings (in dollars per day) were calculated based on the total average heat flow savings per day and the electricity price per kWh in Algeria, using Eq. (6.1):

$$Electricity \text{ cost } saving = \text{Average heat flux reduction} \times electricity\ cost\ /\ kWh \times 24h \quad (6.1)$$

The electricity price was assumed to be \$0.031 per kWh, based on the latest Algerian tariff for buildings. The calculation assumes the use of a medium power air conditioner running for 10 hours on a summer day, with an energy consumption range of 15 to 25 kWh per day. For a building with an external surface area of 200 m², requiring 180 kg of phase change material, the results are shown in Figure 22. The electricity cost savings calculations using phase change materials at site 2 suggest a daily saving of \$9. While this amount may seem modest compared to the initial PCM integration cost of \$1188, its significance increases in the long term, especially for larger buildings. After just 130 days, the total savings in electricity costs due to reduced cooling demand equal the initial investment in the PCM. Beyond this point, the economic benefits of using phase change materials in buildings become more apparent.

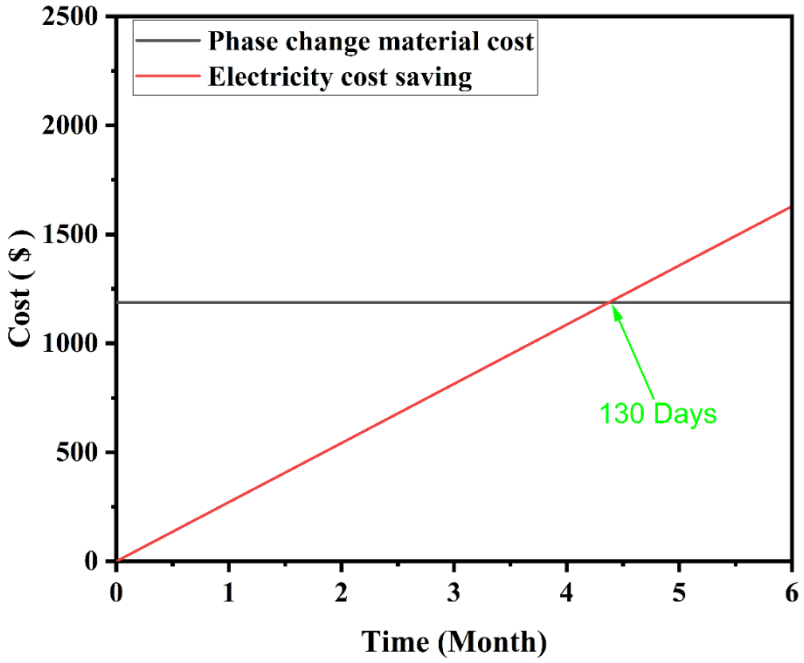

Figure 6.7. PCM cost versus three months of cooling saving in the building

6.3 Numerical study of the integration of new bio-based PCMs into building envelopes during the summer in Algerian cities.

6.3.1 Impact of PCM integration in walls for each city

This study evaluated the effects of incorporating a new bio-based phase change material (PCM) into building walls in different Algerian cities. The main objective was to assess the influence of this PCM on the thermal insulation, energy efficiency and internal thermal stability of the walls. The study compared the performance of a standard wall without PCM with that of walls incorporating a layer of the bio-based PCM.

The results provide valuable insights into the design and construction of more energy-efficient buildings, improving thermal comfort, reducing carbon emissions and minimising reliance on energy-intensive cooling systems. The impact of the bio-based PCM was assessed by analysing temperature variations and heat flow at the inner surface of the walls during summer, and by computing the total reduction in heat exchange at the inner wall surface over three months of summer.

6.3.1.1 Adrar city

In Adrar, the summer temperature can reach approximately 46°C (Figure 9), making it one of the hottest regions in Algeria. Figures 6.8 (1 and 2) show the variation of temperature and heat flux at the inner surface of the wall in summer in Adrar. This study investigated the effect of incorporating bio-based phase change materials (PCMs) into walls on temperature and heat flux. Comparing walls with and without PCMs, the results show that walls with PCMs have lower maximum heat flux and reduced temperature peaks. This shows that the integration of PCMs increases the thermal storage capacity of the wall. For example, on 1 July, the temperature range for the wall with PCMs was 29°C to 30.4°C, whereas the wall without PCMs showed a range of 30.5°C to 32.8°C, resulting in a temperature reduction of 2.4°C due to the phase change process.

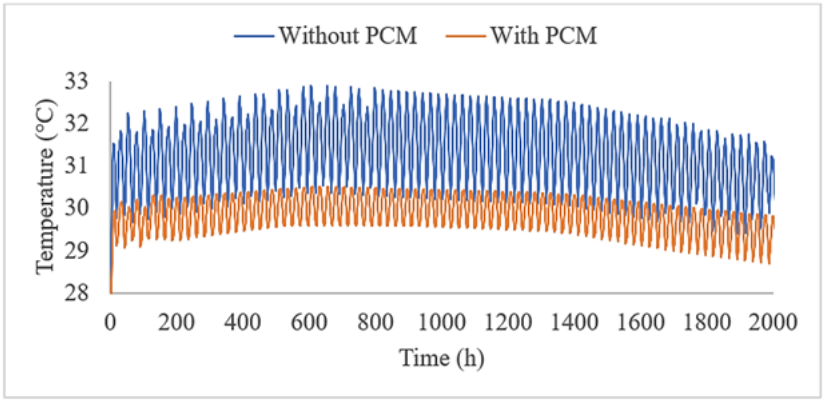

(1)

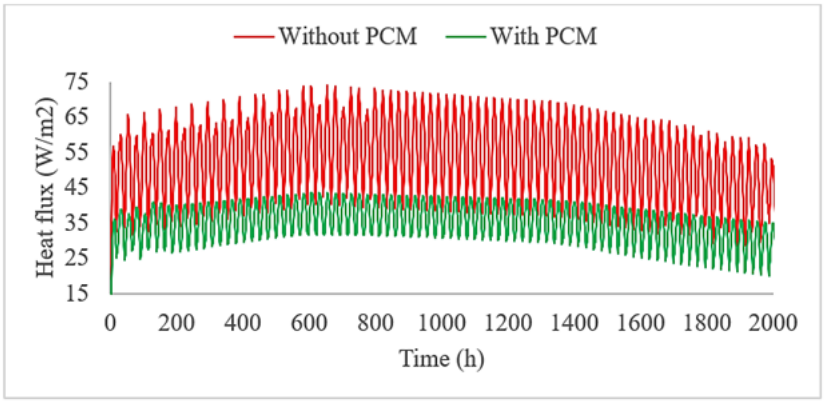

(2)

Figure 6.8. Temperature and total heat flux variations in the inner wall surface without PCM and with PCM for Adrar city: 1) Temperature, 2) Total heat flux.

6.3.1.2 Tindouf city

In Tindouf, summer temperature can reach about 44°C, which is an extremely hot condition. Figure 6.9 (1 and 2) illustrates the variation in temperature and heat flux at the inner surface of the wall during the summer in Tindouf. This study explores the application of bio-based phase change materials (PCMs) in walls to assess their impact on temperature and heat flux.

The results show that walls containing PCMs have lower maximum heat flux and reduced temperature peaks compared to walls without PCMs, indicating an increased heat storage capacity. For example, on 1 July, the temperature range for the wall with PCMs was 28.8°C to 30.1°C, while the wall without PCMs ranged from 29.6°C to 32.2°C, resulting in a temperature reduction of 2.1°C due to the phase change process.

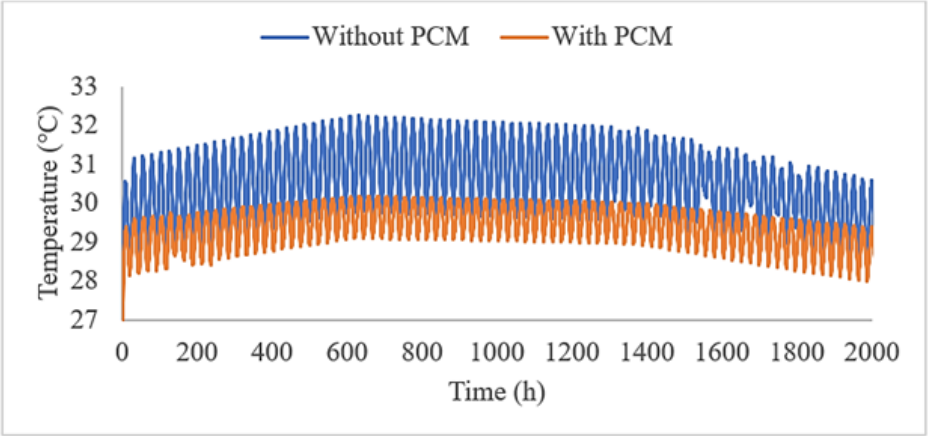

(1)

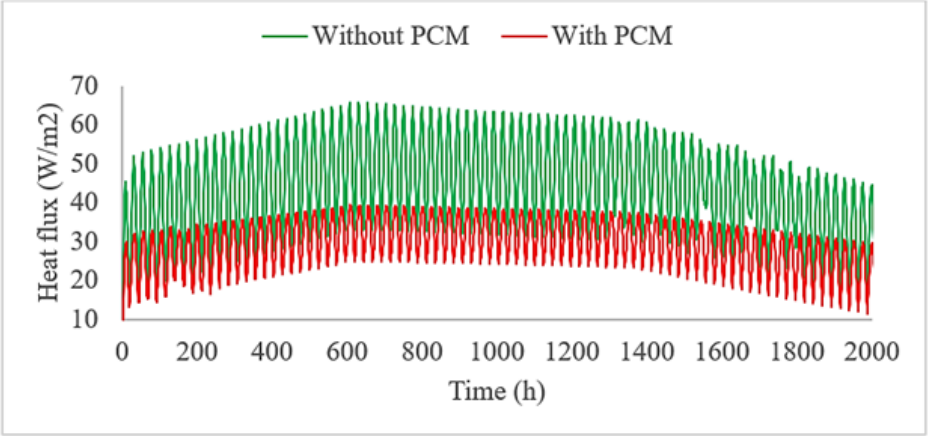

(2)

*Figure 6.9***.** Temperature and total heat flux variations in the inner wall surface without PCM and with PCM for Tindouf city: 1) Temperature, 2) Total heat flux.

6.3.1.3 Ain Salah

In Ain Salah, summer temperatures can reach around 41°C, creating very hot conditions. This research investigates the effect of incorporating bio-based phase change materials (PCMs) into walls on temperature and heat flux during summer, as shown in Figure 6.10 (1 and 2). A comparison between walls with and without PCMs shows that walls incorporating PCMs have lower maximum heat flux and temperature peaks, indicating improved thermal storage capacity. For example, on 1 July, the wall with PCMs had a temperature range of 28.5°C to 29.6°C, whereas the wall without PCMs had a range of 29.0°C to 31.2°C, resulting in a reduction of 1.6°C due to the phase change process.

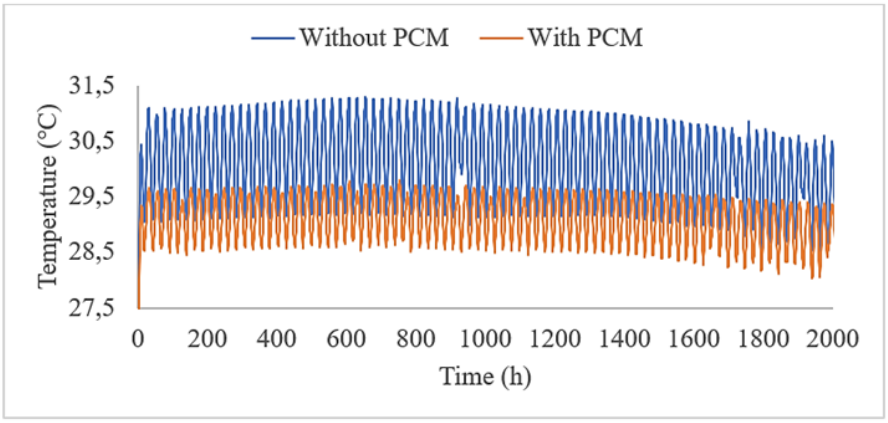

(1)

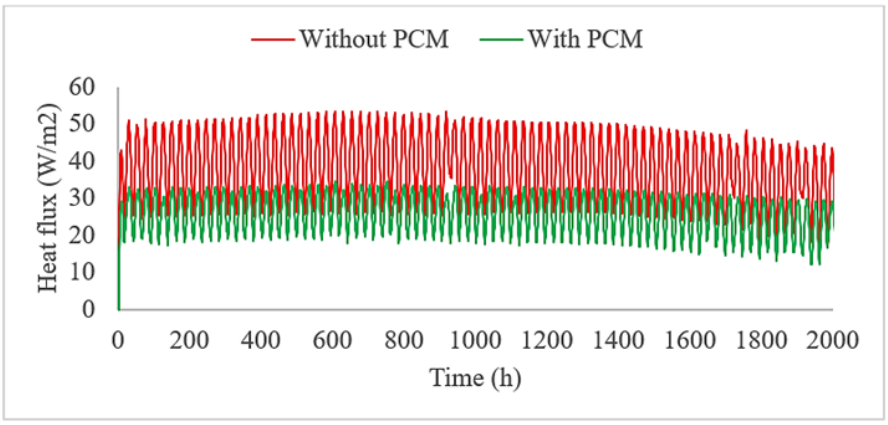

(2)

Figure 6.10. Temperature and total heat flux variations in the inner wall surface without PCM and with PCM for Ain Salah city: 1) Temperature, 2) Total heat flux.

6.3.2 Impact of the PCM bio-based states on the wall

Figure 6.11 shows the variation in the liquid fraction of the bio-based PCM layer over a four-day period in the different climates of Adrar, Tindouf, and Ain Salah. In Tindouf and Ain Salah, where external temperatures remain relatively stable, the liquid fraction cycles consistently over the four days. In contrast, in Adrar, which is characterised by exceptionally high temperatures, the PCM liquefies earlier than in the other cities. In addition, there are cases in Adrar where the PCM does not fully solidify during the night due to the persistently high nighttime temperatures.

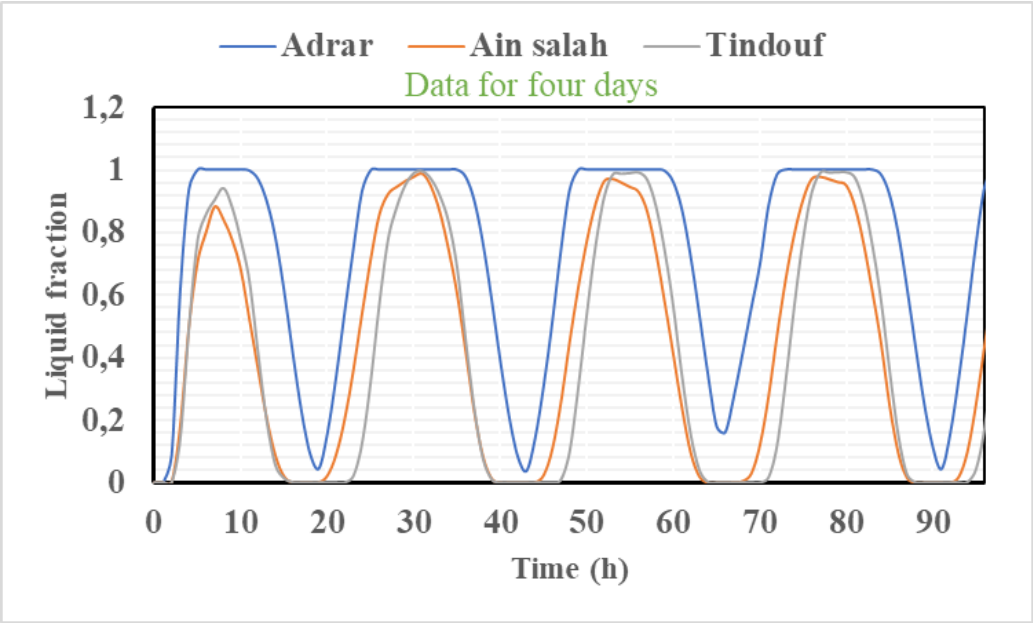

Figure 6.11. The change in the liquid fraction of the PCM in the wall over four days in the cities of Adrar, Tindouf, and Ain Salah.

Incorporating an MA-SA eutectic layer into the wall significantly impacts the temperature and heat flux at the inner surface. The MA-SA eutectic layer plays a crucial role in reducing heat flux fluctuations within the wall. These fluctuations are minimized because a substantial portion of the heat passing through the wall during the day is absorbed as latent heat during the melting process of the MA-SA eutectic. This latent heat is subsequently released at night when the outside temperature decreases, helping to maintain thermal stability and reduce heat exchange within the wall [167]. Figure 6.12 illustrates a noticeable reduction in heat flux during summer across the studied cities due to the presence of phase change materials (PCMs). In Adrar, the heat flux reduction is approximately 40% compared to walls without PCM. In Tindouf, the reduction is 49%, and in Ain Salah, it reaches 53%. These results underscore the effectiveness of integrating a PCM layer in walls for regulating heat exchange at the interior surface during Algeria's summer months. This approach significantly decreases heat flux, contributing to a more stable and comfortable indoor temperature. These findings are valuable for designers and policymakers aiming to improve building energy efficiency in hot climates such as those found in Algerian cities. By comparing our findings with a recent study carried out under nearly identical environmental conditions—a barren desert in Iraq—where petroleum-based paraffin wax was integrated into the building wall, a temperature reduction of 2°C was achieved [64]. In contrast, our study using fatty acids yielded more promising results. Table 6.2 shows the results of using a 3 cm thick bio-based phase change material (PCM) placed

in the middle of a wall in three Algerian cities with an arid desert climate, compared to previous studies using petroleum-based PCMs to improve building performance in hot environments. The results show that this bio-based PCM effectively stabilises indoor temperatures, resulting in a significant reduction in energy consumption for air conditioning. Moreover, the PCM formulated from a blend of myristic and stearic acids proves to be a strong competitor to petroleum-based PCMs, further demonstrating its effectiveness in regulating heat transfer through building surfaces and maintaining indoor thermal comfort, especially in the hot Algerian climate.

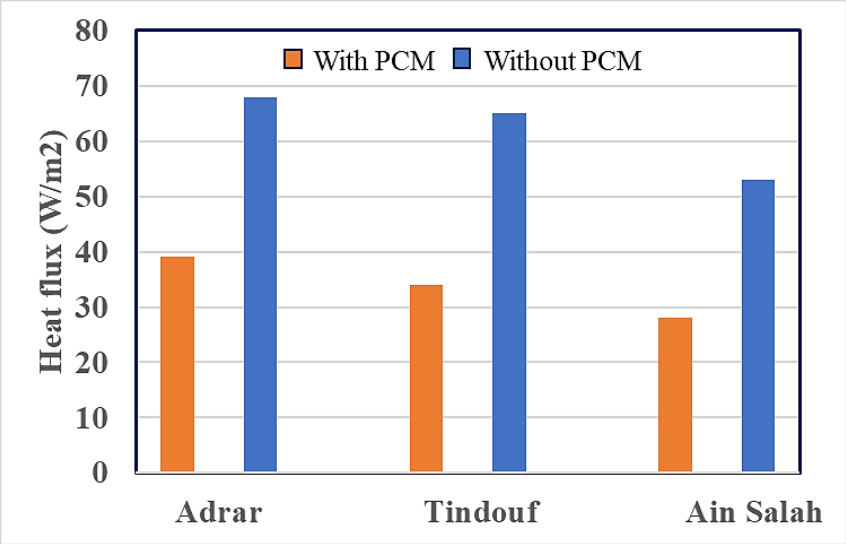

Figure 6.12. Effect of PCM in the wall brick on heat transfer reduction for each city.

Table 6.2 A comparison between the results of this study, which utilized a bio-based PCM, and previous studies that used petroleum-based PCM from the literature.

Type of PCM	**Melting point [°C]**	**Max ΔT [°C]**	**Reference**
paraffin	44	2	[64]
Chloride hexahydrate	31	4	[168]
Paraffin	28.5	1	[166]
Bio-based PCM	35	Adrar (2.4) Tindouf (2.1) Ain Salah (1.6)	Present study

6.4 Thermo-mechanical analysis of clay bricks (Adobe) containing palm fibers and phase change materials (PCM)

6.4.1 Effect of DPF/MA-SA content ratio on the physical properties of Earth bloc

6.4.1.1 Apparent density

The density of adobe, as reported by researchers in the literature, ranges from 1540 kg/m³ to 1950 kg/m³ [169]. This study determined the apparent density of dried specimens by comparing the weight of the soil block to its volume. Figure 6.13 shows the average density values of the formulated material for different DPF/MA-SA contents, ranging from 1542 kg/m³ to1608 kg/m³. Notably, a significant decrease (606 kg/m³) was observed for the 2% DPF/MA-SA content compared to the control material without DPF/MA-SA. This reduction is attributed to the lower apparent density of date palm fiber and the lower apparent density of the MA-SA mixture (840 kg/m³) compared to the adobe mixture (soil + dune sand + lime = adobe) with an apparent density of 1608 kg/m³. The evaporation of water resulted in the detachment of DPF/MA-SA particles from the clay matrix after shrinkage and the increase of the porous network within the material. Similar trends were reported in other studies [169].

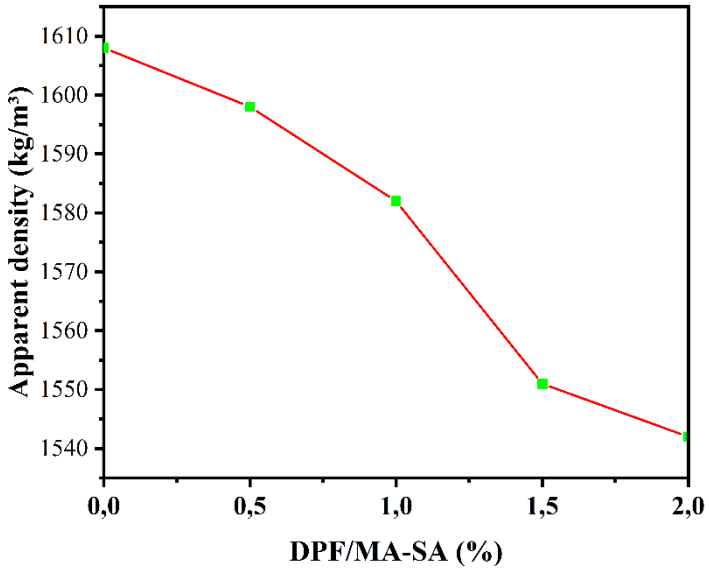

Figure 6.13. Variation of the apparent density as a function of the percentage of MA-SA/DPF.

6.4.1.2 Total absorption

Figure 6.14 illustrates the relationship between the total water absorption of bricks and the amount of DPF/MA-SA over a twenty-four-hour immersion period (in two cases 30 and 50 °C). Firstly, the total water absorption rates ranged from 18.22% for 0% DPF/MA-SA to 18.56%

for 2% DPF/MA-SA, under conditions of temperature below 30°C. This increase is considered minimal compared to previous studies using date palm fibers, attributed to pore closure with the eutectic mixture. The slight rise in absorption is due to DPF/MA-SA disintegration within the matrix (soil + dune sand + lime). Secondly, at 50°C, the rate reaches 18.95% for 2% DPF/MA-SA due to the eutectic mixture transitioning to a liquid state, enabling water access to resulting pores. Moreover, total water absorption increases with higher DPF/MA-SA content. Conclusively, Figure 9 indicates that adding DPF/MA-SA to the mixtures does not substantially increase total water absorption. The test revealed that the materials stayed stable and unchanged after 6 days of immersion, with all blocks retaining their original shape and integrity, a significant advantage for earthen construction.

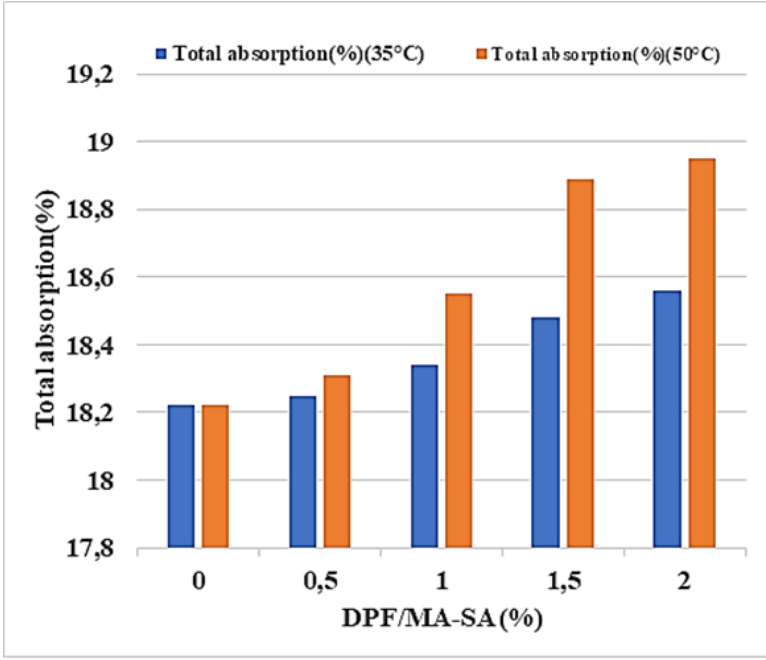

Figure 6.14. Effect of MA-SA/DPF on total absorption of bricks.

6.4.2 Effect of MA-SA/DPF content on the thermo-mechanical properties of adobes

6.4.2.1 Compressive strength

This study investigated how changing the content of DPF/MA-SA affected the compressive strength of bricks at different temperatures. The bricks, measuring 10x10x10 cm^3, were tested at 30°C and 50°C. Through the Figure 6.15, increasing the DPF/MA-SA content reduced the bulk density but also decreased the compressive strength. The highest strength was seen in control bricks without DPF/MA-SA, averaging 4.8 MPa.

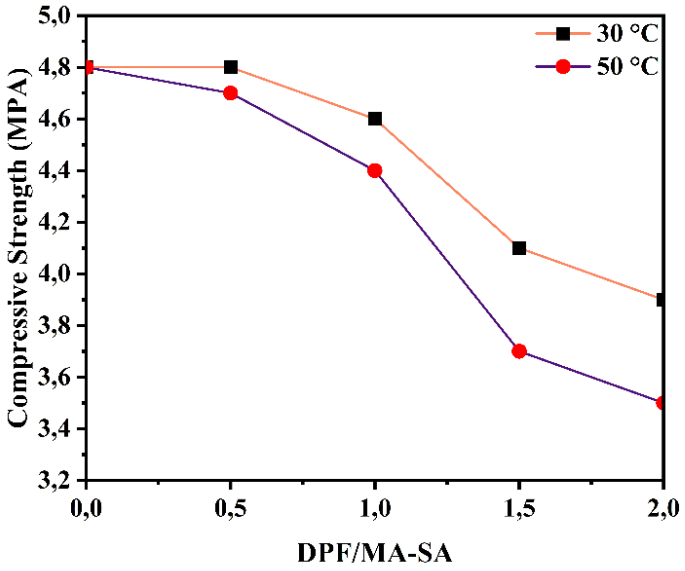

Figure 6.15. Effect of MA-SA/DPF content on the dry compressive strength of adobe.

Even with a 2% DPF/MA-SA content, the decrease in strength was minimal, which was not considered significant. At around 0.5% DPF/MA-SA, the compressive strength was similar to bricks without DPF/MA-SA. Contrary to expectations from previous studies, adding DPF to earthen bricks did not significantly reduce their strength. This was attributed to treating the fibers with MA-SA, which closed all pores when in the solid state. However, when the bricks were exposed to 50°C for 2 hours, ensuring the MA-SA mixture became liquid, the compressive strength decreased compared to the first case. This was because the liquid MA-SA mixture opened the pores, leading to lower strength. The lowest compressive strength values in both cases still met the building requirements in Algeria [170]. The decrease in strength was attributed to an increase in voids within the blocks due to the separation of DPF/MA-SA aggregates from the stabilized ground matrix in dry bricks and the separation of MA-SA from DPF in the liquid state. Because Dry compressive strength of earthen bricks depends on the strength of the binder, the bond strength of clay putty stabilized with lime sand grains, and the internal strength of the sand particles [171].

6.4.2.2 Thermal Conductivity

Thermal conductivity was assessed on brick samples with dimensions of 10 x 10 x 4 cm. The measurements were conducted using a hot wire probe and a heating resistor, along with a sensor that records temperature changes in a transient state. To ensure accuracy, the probe was positioned between two smooth blocks to eliminate air contact. This method is widely utilized in various research studies [172]. All measurements were conducted at an ambient laboratory

temperature of 24°C with 60% humidity. The results align with findings from other researchers [169], [173]. Figure 6.16 shows that thermal conductivity decreases as the DPF/MA-SA content increases, improving thermal insulation by 11% for adobe with 2% DPF/MA-SA, which has a thermal conductivity of 0.554 W/m.K compared to 0.677 W/m.K for control adobe. This improvement in thermal conductivity is due to the improved pore structure of the bricks containing DPF/MA-SA [174].

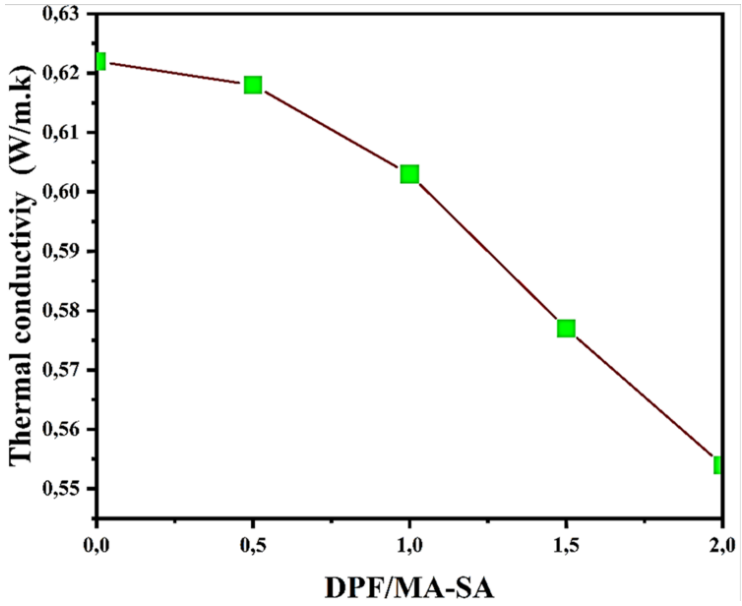

Figure 6.16. Effect of MA-SA/DPF ratio on thermal conductivity.

This reduction is due to the lower density of MA-SA/DPF compared to the clay matrix and its low thermal conductivity. The difference in thermal conductivity between the clay matrix and date palm aggregates is mainly due to their pore sizes and the volume of PCM, which has a very low conductivity (0.17 W/m.K). These findings are consistent with those reported by other researchers [175]. The thermal conductivity value obtained according to the Algerian building code, which limits this value to between 0.1 and 2 W/m.°K [176].

General Conclusion

This study focuses on improving the thermal performance of building walls through the use of bio-organic phase change materials (BIO-PCMs). The primary objective is to replace traditional petroleum-based phase change materials (PCMs) with more sustainable and environmentally friendly options. The research specifically explores the use of fatty acid-based BIO-PCMs, in particular myristic acid (MA) and stearic acid (SA), which are renewable, cost-effective and natural materials with great potential for improving energy efficiency in buildings.

The work begins with the selection of fatty acids based on factors such as cost, availability, renewability and safety. Myristic and stearic acids were selected for their favourable thermophysical properties, including suitable melting points and thermal stability. A eutectic blend of 70% MA and 30% SA was created to provide the desired thermal performance for building applications, with a melting point around 35°C and excellent energy storage capabilities.

The thermal properties of the eutectic mixture were analysed using Differential Scanning Calorimetry (DSC), which revealed a melting enthalpy of 240.1 J/g and a solidification enthalpy of 212.6 J/g, demonstrating its ability to effectively store and release latent heat. This heat storage property is essential for indoor temperature control. In addition, thermogravimetric analysis (TGA) confirmed that the blend is thermally stable, with degradation occurring only at temperatures well above its working range, making it ideal for long-term use in building materials.

The research also includes a numerical study using COMSOL Multiphysics 6.0 to simulate the thermal behaviour of hollow brick walls containing the MA-SA PCM under extreme summer conditions, specifically in Adrar, Algeria. Two types of walls were compared: one with a PCM integrated into the cavity of the bricks and the other without a PCM as a control. The results showed that the PCM-integrated wall reduced the internal temperature by about 2.8°C, improving the thermal comfort of the buildings.

A key finding was the optimal placement of the PCM within the brick walls. Placing the PCM close to the outer surface of the wall gave the best performance, delaying peak temperatures by up to 2 hours. This highlights the importance of PCM placement in building materials for effective thermal management. The simulations also showed that using BIO-

PCMs in walls could lead to significant energy savings, with a daily reduction in electricity costs of around $9 and a payback period of around 150 days. This suggests that BIO-PCMs can play a key role in reducing energy consumption and CO_2 emissions in buildings, particularly in regions such as Algeria where conventional energy sources remain dominant.

In addition to the thermal analysis of PCM-integrated walls, the study also explores the combination of bio-based PCMs with date palm fibers (DPF) to create an eco-friendly composite material for earthen construction. Date palm fibers, a renewable and abundant resource in Algeria, were impregnated with the MA-SA eutectic blend to improve the thermal and mechanical properties of the composite. These PCM-impregnated fibers were successfully incorporated into lime-stabilised soil to form a sustainable, low-cost building material.

The research found that the PCM-infused composite had a melting temperature of 34.5°C and a melting enthalpy of 124 J/g, which is lower than the pure MA-SA blend but still suitable for building applications. The composite showed promising thermal properties and stability, making it a viable option for improving the energy efficiency of clay bricks in hot climates. The mechanical properties of the composite were also evaluated and the results showed that the new PCM-infused bricks met the required strength standards for construction in Algeria.

Further thermal analysis of the PCM-enhanced composite was carried out using techniques such as DSC and TGA, which confirmed the stability and effectiveness of the PCM when incorporated into natural building materials. These results support the potential use of BIO-PCMs in sustainable building practices.

The research also investigated the energy storage capabilities of bio-based PCMs under different climatic conditions in different cities in Algeria. The simulations showed that the incorporation of BIO-PCMs into building materials could help lower indoor temperatures and reduce heat fluxes in summer, thereby improving thermal comfort and reducing the need for air conditioning. Specifically, PCM-integrated walls in Adrar, Tindouf and Ain Salah showed temperature reductions of up to 2.4°C, 2.1°C and 1.6°C respectively. These results highlight the potential of BIO-PCMs to improve energy efficiency in buildings, particularly in hot climates.

The study concludes that bio-organic phase change materials, such as the MA-SA eutectic blend, represent a promising and sustainable solution for better thermal regulation in buildings. By replacing petroleum-based PCMs with renewable, low-cost materials such as fatty acids and combining them with local resources such as date palm fibers, it is possible to

create environmentally friendly and economically viable building materials. The results provide valuable insights for the development of energy efficient and sustainable building materials that can significantly reduce energy consumption, lower CO_2 emissions and contribute to a more sustainable future.

In conclusion, the thesis provides a comprehensive study of the use of bio-based PCMs to improve thermal performance and energy efficiency in buildings. The integration of these materials into construction represents an innovative approach to addressing energy challenges in the building sector, particularly in regions with extreme temperatures. The research shows that bio-based PCMs, particularly those derived from fatty acids and date palm fibers, have the potential to revolutionise building materials by increasing energy efficiency, reducing environmental impact and promoting sustainable building practices.

- **Recommendations**

Future work should focus on optimizing BIO-PCM formulations (e.g., testing new fatty acid blends) and scaling up production for industrial viability. Advanced integration techniques, such as validating optimal PCM wall placement and combining PCMs with passive cooling should be explored to enhance performance. Long-term durability studies under real-world conditions are needed to assess material stability. Region-specific adaptations and policy frameworks can promote BIO-PCM adoption in building codes, while lifecycle analyses will quantify energy and CO_2 savings. Collaborations with industry and material scientists can accelerate commercialization.

References

[1] S. R. L. da Cunha and J. L. B. de Aguiar, “Phase change materials and energy efficiency of buildings: A review of knowledge,” *J Energy Storage, vol. 27, Feb. 2020*. doi: 10.1016/j.est.2019.101083.

[2] J. Min *et al.*, “The effect of carbon dioxide emissions on the building energy efficiency,” *Fuel*, vol. 326, Oct. 2022, doi: 10.1016/j.fuel.2022.124842.

[3] C. Dominguez, E. Kakkos, D. Gross, R. Hischier, and K. Orehounig, “Renovated or replaced? Finding the optimal solution for an existing building considering cumulative CO2 emissions, energy consumption and costs – A case study,” *Energy Build*, vol. 303, Jan. 2024, doi: 10.1016/j.enbuild.2023.113767.

[4] M. Ahangari and M. Maerefat, “An innovative PCM system for thermal comfort improvement and energy demand reduction in building under different climate conditions,” *Sustain Cities Soc*, vol. 44, pp. 120–129, Jan. 2019, doi: 10.1016/j.scs.2018.09.008.

[5] L. Xu *et al.*, “Research on the climate response of variable thermo-physical property building envelopes: A literature review,” Nov. 01, 2020, *Elsevier Ltd*. doi: 10.1016/j.enbuild.2020.110398.

[6] A. Kasaeian, L. bahrami, F. Pourfayaz, E. Khodabandeh, and W. M. Yan, “Experimental studies on the applications of PCMs and nano-PCMs in buildings: A critical review,” Nov. 01, 2017, *Elsevier Ltd*. doi: 10.1016/j.enbuild.2017.08.037.

[7] F. Kuznik, D. David, K. Johannes, and J. J. Roux, “A review on phase change materials integrated in building walls,” 2011, *Elsevier Ltd*. doi: 10.1016/j.rser.2010.08.019.

[8] S. Duan, L. Wang, Z. Zhao, and C. Zhang, “Experimental study on thermal performance of an integrated PCM Trombe wall,” *Renew Energy*, vol. 163, pp. 1932–1941, Jan. 2021, doi: 10.1016/j.renene.2020.10.081.

[9] EIA, “ Annual Energy Outlook 2018 with projections to 2050,” p. 74, 2018.

[10] “Technology Roadmap Energy Efficient Building Envelopes,” www.iea.org.

[11] MINISTERE DE L’ÉNERGIE ET DES MINES, “Bilan énergétique national de l’année 2012,” 2013.

[12] K. Faraj, M. Khaled, J. Faraj, F. Hachem, and C. Castelain, “A review on phase change materials for thermal energy storage in buildings: Heating and hybrid applications,” Jan. 01, 2021, *Elsevier Ltd*. doi: 10.1016/j.est.2020.101913.

[13] M. Maliki, N. Laredj, K. Bendani, and H. Missoum, “Two-Dimensional Transient Modeling of Energy and Mass Transfer in Porous Building Components Using COMSOL Multiphysics,” *Journal of Applied Fluid Mechanics*, vol. 10, Jan. 2017, doi: .DOI:10.18869/acadpub.jafm.73.238.26484.

[14] M. Maliki, Laredj, H. Naji, K. Bendani, and H. Missoum, “Numerical Modelling of Hygrothermal Response in Building Envelopes,” *Gradjevinar*, vol. 66, Nov. 2014, doi: DOI:10.14256/JCE.994.2013.

[15] U. Djillali, L. De Sidi, and B. Abbès, “République Algérienne Démocratique et Populaire Ministère de l’Enseignement Supérieur et de la Recherche Scientifique THESE Présentée pour l’obtention du Diplôme de Doctorat 3ème cycle Par : GOUAREH Abderrahmane Spécialité : Génie Mécanique Option : Energétique et Environnement.”

[16] W. I. F. David *et al.*, “2023 roadmap on ammonia as a carbon-free fuel,” Apr. 01, 2024, *Institute of Physics*. doi: 10.1088/2515-7655/ad0a3a.

[17] MINISTERE DE L’ÉNERGIE ET DES MINES, “Bilan énergétique national de l’année 2016,” 2017.

[18] “Technology Roadmap Energy Efficient Building Envelopes,” www.iea.org.

[19] “Technology Roadmap Energy Efficient Building Envelopes,” www.iea.org.

[20] B. Allibe and A. Benoit, “Modélisation des consommations d’énergie du secteur résidentiel français à long terme-Amélioration du réalisme comportemental et scénarios volontaristes.” [Online]. Available: https://theses.hal.science/tel-00872403v1

[21] MINISTERE DE L’ÉNERGIE ET DES MINES, “Bilan énergétique national de l’année 2011,” 2012.

[22] MINISTERE DE L’ÉNERGIE ET DES MINES, “Bilan énergétique national de l’année 2021,” 2022.

[23] M. Maliki, “Modélisation tridimensionnelle du comportement hygrothermique dans les parois multicouches de bâtiments,” PhD Thesis, Universite Abdelhamid Ibn Badis Mostaganem, 2015.

[24] A. Sarri, D. Bechki, S. Boughali, and H. Bouguettaia, “Review on thermal insulation of buildings with phase change materials: incorporation methods and applications,” 2019, doi: 10.4314/jfas.v11i1.17.

[25] X. Wang, W. Li, Z. Luo, K. Wang, and S. P. Shah, “A critical review on phase change materials (PCM) for sustainable and energy efficient building: Design, characteristic, performance and application,” Apr. 01, 2022, *Elsevier Ltd*. doi: 10.1016/j.enbuild.2022.111923.

[26] P. Arumugam, V. Ramalingam, and P. Vellaichamy, “Effective PCM, insulation, natural and/or night ventilation techniques to enhance the thermal performance of buildings located in various climates – A review,” Mar. 01, 2022, *Elsevier Ltd*. doi: 10.1016/j.enbuild.2022.111840.

[27] Dr. Mohammad S. Al-Homoud, “Performance characteristics and practical applications of common building thermal insulation materials,” *Building and Envirenment*, vol. 40, no. 3, pp. 353–360, Mar. 2005, doi: https://doi.org/10.1016/j.buildenv.2004.05.013.

[28] D. Bozsaky, “The historical development of thermal insulation materials,” *Periodica Polytechnica Architecture*, vol. 41, no. 2, pp. 49–56, Jun. 2011, doi: 10.3311/pp.ar.2010-2.02.

[29] S. Jalali. F. Pacheco-Torgal, “Earth construction: Lessons from the past for future eco-efficient construction,” *Construction and Building Materials* , vol. 29, pp. 512–519, Apr. 2012, doi: https://doi.org/10.1016/j.conbuildmat.2011.10.054.

[30] H. Niroumand, M. F. M. Zain, and M. Jamil, “Assessing of Critical Parametrs on Earth Architecture and Earth Buildings as a Vernacular and Sustainable Architecture in Various Countries,” *Procedia Soc Behav Sci*, vol. 89, pp. 248–260, Oct. 2013, doi: 10.1016/j.sbspro.2013.08.843.

[31] S. L. M. Iorio. Enrico Quagliarini, “Mechanical properties of adobe walls in a Roman Republican domus at Suasa,” *J Cult Herit*, vol. 11, no. 2, pp. 130–137, Apr. 2011, doi: https://doi.org/10.1016/j.culher.2009.01.006.

[32] G. Lan, S. Chao, Y. Wang, and Y. Cui, “Methods to Test the Compressive Strength of Earth Blocks,” *Advances in Materials Science and Engineering*, vol. 2021, 2021, doi: 10.1155/2021/1767238.

[33] Bouhemame. N; Aiadi. K., “Tensile Properties Optimization of Date Palm Leaflets Using Taguchi Method,” *Journal of Natural Fibers*, vol. 19, pp. 6348–6364, 2011, doi: https://doi.org/10.1080/15440478.2021.

[34] K. Almi, Benchabane. A, Lakel S, and Kriker A., “ Potential utilization of date palm wood as composite reinforcement,” *Journal of Reinforced Plastics and Composites.*, vol. 34, pp. 1231–1240, 2015, doi: doi:10.1177/0731684415588356.

[35] B. P. Jelle, “Traditional, state-of-the-art and future thermal building insulation materials and solutions - Properties, requirements and possibilities,” 2011, *Elsevier Ltd*. doi: 10.1016/j.enbuild.2011.05.015.

[36] S. Layachi *et al.*, “Effect of incorporating Expanded polystyrene beads on Thermophysical, mechanical properties and life cycle analysis of lightweight earth blocks,” *Constr Build Mater*, vol. 375, Apr. 2023, doi: 10.1016/j.conbuildmat.2023.130948.

[37] N. Kapilan. K. Ashok Kumar. Keshav Gowda, “Recent advances in applications of phase change materials in cold storage – A review,” *Mater Today Proc*, vol. 47, pp. 2410–2414, 2021, doi: https://doi.org/10.1016/j.matpr.2021.04.442.

[38] F. Agyenim, N. Hewitt, P. Eames, and M. Smyth, “A review of materials, heat transfer and phase change problem formulation for latent heat thermal energy storage systems (LHTESS),” Feb. 2010. doi: 10.1016/j.rser.2009.10.015.

[39] C. Alkan and A. Sari, “Fatty acid/poly(methyl methacrylate) (PMMA) blends as form-stable phase change materials for latent heat thermal energy storage,” *Solar Energy*, vol. 82, no. 2, pp. 118–124, Feb. 2008, doi: 10.1016/j.solener.2007.07.001.

[40] K. Kant, A. Shukla, and A. Sharma, “Advancement in phase change materials for thermal energy storage applications,” *Solar Energy Materials and Solar Cells*, vol. 172, pp. 82–92, Dec. 2017, doi: 10.1016/j.solmat.2017.07.023.

[41] P. K. S. Rathore, N. K. Gupta, D. Yadav, S. K. Shukla, and S. Kaul, “Thermal performance of the building envelope integrated with phase change material for thermal energy storage: an updated review.,” *Sustain Cities Soc*, vol. 79, Apr. 2022, doi: 10.1016/j.scs.2022.103690.

[42] D. Zhou, C. Y. Zhao, and Y. Tian, “Review on thermal energy storage with phase change materials (PCMs) in building applications,” 2012, *Elsevier Ltd*. doi: 10.1016/j.apenergy.2011.08.025.

[43] X. Wang, W. Li, Z. Luo, K. Wang, and S. P. Shah, “A critical review on phase change materials (PCM) for sustainable and energy efficient building: Design, characteristic, performance and application,” Apr. 01, 2022, *Elsevier Ltd*. doi: 10.1016/j.enbuild.2022.111923.

[44] J. Giro-Paloma, M. Martínez, L. F. Cabeza, and A. I. Fernández, “Types, methods, techniques, and applications for microencapsulated phase change materials (MPCM): A review,” Jan. 01, 2016, *Elsevier Ltd*. doi: 10.1016/j.rser.2015.09.040.

[45] P. Uthaichotirat, P. Sukontasukkul, P. Jitsangiam, C. Suksiripattanapong, V. Sata, and P. Chindaprasirt, “Thermal and sound properties of concrete mixed with high porous aggregates from manufacturing waste impregnated with phase change material,” *Journal of Building Engineering*, vol. 29, May 2020, doi: 10.1016/j.jobe.2019.101111.

[46] Ye Hong. Ge Xin-shi., “Preparation of polyethylene–paraffin compound as a form-stable solid-liquid phase change material,” *Solar Energy Materials and Solar Cells*, vol. 64, no. 1, Sep. 2000, doi: https://doi.org/10.1016/S0927-0248(00)00041-6.

[47] B. Lamrani, K. Johannes, and F. Kuznik, “Phase change materials integrated into building walls: An updated review,” Apr. 01, 2021, *Elsevier Ltd*. doi: 10.1016/j.rser.2021.110751.

[48] M. Duquesne, C. Mailhé, K. Ruiz-Onofre, and F. Achchaq, “Biosourced organic materials for latent heat storage: an economic and eco-friendly alternative,” *Energy*, Dec. 2019, doi: .org/10.1016/j.energy.2019.116067.

[49] A. Sharma, V. v. Tyagi, C. R. Chen, and D. Buddhi, “Review on thermal energy storage with phase change materials and applications,” Feb. 2009. doi: 10.1016/j.rser.2007.10.005.

[50] M. Sun *et al.*, “A review on thermal energy storage with eutectic phase change materials: Fundamentals and applications,” Sep. 15, 2023, *Elsevier Ltd*. doi: 10.1016/j.est.2023.107713.

[51] K. Sergei, C. Shen, and Y. Jiang, “A review of the current work potential of a trombe wall,” Sep. 01, 2020, *Elsevier Ltd*. doi: 10.1016/j.rser.2020.109947.

[52] B. Wang *et al.*, “Preparation and application of low-temperature binary eutectic lauric acid-stearic acidSiO2 phase change microcapsules,” *Energy Build*, vol. 279, Jan. 2023, doi: 10.1016/j.enbuild.2022.112706.

[53] A. Sari and A. Karaipekli, “Preparation and thermal properties of capric acid/palmitic acid eutectic mixture as a phase change energy storage material,” *Mater Lett*, vol. 62, no. 6–7, pp. 903–906, Mar. 2008, doi: 10.1016/j.matlet.2007.07.025.

[54] S. Kahwaji and M. A. White, “Prediction of the properties of eutectic fatty acid phase change materials,” *Thermochim Acta*, vol. 660, pp. 94–100, Feb. 2018, doi: 10.1016/j.tca.2017.12.024.

[55] J. Zuo, W. Li, and L. Weng, “Thermal properties of lauric acid/1-tetradecanol binary system for energy storage,” *Appl Therm Eng*, vol. 31, no. 6–7, pp. 1352–1355, May 2011, doi: 10.1016/j.applthermaleng.2011.01.008.

[56] K. Kant, A. Shukla, and A. Sharma, “Ternary mixture of fatty acids as phase change materials for thermal energy storage applications,” *Energy Reports*, vol. 2, pp. 274–279, Nov. 2016, doi: 10.1016/j.egyr.2016.10.002.

[57] H. Ke, “Phase diagrams, eutectic mass ratios and thermal energy storage properties of multiple fatty acid eutectics as novel solid-liquid phase change materials for storage and retrieval of thermal energy,” *Appl Therm Eng*, vol. 113, pp. 1319–1331, Feb. 2017, doi: 10.1016/j.applthermaleng.2016.11.158.

[58] T. Khadiran, M. Z. Hussein, Z. Zainal, and R. Rusli, “Advanced energy storage materials for building applications and their thermal performance characterization: A review,” May 01, 2016, *Elsevier Ltd*. doi: 10.1016/j.rser.2015.12.081.

[59] Song Mengjie, Niu Fuxin Mao Ning. Hu Yanxin, and Deng Shiming., “Review on building energy performance improvement using phase change materials,” *Energy Build*, vol. 158, pp. 776–793, Jan. 2018, doi: https://doi.org/10.1016/j.enbuild.2017.10.066.

[60] Y. ZOHIR, “Etude expérimental et numérique du comportement thermique de matériaux à changement de phase. Intégration dans un composant solaire passif pour L’habitat ,” PhD Thesis, Université d’Artois, 2008.

[61] Q. Al-Yasiri and M. Szabó, “Incorporation of phase change materials into building envelope for thermal comfort and energy saving: A comprehensive analysis,” Apr. 01, 2021, *Elsevier Ltd*. doi: 10.1016/j.jobe.2020.102122.

[62] M. Sawadogo, F. Benmahiddine, A. E. A. Hamami, R. Belarbi, A. Godin, and M. Duquesne, “Investigation of a novel bio-based phase change material hemp concrete for passive energy storage in buildings,” *Appl Therm Eng*, vol. 212, Jul. 2022, doi: 10.1016/j.applthermaleng.2022.118620.

[63] A. Sarri, D. Bechki, H. Bouguettaia, S. N. Al-Saadi, S. Boughali, and M. M. Farid, “Effect of using PCMs and shading devices on the thermal performance of buildings in different Algerian climates. A simulation-based optimization,” *Solar Energy*, vol. 217, pp. 375–389, Mar. 2021, doi: 10.1016/j.solener.2021.02.024.

[64] Q. Al-Yasiri and M. Szabó, “Experimental study of PCM-enhanced building envelope towards energy-saving and decarbonisation in a severe hot climate,” *Energy Build*, vol. 279, Jan. 2023, doi: 10.1016/j.enbuild.2022.112680.

[65] Z. A. Al-Absi, M. I. M. Hafizal, and M. Ismail, “Experimental study on the thermal performance of PCM-based panels developed for exterior finishes of building walls,” *Journal of Building Engineering*, vol. 52, Jul. 2022, doi: 10.1016/j.jobe.2022.104379.

[66] Z. Liu, J. Hou, D. Wei, X. Meng, and B. J. Dewancker, “Thermal performance analysis of lightweight building walls in different directions integrated with phase change materials (PCM),” *Case Studies in Thermal Engineering*, vol. 40, p. 102536, Dec. 2022, doi: 10.1016/j.csite.2022.102536.

[67] C. G. Rangel, C. I. Rivera-Solorio, M. Gijón-Rivera, and S. Mousavi, “The effect on thermal comfort and heat transfer in naturally ventilated roofs with PCM in a semi-arid climate: An experimental research,” *Energy Build*, vol. 274, Nov. 2022, doi: 10.1016/j.enbuild.2022.112453.

[68] C. Arumugam and S. Shaik, “Air-conditioning cost saving and CO2 emission reduction prospective of buildings designed with PCM integrated blocks and roofs,” *Sustainable Energy Technologies and Assessments*, vol. 48, Dec. 2021, doi: 10.1016/j.seta.2021.101657.

[69] Q. Li *et al.*, “Effect of sunspace and PCM louver combination on the energy saving of rural residences: Case study in a severe cold region of China,” *Sustainable Energy Technologies and Assessments*, vol. 45, Jun. 2021, doi: 10.1016/j.seta.2021.101126.

[70] Q. Al-Yasiri and M. Szabó, “Experimental evaluation of the optimal position of a macroencapsulated phase change material incorporated composite roof under hot climate conditions,” *Sustainable Energy Technologies and Assessments*, vol. 45, Jun. 2021, doi: 10.1016/j.seta.2021.101121.

[71] H. M. Abbas, J. M. Jalil, and S. T. Ahmed, “Experimental and numerical investigation of PCM capsules as insulation materials inserted into a hollow brick wall,” *Energy Build*, vol. 246, Sep. 2021, doi: 10.1016/j.enbuild.2021.111127.

[72] X. Sun, L. Liu, Y. Mo, J. Li, and C. Li, “Enhanced thermal energy storage of a paraffin-based phase change material (PCM) using nano carbons,” *Appl Therm Eng*, vol. 181, Nov. 2020, doi: 10.1016/j.applthermaleng.2020.115992.

[73] R. Saxena, D. Rakshit, and S. C. Kaushik, “Experimental assessment of Phase Change Material (PCM) embedded bricks for passive conditioning in buildings,” *Renew Energy*, vol. 149, pp. 587–599, Apr. 2020, doi: 10.1016/j.renene.2019.12.081.

[74] P. K. S. Rathore and S. K. Shukla, “An experimental evaluation of thermal behavior of the building envelope using macroencapsulated PCM for energy savings,” *Renew Energy*, vol. 149, pp. 1300–1313, Apr. 2020, doi: 10.1016/j.renene.2019.10.130.

[75] S. Dabiri, M. Mehrpooya, and E. G. Nezhad, “Latent and sensible heat analysis of PCM incorporated in a brick for cold and hot climatic conditions, utilizing computational fluid dynamics,” *Energy*, vol. 159, pp. 160–171, Sep. 2018, doi: 10.1016/j.energy.2018.06.074.

[76] H. Elarga, S. Fantucci, V. Serra, R. Zecchin, and E. Benini, “Experimental and numerical analyses on thermal performance of different typologies of PCMs integrated in the roof space,” *Energy Build*, vol. 150, pp. 546–557, Sep. 2017, doi: 10.1016/j.enbuild.2017.06.038.

[77] Vineet Veer Tyagi. D. Buddhi., “PCM thermal storage in buildings: A state of art ,” *Renewable and Sustainable Energy Reviews*, vol. 11, no. 6, pp. 1146–1166, Aug. 2007, doi: https://doi.org/10.1016/j.rser.2005.10.002.

[78] D. W. Hawes, D. Feldman, and D. Banu, “Latent heat storage in building materials Objectives of research in thermal storage building materials,” 1993. doi: https://doi.org/10.1016/0378-7788(93)90040-2.

[79] D. Feldman, D. Banu, D. Hawes, and E. Ghanbari, “Obtaining an energy storing building material by direct incorporation of an organic phase change material in gypsum wallboard,” 1991. doi: https://doi.org/10.1016/0165-1633(91)90021-C.

[80] S. A. Memon, “Phase change materials integrated in building walls: A state of the art review,” 2014, *Elsevier Ltd*. doi: 10.1016/j.rser.2013.12.042.

[81] L. Navarro *et al.*, “Thermal energy storage in building integrated thermal systems: A review. Part 1. active storage systems,” Apr. 01, 2016, *Elsevier Ltd*. doi: 10.1016/j.renene.2015.11.040.

[82] Sarri abdelkader, “Etude du Stockage d’Energie Thermique par Matériaux à Changements de Phase dans le Sud-Est Algérien,” UNIVERSITE KASDI MERBAH OUARGLA, OUARGLA, 2021.

[83] Y. Cui, J. Xie, J. Liu, and S. Pan, “Review of Phase Change Materials Integrated in Building Walls for Energy Saving,” in *Procedia Engineering*, Elsevier Ltd, 2015, pp. 763–770. doi: 10.1016/j.proeng.2015.09.027.

[84] R. K. Sharma, P. Ganesan, V. v. Tyagi, H. S. C. Metselaar, and S. C. Sandaran, “Developments in organic solid-liquid phase change materials and their applications in thermal energy storage,” *Energy Convers Manag*, vol. 95, pp. 193–228, May 2015, doi: 10.1016/j.enconman.2015.01.084.

[85] X. Shi, M. R. Yazdani, R. Ajdary, and O. J. Rojas, “Leakage-proof microencapsulation of phase change materials by emulsification with acetylated cellulose nanofibrils,” *Carbohydr Polym*, vol. 254, Feb. 2021, doi: 10.1016/j.carbpol.2020.117279.

[86] B. Muñoz-Sánchez, I. Iparraguirre-Torres, V. Madina-Arrese, U. Izagirre-Etxeberria, A. Unzurrunzaga-Iturbe, and A. García-Romero, “Encapsulated High Temperature PCM as Active Filler Material in a Thermocline-based Thermal Storage System,” in *Energy Procedia*, Elsevier Ltd, May 2015, pp. 937–946. doi: 10.1016/j.egypro.2015.03.177.

[87] C. Suresh, T. Kumar Hotta, and S. K. Saha, “Phase change material incorporation techniques in building envelopes for enhancing the building thermal Comfort-A review,” Aug. 01, 2022, *Elsevier Ltd*. doi: 10.1016/j.enbuild.2022.112225.

[88] Z. Liu *et al.*, “A review on macro-encapsulated phase change material for building envelope applications,” Oct. 15, 2018, *Elsevier Ltd*. doi: 10.1016/j.buildenv.2018.08.030.

[89] F. Souayfane, F. Fardoun, and P. H. Biwole, “Phase change materials (PCM) for cooling applications in buildings: A review,” Oct. 01, 2016, *Elsevier Ltd*. doi: 10.1016/j.enbuild.2016.04.006.

[90] Xiangfei Kong ; Chengqiang Yao ; Pengfei Jie ; Yun Liu ; Chengying Qi ; Xian Rong, “Development and thermal performance of an expanded perlite-based phase change material wallboard for passive cooling in building,” *Energy and Buildings* , vol. 152, pp. 547–557, Oct. 2017, doi: https://doi.org/10.1016/j.enbuild.2017.06.067.

[91] Xiangfei Kong ; Lu Wang ; Han Li ; Guangpu Yuan ; Chengqiang Yao, “Experimental study on a novel hybrid system of active composite PCM wall and solar thermal system for clean heating supply in winter,” *Solar Energy* , vol. 195, pp. 259–270, Jan. 2020, doi: https://doi.org/10.1016/j.solener.2019.11.081.

[92] Luisa F. Cabeza ; Lidia Navarro ; Anna Laura Pisello ; Lorenzo Olivieri ; Cesar Bartolomé ; José Sánchez g; Servando Álvarez ; Jose Antonio Tenorio, “Behaviour of a concrete wall containing micro-encapsulated PCM after a decade of its construction,” *Solar Energy* , vol. 200, pp. 108–113, Apr. 2020, doi: https://doi.org/10.1016/j.solener.2019.12.003.

[93] F. Kuznik, J. Virgone, and K. Johannes, “In-situ study of thermal comfort enhancement in a renovated building equipped with phase change material wallboard,” *Renew Energy*, vol. 36, no. 5, pp. 1458–1462, 2011, doi: 10.1016/j.renene.2010.11.008.

[94] Cabeza. C. C. M. N. M. M. R. Leppers. O. Zubillaga. Luisa F, “Use of microencapsulated PCM in concrete walls for energy savings,” *Energy Build*, vol. 39, no. 2, pp. 113–119, Feb. 2007, doi: https://doi.org/10.1016/j.enbuild.2006.03.030.

[95] A. Castell ; I. Martorell ; M. Medrano; G. Pérez ; L.F. Cabeza, “Experimental study of using PCM in brick constructive solutions for passive cooling,” *Energy Build*, vol. 42, no. 4, pp. 534–540, Apr. 2010, doi: https://doi.org/10.1016/j.enbuild.2009.10.022.

[96] N. Hichem, S. Noureddine, S. Nadia, and D. Djamila, “Experimental and numerical study of a usual brick filled with PCM to improve the thermal inertia of buildings,” in *Energy Procedia*, Elsevier Ltd, 2013, pp. 766–775. doi: 10.1016/j.egypro.2013.07.089.

[97] Frédéric Kuznik; Joseph Virgone; Jean-Jacques Roux, “Energetic efficiency of room wall containing PCM wallboard: A full-scale experimental investigation,” *Energy Build*, vol. 40, no. 2, pp. 148–156, 2008, doi: https://doi.org/10.1016/j.enbuild.2007.01.022.

[98] Hassan Nazir ; Mariah Batool ; Francisco J. Bolivar Osorio ;Marllory Isaza-Ruiz ; Xinhai Xu ; K. Vignarooban; Patrick Phelan; Inamuddin; Arunachala. Kannan, “Recent developments in phase change materials for energy storage applications: A review,” *Int J Heat Mass Transf*, vol. 129, pp. 491–523, Feb. 2019, doi: https://doi.org/10.1016/j.ijheatmasstransfer.2018.09.126.

[99] Tung-Chai Ling; Chi-Sun Poon, “Use of phase change materials for thermal energy storage in concrete: An overview,” *Constr Build Mater*, vol. 46, pp. 55–62, Sep. 2013, doi: https://doi.org/10.1016/j.conbuildmat.2013.04.031.

[100] Rhys Jacob; Frank Bruno, “Review on shell materials used in the encapsulation of phase change materials for high temperature thermal energy storage,” *Renewable and Sustainable Energy Reviews*, vol. 48, pp. 79–87, Aug. 2015, doi: https://doi.org/10.1016/j.rser.2015.03.038.

[101] G. B and T. S, “Effectiveness of CFD simulation for the performance prediction of phase change building boards in the thermal environment control of indoor spaces,” *Build Environ*, vol. 59, pp. 612–625, Jan. 2013, doi: https://doi.org/10.1016/j.buildenv.2012.10.004.

[102] M.A. Izquierdo-Barrientos ; J.F. Belmonte ; D. Rodríguez-Sánchez ; A.E. Molina ; J.A. Almendros-Ibáñez, “A numerical study of external building walls containing phase change materials (PCM),” *Applied Thermal Engineering* , vol. 47, pp. 73–85, Dec. 2012, doi: https://doi.org/10.1016/j.applthermaleng.2012.02.038.

[103] F. Kuznik ; K. Johannes ; E. Franquet ; L. Zalewski ; S. Gibout ; P. Tittelein; J.-P. Dumas; D. David ; J.-P. Bédécarrats ; S. Lassue, “Impact of the enthalpy function on the simulation of a building with phase change material wall,” *Energy and Buildings* , vol. 126, pp. 220–229, Aug. 2016, doi: https://doi.org/10.1016/j.enbuild.2016.05.046.

[104] Mohammad Saffari ; Alvaro de Gracia ; Cèsar Fernández ; Luisa F. Cabeza, “Simulation-based optimization of PCM melting temperature to improve the energy performance in buildings,” *Appl Energy*, vol. 202, pp. 420–434, Sep. 2017, doi: https://doi.org/10.1016/j.apenergy.2017.05.107.

[105] Na Zhu ; Fuli Liu ; Pengpeng Liu ; Pingfang Hu ; Mengdu Wu, “Energy saving potential of a novel phase change material wallboard in typical climate regions of China,” *Energy and Buildings* , vol. 128, pp. 360–369, Sep. 2016, doi: https://doi.org/10.1016/j.enbuild.2016.06.093.

[106] Amirreza Fateh ; Davide Borelli ; Francesco Devia ; Helmut Weinläder, “Summer thermal performances of PCM-integrated insulation layers for light-weight building walls: Effect of orientation and melting point temperature,” *Thermal Science and Engineering Progress* , vol. 6, pp. 361–369, Jun. 2018, doi: https://doi.org/10.1016/j.tsep.2017.12.012.

[107] Z. Guermat, Y. Kabar, F. Kuznik, and T. E. Boukelia, “Numerical investigation of the integration of new bio-based PCM in building envelopes during the summer in Algerian cities,” *J Energy Storage*, vol. 79, Feb. 2024, doi: 10.1016/j.est.2023.110111.

[108] M. E. Brahimi, M. Maliki, N. Laredj, F. Kuznik, M. Sardou, and H. Missoum, “Investigation of the thermal efficiency of hollow bricks filled with bio-organic phase change material mixture,” *J Energy Storage*, vol. 122, p. 116667, Jun. 2025, doi: 10.1016/j.est.2025.116667.

[109] M. E. Brahimi, M. Maliki, L. Nadia, Hanifi Missoum, and Sardou Miloud., “Thermal Analysis of a Novel Phase Change Material (PCM) and Its Impact on Building Energy

Performance: A Case Study in Arid Climates," *Heat Transf Res*, 2025, doi: http://dx.doi.org/10.1615/HeatTransRes.2025057101.

[110] Z.X. Li ; Abdullah A.A.A. Al-Rashed ; Mahfouz Rostamzadeh; Rasool Kalbasi ; Amin Shahsavar ; Masoud Afrand, "Heat transfer reduction in buildings by embedding phase change material in multi-layer walls: Effects of repositioning, thermophysical properties and thickness of PCM," *Energy Conversion and Management* , vol. 195, pp. 43–56, Sep. 2019, doi: https://doi.org/10.1016/j.enconman.2019.04.075.

[111] Müslüm Arıcı ; Feyza Bilgin ; Sandro Nižetić ; Hasan Karabay, "PCM integrated to external building walls: An optimization study on maximum activation of latent heat," *Applied Thermal Engineering Volume 165, 25 January 2020, 114560*, vol. 165, Jan. 2020, doi: https://doi.org/10.1016/j.applthermaleng.2019.114560.

[112] Qian Wang ; Runqi Wu ; Yu Wu ; C.Y. Zhao, "Parametric analysis of using PCM walls for heating loads reduction," *Energy and Buildings* , vol. 172, pp. 328–336, Aug. 2018, doi: https://doi.org/10.1016/j.enbuild.2018.05.012.

[113] Feng Jiang ; Xin Wang ; Yinping Zhang, "A new method to estimate optimal phase change material characteristics in a passive solar room," *Energy Conversion and Management* , vol. 52, no. 6, pp. 2437–2441, Jun. 2011, doi: https://doi.org/10.1016/j.enconman.2010.12.051.

[114] L. Erlbeck ; P. Schreiner ; K. Schlachter ; P. Dörnhofer ; F. Fasel ; F.-J. Methner ; M. Rädle, "Adjustment of thermal behavior by changing the shape of PCM inclusions in concrete blocks," *Energy Conversion and Management* , vol. 158, pp. 256–265, Feb. 2018, doi: https://doi.org/10.1016/j.enconman.2017.12.073.

[115] E. Tunçbilek, M. Arıcı, and S. Bouadila, "Seasonal and annual performance analysis of PCM-integrated building brick under the climatic conditions of Marmara region," *J Therm Anal Calorim* , vol. 141, pp. 613–624, Jan. 2020, doi: https://doi.org/10.1007/s10973-020-09320-8.

[116] M. Mahdaoui *et al.*, "Building bricks with phase change material (PCM): Thermal performances," *Constr Build Mater*, vol. 269, Feb. 2021, doi: 10.1016/j.conbuildmat.2020.121315.

[117] R. Aridi and A. Yehya, "Review on the sustainability of phase-change materials used in buildings," Aug. 01, 2022, *Elsevier Ltd*. doi: 10.1016/j.ecmx.2022.100237.

[118] S. G. Jeong, J. H. Lee, J. Seo, and S. Kim, "Thermal performance evaluation of Bio-based shape stabilized PCM with boron nitride for energy saving," *Int J Heat Mass Transf*, vol. 71, pp. 245–250, Apr. 2014, doi: 10.1016/j.ijheatmasstransfer.2013.12.017.

[119] A. Saria and K. Kaygusuzb, "Thermal Energy Storage Characteristics of Myristic and Stearic Acids Eutectic Mixture for Low Temperature Heating Applications*," *Chinese J. Chem. Eng*, vol. 14, no. 2, pp. 270–275, Apr. 2006, doi: 10.1016/S1004-9541(06)60070-0.

[120] S. Homlakorn, A. Suksri, and T. Wongwuttanasatian, "Efficiency improvement of PV module using a binary-organic eutectic phase change material in a finned container," *Energy Reports*, vol. 8, pp. 121–128, Nov. 2022, doi: 10.1016/j.egyr.2022.05.147.

[121] P. Kauranen, K. Peippo, and P. D. Lund, “An organic PCM storage system with adjustable melting temperature,” *solar Energy*, vol. 46, no. 5, pp. 275–278, Nov. 1991.

[122] G. M. Demirbolat, G. P. Coskun, O. Erdogan, and O. Cevik, “Long chain fatty acids can form aggregates and affect the membrane integrity,” *Colloids Surf B Biointerfaces*, vol. 204, p. 111795, Aug. 2021, doi: 10.1016/J.COLSURFB.2021.111795.

[123] R. Zhang, D. Chen, L. Chen, X. Cao, X. Li, and Y. Qu, “Preparation and thermal properties analysis of fatty acids/1-hexadecanol binary eutectic phase change materials reinforced with TiO2 particles,” *J Energy Storage*, vol. 51, Jul. 2022, doi: 10.1016/j.est.2022.104546.

[124] M. B, T. Kumara, and Veershetty Gumtapure., “Experimental investigation of shellac wax as potential bio-phase change material for medium temperature solar thermal energy storage applications,” *Solar Energy*, vol. 231, pp. 1002–1014, Jan. 2022, doi: doi.org/10.1016/j.solener.2021.12.019.

[125] M. Rudra and Veershetty Gumtapure., “Thermo-physical analysis of natural shellac wax as novel bio-phase change material for thermal energy storage applications,” *The Journal of Energy Storage*, vol. 29, Jun. 2020, doi: doi.org/10.1016/j.est.2020.101390.

[126] T. Titin, K. Eny, Dwi; Marta Nurjaya, Nandy; Putra, M. Teuku, and M. Indra, “Experimental analysis of natural wax as phase change material by thermal cycling test using thermoelectric system,” *The journal of energy storage*, vol. 40, Aug. 2021, doi: 10.1016/j.est.2021.102703.

[127] E. Cibele, Mohamad Rida, C. Gabriela, L. Lucila, and Sabine Hoffmann., “Climate-Based Analysis for the Potential Use of Coconut Oil as Phase Change Material in Buildings,” *Sustainability*, vol. 13, 2021, doi: 10.3390/su131910731.

[128] Y. Tang, G. Alva, X. Huang, D. Su, L. Liu, and G. Fang, “Thermal properties and morphologies of MA-SA eutectics/CNTs as composite PCMs in thermal energy storage,” *Energy Build*, vol. 127, pp. 603–610, Sep. 2016, doi: 10.1016/j.enbuild.2016.06.031.

[129] Z. L. Yang, R. Walvekar, W. P. Wong, R. K. Sharma, S. Dharaskar, and M. Khalid, “Advances in phase change materials, heat transfer enhancement techniques, and their applications in thermal energy storage: A comprehensive review,” *J Energy Storage*, vol. 87, p. 111329, May 2024, doi: 10.1016/J.EST.2024.111329.

[130] I. Shamseddine, F. Pennec, P. Biwole, and F. Fardoun, “Supercooling of phase change materials: A review,” *Renewable and Sustainable Energy Reviews*, vol. 158, p. 112172, Apr. 2022, doi: 10.1016/J.RSER.2022.112172.

[131] E. D. Kravvaritis, K. A. Antonopoulos, and C. Tzivanidis, “Experimental determination of the effective thermal capacity function and other thermal properties for various phase change materials using the thermal delay method,” *Appl Energy*, vol. 88, no. 12, pp. 4459–4469, 2011, doi: 10.1016/j.apenergy.2011.05.032.

[132] A. Keziz, M. Rasheed, M. Heraiz, F. Sahnoune, and A. Latif, “Structural, morphological, dielectric properties, impedance spectroscopy and electrical modulus of sintered Al6Si2O13–Mg2Al4Si5O18 composite for electronic applications,” *Ceram Int*, vol. 49, no. 23, pp. 37423–37434, Dec. 2023, doi: 10.1016/j.ceramint.2023.09.068.

[133] M. Garcia-Valles, P. Alfonso, S. Martínez, and N. Roca, "Mineralogical and thermal characterization of kaolinitic clays from terra alta (Catalonia, Spain)," *Minerals*, vol. 10, no. 2, Feb. 2020, doi: 10.3390/min10020142.

[134] A. Bassoud, H. Khelafi, A. M. Mokhtari, and A. Bada, "Effectivenessof salty sand in improving the adobe's thermomechanical properties: Adrar case study (south Algeria)," *Trends in Sciences*, vol. 18, no. 19, Oct. 2021, doi: 10.48048/tis.2021.6.

[135] A. Bada, H. Khelafi, and A. Mokhtari, "Etude et Caractérisation Thermomécanique Des Matériaux Locaux A Base D'argile-Argile D'Adrar," International Journal of Scientific Research & Engineering Technology - IJSET Vol.5 pp.5-8, 2017.

[136] A. Bassoud, H. Khelafi, A. M. Mokhtari, and A. Bada, "Effectivenessof salty sand in improving the adobe's thermomechanical properties: Adrar case study (south Algeria)," *Trends in Sciences*, vol. 18, no. 19, Oct. 2021, doi: 10.48048/tis.2021.6.

[137] M. L. Bakhaled, M. Bentchikou, R. Belarbi, and M. Maliki, "Elaboration and characterization of extruded clay bricks with light weight date palm fibers," *Materials Testing*, vol. 63, no. 9, pp. 872–877, Sep. 2021, doi: 10.1515/mt-2021-0011.

[138] C. Cárdenas-Ramírez, M. A. Gómez, and F. Jaramillo, "Comprehensive analysis of the thermal properties of capric-myristic, lauric-myristic and palmitic-stearic acids and their shape-stabilization in an inorganic support," *J Energy Storage*, vol. 34, p. 102015, Feb. 2021, doi: 10.1016/J.EST.2020.102015.

[139] W. Zhang *et al.*, "Lauric-stearic acid eutectic mixture/carbonized biomass waste corn cob composite phase change materials: Preparation and thermal characterization," *Thermochim Acta*, vol. 674, pp. 21–27, Apr. 2019, doi: 10.1016/j.tca.2019.01.022.

[140] G. Hekimoğlu *et al.*, "Walnut shell derived bio-carbon/methyl palmitate as novel composite phase change material with enhanced thermal energy storage properties," *J Energy Storage*, vol. 35, Mar. 2021, doi: 10.1016/j.est.2021.102288.

[141] X. Jingchen *et al.*, "Form-stable phase change material based on fatty acid/wood flour composite and PVC used for thermal energy storage," *Energy Build*, vol. 209, Feb. 2020, doi: 10.1016/j.enbuild.2019.109663.

[142] A. Sarı, G. Hekimoğlu, and V. V. Tyagi, "Low cost and eco-friendly wood fiber-based composite phase change material: Development, characterization and lab-scale thermoregulation performance for thermal energy storage," *Energy*, vol. 195, Mar. 2020, doi: 10.1016/j.energy.2020.116983.

[143] T. Dong *et al.*, "A phase change material embedded composite consisting of kapok and hollow PET fibers for dynamic thermal comfort regulation," *Ind Crops Prod*, vol. 158, Dec. 2020, doi: 10.1016/j.indcrop.2020.112945.

[144] Z. Assia, F. Fazia, and H. Abdelmadjid, "Sustainability of the stabilized earth blocs under chemicals attack's effects and environmental conditions," *Constr Build Mater*, vol. 212, pp. 787–798, Jul. 2019, doi: 10.1016/j.conbuildmat.2019.03.324.

[145] A. Karaipekli and A. Sari, "Preparation, thermal properties and thermal reliability of eutectic mixtures of fatty acids/expanded vermiculite as novel form-stable composites

for energy storage," *Journal of Industrial and Engineering Chemistry*, vol. 16, no. 5, pp. 767–773, Sep. 2010, doi: 10.1016/j.jiec.2010.07.003.

[146] O. Chung, S. G. Jeong, and S. Kim, "Preparation of energy efficient paraffinic PCMs/expanded vermiculite and perlite composites for energy saving in buildings," *Solar Energy Materials and Solar Cells*, vol. 137, pp. 107–112, 2015, doi: 10.1016/j.solmat.2014.11.001.

[147] B.L.S. Gowreesunker, "Phase change thermal energy storage for the thermal control of large thermally lightweight indoor spaces," PhD Theses, Brunel University School of Engineering and Design , 2013.

[148] Raza Gulfam ; Peng Zhang ; Zhaonan Meng, "Advanced thermal systems driven by paraffin-based phase change materials – A review," *Applied Energy* , vol. 238, pp. 582–611, Mar. 2019, doi: https://doi.org/10.1016/j.apenergy.2019.01.114.

[149] H. B. Pascal, E. Pierre, and K. Frederic, "Phase-change materials to improve solar panel's performance," *Energy and Buildings* , vol. 62, pp. 59–67, Jul. 2013, doi: https://doi.org/10.1016/j.enbuild.2013.02.059.

[150] M. S. D. Poirier, "On Numerical Methods Used in Mathematical Modeling of Phase Change in Liquid Metals," *J. Heat Transfer*, 1988.

[151] C. R. Swaminathan ; V. R. Voller, "A general enthalpy method for modeling solidification processes," *Metall Trans*, vol. 23, pp. 651–664, 1992, doi: https://doi.org/10.1007/BF02649725.

[152] E. M. Alawadhi, "Thermal analysis of a building brick containing phase change material," *Energy Build*, vol. 40, pp. 351–357, 2008, doi: https://doi.org/10.1016/j.enbuild.2007.03.001.

[153] K. Kant; A. Shukla; A.l Sharma, "Heat transfer studies of building brick containing phase change materials," *Solar Energy*, vol. 155, pp. 1233–1242, 2017, doi: https://doi.org/10.1016/j.solener.2017.07.072.

[154] M.I. Hasan; H.O. Basher; A.O. Shdhan, "Experimental investigation of phase change materials for insulation of residential buildings," *Sustain Cities Soc*, vol. 36, pp. 42–58, 2018, doi: https://doi.org/10.1016/j.scs.2017.10.009.

[155] M. Li; G. Gui; Z. Lin; L. Jiang; H. Pan; X. Wang, "Numerical Thermal Characterization and Performance Metrics of Building Envelopes Containing Phase Change Materials for Energy-Efficient Buildings," *Sustainability*, vol. 10, p. 2657, 2018, doi: https://doi.org/10.3390/su10082657.

[156] M. E. Brahimi, M. Maliki, N. Laredj, H. Missoum, and M. Sardou, "Thermo-Mechanical Assessment of Bio-based Insulating Material Using Phase Change Materials and Date Palm Fibers," *Science, Engineering and Technology*, vol. 5, no. 1, Mar. 2025, doi: 10.54327/set2025/v5.i1.209.

[157] Y. Hamidi, Z. Aketouane, M. Malha, D. Bruneau, A. Bah, and R. Goiffon, "Integrating PCM into hollow brick walls: Toward energy conservation in Mediterranean regions," *Energy Build*, vol. 248, Oct. 2021, doi: 10.1016/j.enbuild.2021.111214.

[158] N. P. Sharifi, G. E. Freeman, and A. R. Sakulich, “Using COMSOL modeling to investigate the efficiency of PCMs at modifying temperature changes in cementitious materials - Case study,” *Constr Build Mater*, vol. 101, pp. 965–974, Dec. 2015, doi: 10.1016/j.conbuildmat.2015.10.162.

[159] A. Ntoumos, P. Hadjinicolaou, G. Zittis, Y. Proestos, and J. Lelieveld, “Projected Air Temperature Extremes and Maximum Heat Conditions Over the Middle-East-North Africa (MENA) Region,” *Earth Systems and Environment*, vol. 6, no. 2, pp. 343–359, Jun. 2022, doi: 10.1007/s41748-022-00297-y.

[160] A. Bachir and N. Taieb, “Numerical analysis for energy performance optimization of hollow bricks for roofing. Case study: Hot climate of Algeria,” *Constr Build Mater*, vol. 367, Feb. 2023, doi: 10.1016/j.conbuildmat.2023.130336.

[161] H. Kitagawa, T. Asawa, T. Kubota, and A. R. Trihamdani, “Numerical simulation of radiant floor cooling systems using PCM for naturally ventilated buildings in a hot and humid climate,” *Build Environ*, vol. 226, Dec. 2022, doi: 10.1016/j.buildenv.2022.109762.

[162] J. Yu, C. Yang, and L. Tian, “Low-energy envelope design of residential building in hot summer and cold winter zone in China,” *Energy Build*, vol. 40, no. 8, pp. 1536–1546, 2008, doi: 10.1016/j.enbuild.2008.02.020.

[163] Y. Hamidi, M. Malha, and A. Bah, “Analysis of the thermal behavior of hollow bricks walls filled with PCM: Effect of PCM location,” *Energy Reports*, vol. 7, pp. 105–115, Nov. 2021, doi: 10.1016/j.egyr.2021.08.108.

[164] M. Sovetova, S. A. Memon, and J. Kim, “Thermal performance and energy efficiency of building integrated with PCMs in hot desert climate region,” *Solar Energy*, vol. 189, pp. 357–371, Sep. 2019, doi: 10.1016/j.solener.2019.07.067.

[165] T. A. Vik, H. B. Madessa, P. Aslaksrud, E. Folkedal, and O. S. Øvrevik, “Thermal Performance of an Office Cubicle Integrated with a Bio-based PCM: Experimental Analyses,” in *Energy Procedia*, Elsevier Ltd, Mar. 2017, pp. 609–618. doi: 10.1016/j.egypro.2017.03.223.

[166] G. Evola, L. Marletta, and F. Sicurella, “A methodology for investigating the effectiveness of PCM wallboards for summer thermal comfort in buildings,” *Build Environ*, vol. 59, pp. 517–527, Jan. 2013, doi: 10.1016/j.buildenv.2012.09.021.

[167] H. Zhan, N. Mahyuddin, R. Sulaiman, and F. Khayatian, “Phase change material (PCM) integrations into buildings in hot climates with simulation access for energy performance and thermal comfort: A review,” Sep. 15, 2023, *Elsevier Ltd*. doi: 10.1016/j.conbuildmat.2023.132312.

[168] Mannivannana. et al., “Simulation and experimental study of thermal performance of a building roof with a phase change material (PCM),” *Sadhana*, vol. 40, pp. 2381–2388, Dec. 2015, doi: https://doi.org/10.1007/s12046-014-0332-8.

[169] D. Khoudja, B. Taallah, O. Izemmouren, S. Aggoun, O. Herihiri, and A. Guettala, “Mechanical and thermophysical properties of raw earth bricks incorporating date palm

waste," *Constr Build Mater*, vol. 270, Feb. 2021, doi: 10.1016/j.conbuildmat.2020.121824.

[170] D. Silveira, H. Varum, A. Costa, T. Martins, H. Pereira, and J. Almeida, "Mechanical properties of adobe bricks in ancient constructions," *Constr Build Mater*, vol. 28, no. 1, pp. 36–44, Mar. 2012, doi: 10.1016/j.conbuildmat.2011.08.046.

[171] F. Parisi, D. Asprone, L. Fenu, and A. Prota, "Experimental characterization of Italian composite adobe bricks reinforced with straw fibers," *Compos Struct*, vol. 122, pp. 300–307, Apr. 2015, doi: 10.1016/j.compstruct.2014.11.060.

[172] H. Niroumand, M. F. M. Zain, M. Jamil, and S. Niroumand, "Earth Architecture from Ancient until Today," *Procedia Soc Behav Sci*, vol. 89, pp. 222–225, Oct. 2013, doi: 10.1016/j.sbspro.2013.08.838.

[173] A. Oushabi, S. Sair, Y. Abboud, O. Tanane, and A. El Bouari, "An experimental investigation on morphological, mechanical and thermal properties of date palm particles reinforced polyurethane composites as new ecological insulating materials in building," *Case Studies in Construction Materials*, vol. 7, pp. 128–137, Dec. 2017, doi: 10.1016/j.cscm.2017.06.002.

[174] G. Matthew, O. Sanya, and N. Mohammed, "Influence of Pore Nature on the Thermal Conductivity of Insulating Refractory Brick," *Chemistry and Materials Research*, Sep. 2020, doi: 10.7176/cmr/12-7-03.

[175] A. B. Cherki, A. Khabbazi, B. Remy, and D. Baillis, "Granular cork content dependence of thermal diffusivity, thermal conductivity and heat capacity of the composite material / Granular cork bound with plaster," in *Energy Procedia*, Elsevier Ltd, 2013, pp. 83–92. doi: 10.1016/j.egypro.2013.11.008.

[176] F. Hadji, N. Ihaddadene, R. Ihaddadene, A. Betga, A. Charick, and P. O. Logerais, "Thermal conductivity of two kinds of earthen building materials formerly used in Algeria," *Journal of Building Engineering*, vol. 32, Nov. 2020, doi: 10.1016/j.jobe.2020.101823.